



## Polymerization in living organisms

Cite this: DOI: 10.1039/d2cs00759b

 Dan Wu,<sup>ab</sup> Jiaqi Lei,<sup>a</sup> Zhankui Zhang,<sup>b</sup> Feihe Huang,<sup>id</sup>\*<sup>cd</sup> Marija Buljan<sup>e</sup> and Guocan Yu<sup>id</sup>\*<sup>af</sup>

Vital biomacromolecules, such as RNA, DNA, polysaccharides and proteins, are synthesized inside cells via the polymerization of small biomolecules to support and multiply life. The study of polymerization reactions in living organisms is an emerging field in which the high diversity and efficiency of chemistry as well as the flexibility and ingeniousness of physiological environment are incisively and vividly embodied. Efforts have been made to design and develop *in situ* intra/extracellular polymerization reactions. Many important research areas, including cell surface engineering, biocompatible polymerization, cell behavior regulation, living cell imaging, targeted bacteriostasis and precise tumor therapy, have witnessed the elegant demeanour of polymerization reactions in living organisms. In this review, recent advances in polymerization in living organisms are summarized and presented according to different polymerization methods. The inspiration from biomacromolecule synthesis in nature highlights the feasibility and uniqueness of triggering living polymerization for cell-based biological applications. A series of examples of polymerization reactions in living organisms are discussed, along with their designs, mechanisms of action, and corresponding applications. The current challenges and prospects in this lifeful field are also proposed.

Received 28th November 2022

DOI: 10.1039/d2cs00759b

[rsc.li/chem-soc-rev](https://rsc.li/chem-soc-rev)

<sup>a</sup> Key Laboratory of Bioorganic Phosphorus Chemistry & Chemical Biology, Department of Chemistry, Tsinghua University, Beijing 100084, P. R. China. E-mail: guocanyu@mail.tsinghua.edu.cn

<sup>b</sup> College of Materials Science and Engineering, Zhejiang University of Technology Hangzhou, 310014, P. R. China

<sup>c</sup> Stoddart Institute of Molecular Science, Department of Chemistry, Zhejiang University, Hangzhou 310027, P. R. China. E-mail: fhuang@zju.edu.cn

<sup>d</sup> ZJU-Hangzhou Global Scientific and Technological Innovation Center, Hangzhou, 311215, P. R. China

<sup>e</sup> Empa, Swiss Federal Laboratories for Materials Science and Technology, 9014 St. Gallen, Switzerland

<sup>f</sup> School of Medicine, Tsinghua University, Beijing 100084, P. R. China

## 1. Introduction

As the basic components of all organisms, biomacromolecules have evolved with nature over billions of years with elegant structures and reliable performances. DNA is a biomacromolecule with a double helical structure for storing hereditary information and hierarchically folded molds of proteins for catalysis and structure recognition.<sup>1–9</sup> Biomacromolecules are produced in living organisms through *in situ* polymerization. Biomacromolecules with precise structures and diverse functions are synthesized through


**Dan Wu**

Dan Wu was born in Henan, China, in 1988. She received her PhD degree from Zhejiang University in 2016 under the supervision of Prof. Guping Tang. She is currently a lecturer at the college of materials science and engineering at Zhejiang University of Technology. Her current research interests are focused on the construction of functional biomaterials.


**Jiaqi Lei**

Jiaqi Lei is a PhD candidate at the Department of Chemistry, Tsinghua University, under the supervision of Dr Guocan Yu. He received his BS degree from Northwestern Polytechnical University majoring in polymer science and engineering. Now, he is interested in understanding and exploring the pathway of immunology (especially the role of saccharides), the mode of cancer growing, and the protein interaction with small molecules or ligands. He is devoted to making potency drugs using supramolecular chemistry to contribute to human health.

the permutations of simple monomers (such as nucleotides, amino acids, and monosaccharides) catalyzed by enzymes (Fig. 1).<sup>10–14</sup> Inspired by nature, the human in-born curiosity drives the motivation to use intracellular conditions to synthesize bioactive macromolecules *in situ*, which is the origin of biomimetic engineered living materials (ELMs).<sup>15–23</sup> Therefore, raising the concept of moving synthetic reactions from laboratory flasks into a cellular microenvironment is promising and crucial.

Recently, ELMs which make use of the dynamic metabolic profile of living organisms to modulate and assemble complicated synthetic structures, have shown promising potential in cell-based biological applications, such as cell-on-a-chips, cell-based sensors, cell therapy, biocatalysis and biomotors.<sup>24–30</sup> Two polymerization strategies, namely, covalent and noncovalent (supramolecular) polymerization, are generally used for constructing ELMs inside and on the surface of living cells. For cell surface engineering, polymer-based cell encapsulation and

direct polymerization on the cell surface are two very active directions. To date, numerous polymer-based strategies, such as layer-by-layer, cell-in-microgel and cell-in-shell, have been explored to encapsulate cells.<sup>31–34</sup> However, these strategies are barely biocompatible and the formed polymer shells are always thick and stiff, thus impairing cell capabilities, to a certain extent.<sup>35</sup> Although some strategies, such as biomolecular assembly, fast kinetic gelation and mussel-inspired chemistry, have been exploited to enrich the sorts of cell envelopes; however the problems of uncontrolled polymerization and low encapsulation efficiency remain.<sup>36–38</sup>

Currently, direct and *in situ* polymerization approaches have been developed to reduce polymer thickness and improve the coating efficiency with the aid of new chemical polymeric reactions, such as biosynthetic reactions and visible light-triggered graft polymerization.<sup>39,40</sup> Chemical or physical polymer grafting reactions (also known as the “grafting-to” strategy) are preferred



**Zhankui Zhang**

*Zhankui Zhang received his BS degree from Henan University of Technology in 2016. Now he is a postgraduate at the College of Materials Science and Engineering, Zhejiang University of Technology under the supervision of Prof. Wu Dan. His research interests focus on functional biomaterials.*



**Feihe Huang**

*Feihe Huang is Changjiang Scholar Chair Professor at Zhejiang University. His current research is focused on supramolecular chemistry. Awards and honours he has received include Chinese Chemical Society AkzoNobel Chemical Sciences Award, The Cram Lehn Pedersen Prize in Supramolecular Chemistry, the Royal Society of Chemistry Polymer Chemistry Lectureship award, Changjiang Scholar, The Royal Society Newton Advanced Fellowship award, and the Germany Bruno Werdelmann Lectureship Award. He sits/sat on the Advisory Boards of J Am Chem Soc, Chem Soc Rev, Chem Commun, Acta Chim Sinica, Macromolecules, ACS Macro Lett, and Polym Chem. He is an Editorial Board Member of Mater Chem Front.*



**Marija Buljan**

*Marija Buljan is a group leader at the Swiss Federal Laboratories for Materials Science and Technology and an associated group leader at the Swiss Institute of Bioinformatics. She obtained her PhD degree in computational biology from the University of Cambridge and after that she worked as a researcher at the MRC Laboratory of Molecular Biology in Cambridge, UK, German Cancer Research Institute in Heidelberg, Germany and ETH Zurich in Switzerland.*

*Her research interests include computational and systems biology, proteomics and immunoengineering.*



**Guocan Yu**

*Guocan Yu received his PhD degree from Zhejiang University in 2015 under the supervision of Prof. Feihe Huang. He spent five years as a postdoctoral fellow in Dr Xiaoyuan (Shawn) Chen's research group at National Institutes of Health (NIH) from 2015 to 2020. He started his independent research career at the Department of Chemistry at Tsinghua University in the late 2020. His research interests are focused on the development of smart delivery systems, supramolecular theranostics and supramolecular strategies for immune modulation.*

*His research interests are focused on the development of smart delivery systems, supramolecular theranostics and supramolecular strategies for immune modulation.*

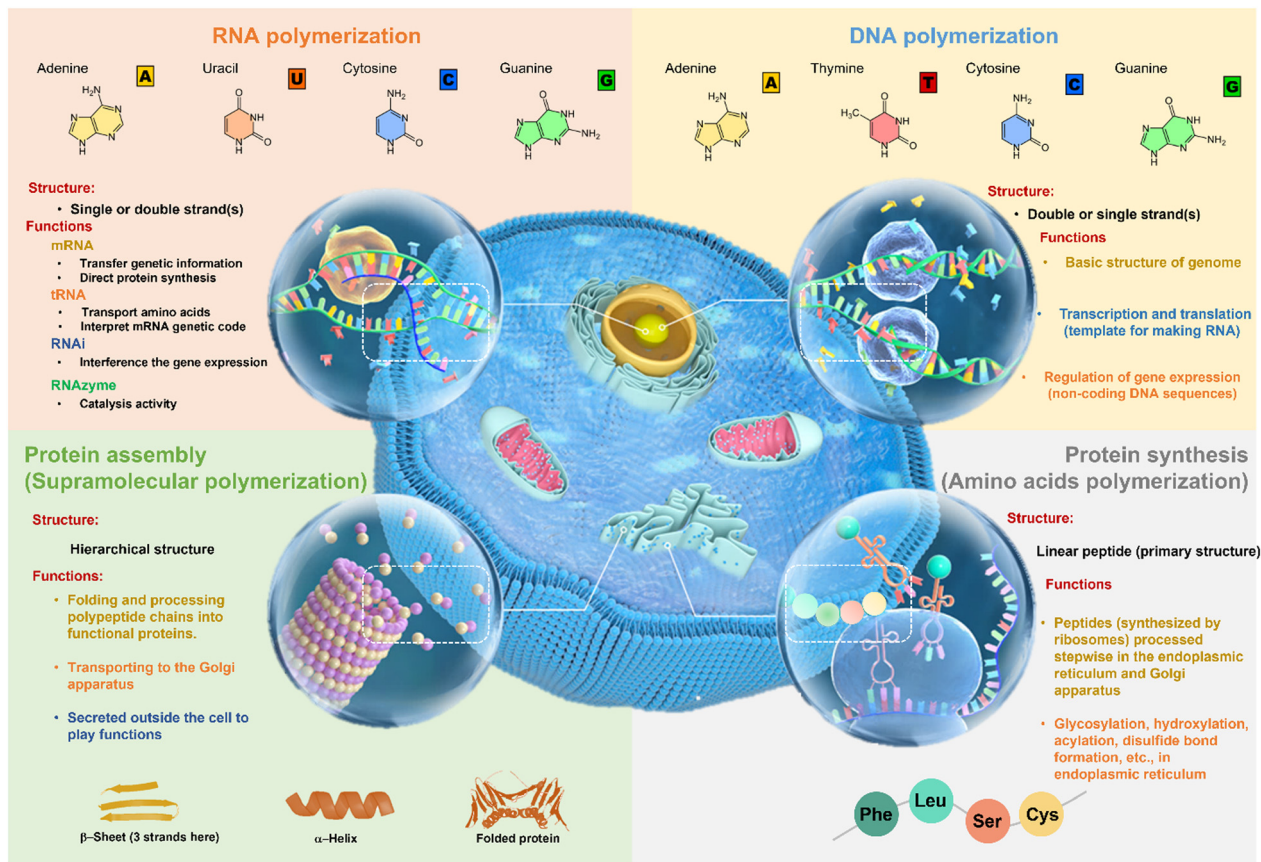


Fig. 1 Schematic diagram of covalent polymerization (RNA, DNA, and protein synthesis) and supramolecular polymerization (protein assembly) in nature.

methods for cell surface polymerization.<sup>41–46</sup> However, these approaches are often limited by low grafting ratios, inefficient cellular mass transport, signal transduction, and the excessive use of reactive polymers.<sup>47–50</sup> The “grafting-from” strategy, where polymers directly grow from the surfaces of cells, can enhance the polymer grafting rate, control polymer chain length and acquire functional block copolymers, thus greatly improving the efficiency of cell surface engineering without affecting cell functions.<sup>51</sup> Radical polymerization reactions are the most popular reactions for *in situ* polymerization on the cell surface. For example, photo-induced electron transfer-reversible addition-fragmentation chain-transfer (PET-RAFT) polymerization and atom-transfer radical polymerization (ATRP) have been extensively used to regulate the metabolic activity of cells. In addition, Pd-mediated cross-coupling reactions and cascade bioorthogonal reactions have attracted considerable scholarly attention in recent years.

For intracellular engineering, although some inorganic nanomaterials,<sup>52–55</sup> such as fluorescent quantum dots,<sup>56,57</sup> have been biosynthesized in cells, the explorations of *in situ* intracellular polymerization are relatively few due to some difficulties: (1) Monomers are hardly accumulated in living cells. (2) Polymerization is slow, which requires a long exposure time for cells to poison polymerization conditions. (3) Intracellular metabolic biomolecules, such as amino acids and dissolved oxygen, easily interfere with the polymerization reactions. (4) External stimuli-initiated polymerization reactions cannot be efficiently conducted

*in vivo* due to the poor tissue penetration capability of external stimuli, such as light. To date, a couple of polymerization reactions have been realized in living cells; however, much work needs to be carried out to fully utilize bio-polymerization.

Biomimetic polymer synthesis has been rapidly developed in the past five years, with remarkable advancements in methods to establish sophisticated sequence-controlled materials. These novel synthetic polymers provide unprecedented possibilities in different fields ranging from biomedical sensing to therapeutic delivery. This review comprehensively summarizes the progress in intra/extracellular polymerization for overcoming the present medical problems. By taking advantage of different biological or cellular characteristics, versatile polymerization processes, such as free radical polymerization, bioorthogonal polymerization, oxidative polymerization and supramolecular polymerization, are ingeniously designed. The sophisticated designs of polymerization reactions and the therapeutic mechanisms are discussed in detail. We also reveal the current limitations of polymerization in living organisms, and propose possible solutions and prospective future development directions, providing new thoughts for the research community.

## 2. Free radical polymerization

### 2.1 Atom-transfer radical polymerization (ATRP)

Achieved with transition metal catalysts, ATRP enables the equilibrium between active growing polymer chains and

dormant inactive polymer chains to obtain final products with controlled molecular weight and low dispersity. The inexpensive catalysts endow ATRP with high efficiency and feasibility. However, once the reaction conditions are transferred from a flask to an organism, problems arise: (1) The sensitivity of the reactions to oxygen and water inhibit the reaction efficiency inside the organisms. (2) The living organisms are likely to be affected by the toxic transition metal-based catalysts. It can be foreseen that the introduction of non-metallic catalysts and optimization of the initiation conditions will be significant directions for *in situ* ATRP inside the organisms in the future investigations.

**2.1.1 Extracellular ATRP initiated by the redox systems of microorganisms.** Bacteria can synthesize various polymers as extracellular matrices (ECMs) to encase and support their cellular communities. Although genetic engineering has been used to regulate the synthesis of ECM-related biopolymers, it will be better to expand the scope of natural ECMs to artificial polymers with “abiotic” chemistry. In fact, a range of cell-mediated polymerization reactions have been developed, although most of them require catalysts or harsh conditions, thus resulting in cytotoxicity or a complex synthetic process.<sup>58–61</sup> Based on the iron reducing system of bacteria, Rawson *et al.* synthesized well-defined polymers *via* ATRP under ambient conditions without

sacrificing bacterial viability (Fig. 2a, I).<sup>62</sup> Polymerization reactions were first conducted in the *Cupriavidus metallidurans* (*C. met.*) system in which poly(ethylene glycol) methyl ether methacrylate (PEGMA) monomers, 2-hydroxyethyl 2-bromoisobutyrate (HEBIB) and Fe<sup>III</sup>/Me<sub>6</sub>TREN were involved. <sup>1</sup>H NMR demonstrated that bacteria and the Fe<sup>III</sup> catalyst were indispensable for ATRP (Fig. 2a, II). Importantly, the bacterial viability was retained as high as 85% after polymerization, a value that was on a par with that of the control group with a viability of 80% (Fig. 2a, III), suggesting that the polymerization did not disturb the metabolism of bacteria. It was found that high concentration of bacteria and the catalyst increased the rate of polymerization (Fig. 2a, IV and V), while the low catalyst concentration increased the molar mass (M<sub>n</sub><sup>SEC</sup>) of polymers (Fig. 2a, VI), which verified that the initiation efficiency was high. Other monomers with hydrophilic and charged side chains could also be utilized as monomers for polymerization in bacterial solutions, indicating that this bacteria-initiated ATRP was tolerant to a series of monomers with different functionalities. Because the oxidation states of iron can be modulated by many bacterial strains, this strategy sets up a polymerization method with a high applicability to fabricate natural–synthetic hybrid conjugates and structures. Of note, live cells were the guarantee for the polymerisation to take place; further work in which devitalized cells regulate the polymerisation is expected to be given more

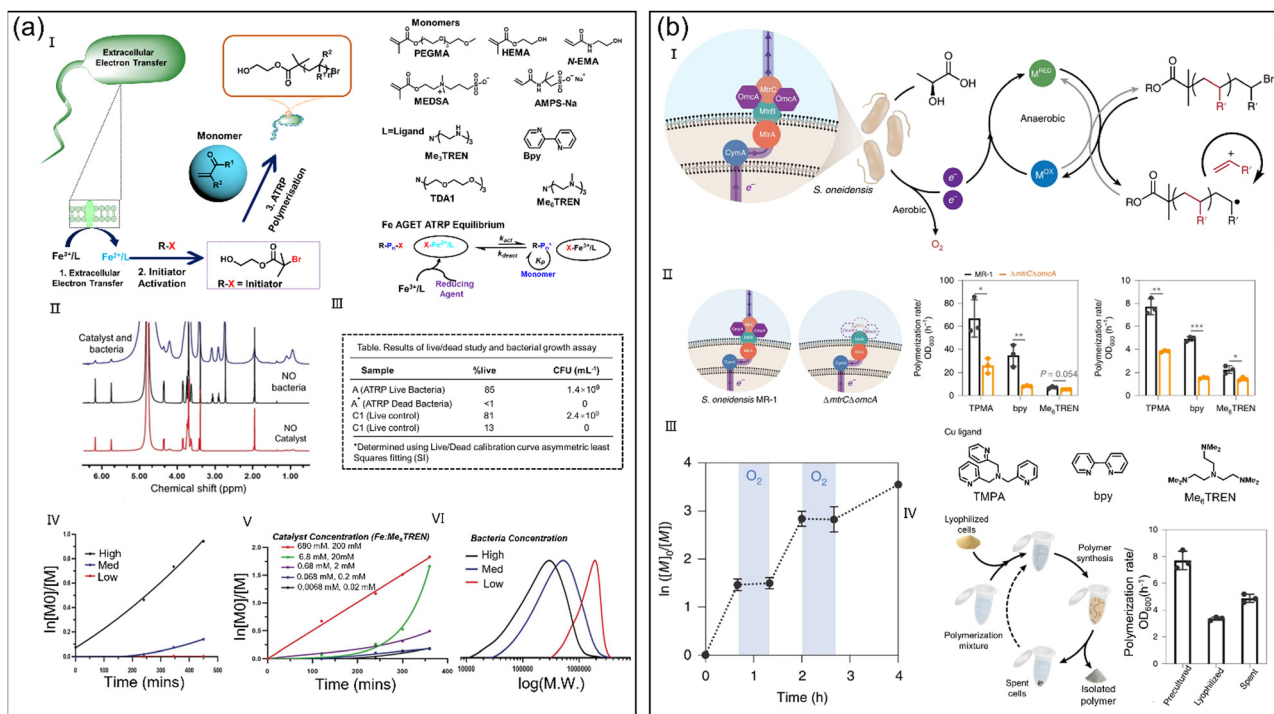


**Fig. 2** (a) Iron-catalyzed ATRP on bacterial surfaces. (I) Concept of iron-mediated ATRP based on the bacteria-initiated polymerization, and the structures of different monomers and ligands for the Fe catalysts. (II) <sup>1</sup>H NMR spectra of *C. met.*-initiated activator generated by electron transfer (ARGET) ATRP. (III) Results of live/dead staining and bacteria growth analysis. (IV) <sup>1</sup>H NMR kinetic graph of AGET ATRP involving different bacterial concentrations. (V) <sup>1</sup>H NMR kinetic graph of AGET ATRP involving different catalyst concentrations. (VI) Size exclusion chromatography overlay of polymers synthesized using different bacterial concentrations. Reproduced with the permission from ref. 62. Copyright 2019, Wiley-VCH Verlag GmbH & Co. KGaA, Weinheim. (b) Microbial metabolism-supported aerobic radical polymerization. (I) Mechanism of aerobic radical polymerization. (II) Comparison of polymerization rate between *S. oneidensis* and Δ*mtrCΔomcA* (*S. oneidensis* strain lacking *mtrC*) strain under different polymerization conditions. (III) Polymerization kinetics with or without oxygen bubbling. (IV) Comparison of polymerization rates among the precultured, lyophilized and spent MR-1 *S. oneidensis*-involved polymerizations. Reproduced with the permission from ref. 67. Copyright 2020, Springer Nature.

emphasis to broaden the applicability of bacteria-based polymerisation.

Although some radical polymerization reactions have been driven in open containers under ambient condition, the reactions usually prefer anaerobic environment and are restricted to the limited catalysts and monomers.<sup>63–66</sup> Inspired by the oxygen consumption capability of glucose oxidase (GOx) in recent living polymerization reactions, Keitz *et al.* utilized microbial aerobic respiration to initiate metal-catalyzed radical polymerization under aerobic conditions. The facultative *Shewanella oneidensis* (*S. oneidensis*, MR-1) regulated radical polymerization reactions under aerobic conditions through a two-step reaction: (1) depleting the dissolved oxygen by aerobic respiration and (2) conducting extracellular electron transfer (EET) to the metal catalysts to initiate the ATRP (Fig. 2b, I).<sup>67</sup> Under anaerobic and aerobic conditions, *S. oneidensis* was able to initiate free radical polymerization without pre-removal of oxygen. Of note, the polymerization efficiency was closely connected with the extracellular electron transfer protein-mediated anaerobic metabolism of *S. oneidensis* (Fig. 2b, II), and the polymerization rate remained high when a series of

metal catalysts and monomers even at a low concentration were utilized. Importantly, polymerization reactions withstood the repeated oxygen perfusions (Fig. 2b, III) and could be activated by the lyophilized and recycled cells (Fig. 2b, IV). This novel hybrid strategy of fermentative metabolism, aerobic respiration and the facultative properties of *S. oneidensis*, will surely provide new ideas for artificial polymerization reactions and improve the biosynthesis abilities of organisms. Although this work promotes the success of bacteria-based radical polymerization reactions in aerobic environments, the cytotoxic Cu-based catalyst is a concern. Obviously, radical polymerization reactions with a high biosafety under aerobic conditions are the priority for future investigations.

Although hybrid structures composed of synthetic polymers and living cells have exhibited brilliant cell-based applications, it is still highly challenging to perform polymerization on the surface of individual living cells as the polymerization conditions are always fatal to cells. Taking surface-initiated ATRP (SI-ATRP), for example, transition-metal catalysts, anaerobic conditions and organic solvents are culprits for the cytotoxicity of SI-ATRP. However, these cytotoxic threats can be circumvented, to

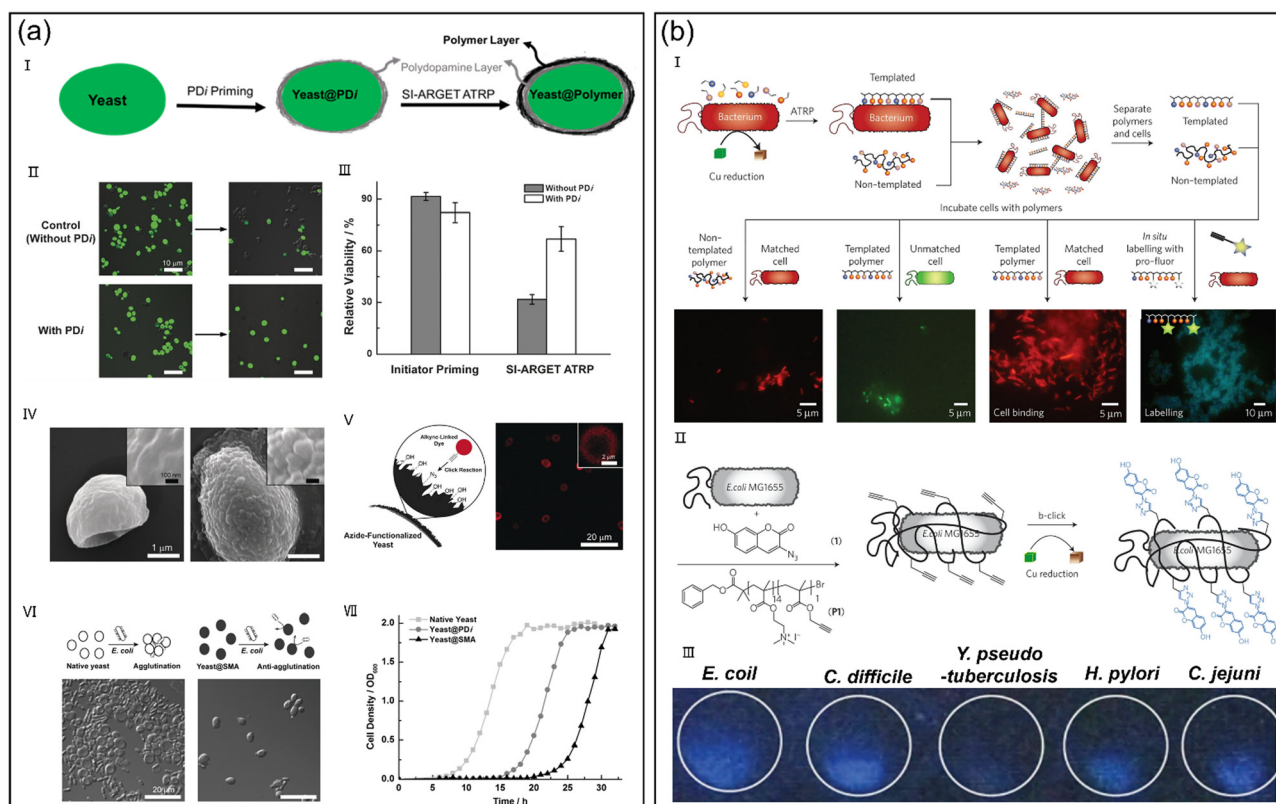


**Fig. 3** (a) PD-based SI-ARGET ATRP on individual yeast cells. (I) Schematic diagram of the cyto-compatible polymers growing from the surfaces of yeast cells. (II) Comparison of viability between the polymer-coated yeasts and native yeasts. (III) Quantitative results of II. (IV) SEM images of the native yeasts (left) and polymer-coated yeasts (right). (V) Confocal laser scanning microscopy (CLSM) image of the polymer-coated yeasts stained with red Alexa Fluor<sup>®</sup>594. (VI) Agglutination assay of the native yeasts and polymer-coated yeasts. (VII) Growth curves of different yeasts. Reproduced with the permission from ref. 68. Copyright 2016, Wiley-VCH Verlag GmbH & Co. KgaA, Weinheim. (b) Bacteria-directed polymer synthesis for microbial self-selective binding and labelling. (I) Schematic diagram of the bacteria-directed synthesis of polymer for matching homologous microbes. (II) Schematic diagram of *in situ* labelling of *E. coli* MG1655 via bacterial-instructed click polymerization. (III) Images revealing the efficient of *in situ* labelling to detect different pathogenic bacteria. Reproduced with the permission from ref. 49. Copyright 2014, Springer Nature.

a certain degree, by adopting ATRP using activators regenerated by electron transfer (ARGET ATRP). Reducing agents (e.g., ascorbic acid) used for ARGET ATRP can reduce Cu(II) to Cu(I), and thus a litter metal catalyst is needed. Moreover, ARGET ATRP is conducted in water under atmospheric conditions, making ARGET ATRP more compatible than traditional ATRP. Nevertheless, cytotoxic radical species generated by ARGET ATRP will attack living cells, possibly leading to a low viability during polymerization reactions. Choi *et al.* utilized the radical-depleting ability of polydopamine (PD) to fabricate cell-polymer hybrid materials based on SI-ARGET ATRP. PD-based layers not only blocked radicals generated during SI-ARGET ATRP, but also acted as ATRP macroinitiators (Pdi) for SI-ATRP (Fig. 3a, I).<sup>68</sup> After SI-ARGET ATRP on Pdi-primed yeast cells, negligible decrease in the viability of the yeast was monitored. However, an obvious cytotoxicity was observed in the control group (Fig. 3a, II and III), suggesting that the Pdi layer effectively reduced the peroxidation damage of the cell membrane. Scanning electron microscopy (SEM) revealed that the surface of the polymer-coated yeasts was rougher than that of native or Pdi-primed yeast cells (Fig. 3a, IV), confirming the generation of polymers on the cell surfaces. With the cooperation of fluorescent co-monomers and bioorthogonal chemistry, a polymer layer on the surface of yeast was obviously visualized (Fig. 3a, V). *E. coli* has abundant  $\alpha$ -D-mannose-binding protein on the cilium, which can trigger the formation of cell aggregates when mixed with yeasts. However, no cell clusters formed in the group with co-culturing yeast and *E. coli* (Fig. 3a, VI), indicating that the compact polymer layer of yeasts efficiently blocked their agglutination. In addition, cell-division activity was suppressed and the lag phase of yeasts was prolonged after polymer grafting (Fig. 3a, VII), indicating that the cytocompatible and highly dense polymers were formed on the surface of individual living cells. Considering the diversity of synthetic polymers, it is believed that grafting polymers on cell surfaces will generate a number of delicate cellular hybrids for various biomedical and biotechnological applications.

Traditional antibiotics have been highly effective in combating microbiological contamination, but the appearance of resistant strains is a growing concern. New methods that do not arouse drug-resistant strains are required.<sup>69</sup> The method of isolating bacteria strains away from the infective sites is attractive from a theranostic perspective.<sup>70,71</sup> Nevertheless, the specific binding of targeted bacterial strains is difficult, and the present practice needs costly “cold-chain” biological reagents, such as aptamers and antibodies, severely limiting their popularization in large areas. Inspired by the role of ECM containing complex macromolecules synthesized by bacteria to support cell communities, synthesis of ECM mimics through naturally metabolic pathways would be greatly advantageous for targeted binding bacteria. Alexander *et al.* exploited the redox systems of bacteria for the polymerization of acrylic monomers *via* a Cu(I)-mediated ATRP on cell surfaces (Fig. 3b, I).<sup>49</sup> In such a manner, the bacteria selected the matched binding monomers with them, and *in situ* grew disparate polymers on cell surfaces. The monomer composition of bacteria-instructed polymers was affected by the bacterial species, and the resulting polymers could specifically bind to the bacteria

which provided the template. Bacterial redox chemistry was also engaged to “click” fluorescent markers onto bacteria-directed polymers on the surface of various clinically isolated strains (Fig. 3b, II), permitting rapid and facile binding and imaging of pathogens (Fig. 3b, III). This cell-mediated chemistry utilizes ready-made materials that do not need cold-chain storage, which is more adaptable for routine laboratory settings. Meanwhile, many possible monomers have been applied in bacteria-supported ATRP reactions, indicating that further refining of binding specificity would be possible *via* judicious choice and diversification of polymer components. Therefore, it is believed that this method would, if developed well, create new platforms for bacteria-specific theranostic applications.

**2.1.2 Intracellular ATRP initiated by the synergistic effect of endogenous and exogenous reductants.** Cu(I)-catalyzed radical polymerization has been conducted in the physiological environment,<sup>72,73</sup> while Cu(I) agents and their ligands always induce cytotoxicity.<sup>74</sup> Meanwhile, the enrichment of Cu(I) catalysts in living cells is hard to control. Hence, it is hard for the current catalysts to balance the catalytic activity and cell viability. Wang *et al.* reported an intracellular radical polymerization reaction based on the *in situ* generated Cu(I) catalyst (Fig. 4a, I).<sup>75</sup> Under the dual-reduction effect of endogenous glutathione (GSH) and exogenous sodium ascorbate (NaAsc), Cu(II)-histidine complexes were *in situ* reduced into active Cu(I) catalysts in living cells. The generated Cu(I) catalysts then activated the alkyl bromide initiator (TEG-Br) and initiated the polymerization of acrylic monomers with designed functionalities. Owing to the fast uptake of catalysts and the high intracellular GSH concentration, a polymer with strong fluorescence was only observed in HepG2 cells (Fig. 4a, II). As expected, the polymerization of prodrug monomers (Acr-PTX) induced a high percentage of cell apoptosis and showed a high anticancer activity due to the prolonged retention time of poly-PTX (Fig. 4a, III). Compared with the easily effluted small-molecular drugs, the *in situ* polymerized drugs in tumor cells prolonged the circulation time and enhanced the drug efficacy. Therefore, these intracellular polymerization reactions doubtlessly offer many possibilities such as the methods to build cellular biosynthetic factories and new theranostic strategies to treat the cell-relevant diseases.

## 2.2 Reversible addition fragmentation chain transfer (RAFT) polymerization

Trithiocarbonate-based agents are added in RAFT polymerization as chain transfer agents to allow degenerate transfer, thereby reducing radicals to achieve controllable polymerization. In RAFT polymerization, polymers with relatively complex structures, integrated multi-functions, and precise molecular weights can be synthesized. Additionally, RAFT is less sensitive to the reaction conditions (even in the aqueous phase), which is the fundamental reason for the promising applications of RAFT polymerization inside the organisms.

**2.2.1 Extracellular RAFT polymerization initiated by the redox systems of microorganisms and light.** Prior research studies have concentrated on the metal reduction ability of bacteria (e.g., *C. metallidurans*, *E. coli* and *S. oneidensis*) to regulate

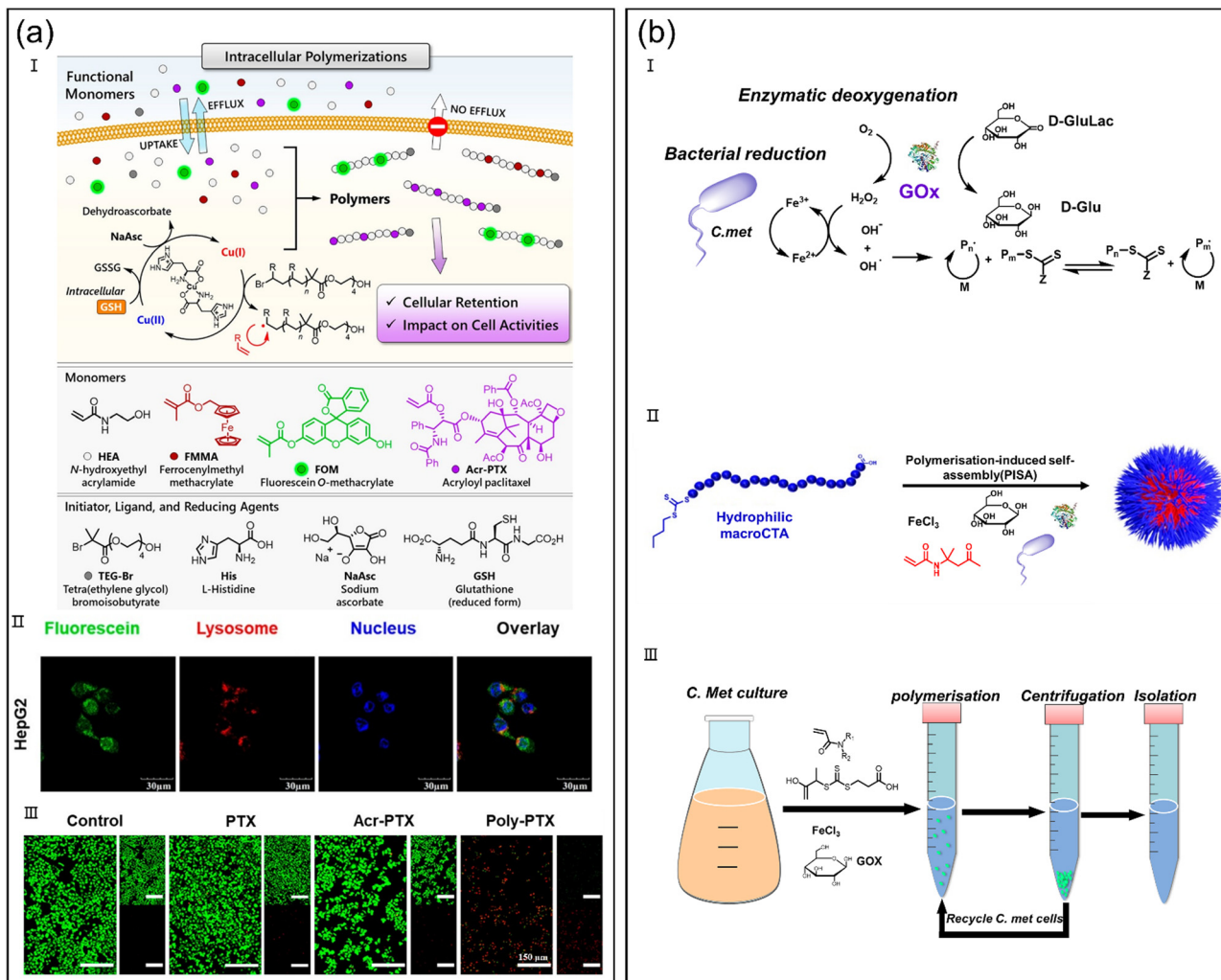


Fig. 4 (a) *In situ* Cu(I)-catalyzed intracellular radical polymerization for enhancing the apoptosis of cancer cells. (I) Schematic diagram of the Cu(I)-catalyzed intracellular radical polymerization reaction. (II) CLSM images of HepG2 cells showing Cu(I)-catalyzed radical polymerization. (III) Live/dead dual-staining of HepG2 cells after different treatments. Reproduced with the permission from ref. 75. Copyright 2021, American Chemical Society. (b) Oxytolerant RAFT polymerization triggered by living bacteria. (I) Schematic diagram of the GOx and bacteria-instructed Fenton reaction-assisted RAFT process. (II) Schematic diagram of bacteria-mediated polymerization-triggered self-assembly. (III) Schematic diagram of bacteria recycling. Reproduced with the permission from ref. 79. Copyright 2022, American Chemical Society.

metal-mediated ATRP.<sup>76</sup> However, these ATRP are easily affected by the bacterial-alternate initiation pathways.<sup>77</sup> In contrast, RAFT polymerization, an external radical-initiated polymerization, might be controlled more easily than cell-instructed ATRP, because radicals are readily available in many physiological environments.<sup>78</sup> Although various oxygen-tolerant RAFT polymerization reactions have been developed, none has been applied in bacterial media. Gurnani *et al.* presented a new bacteria-initiated oxygen-tolerant RAFT polymerization based on the Fenton reaction (Fig. 4b, I).<sup>79</sup> By utilizing the reducing ability of *C. metallidurans* CH34, Fe<sup>2+</sup> could be *in situ* formed from Fe<sup>3+</sup> that accelerated the generation of hydroxyl radicals to trigger the RAFT process. Inspired by its deoxidizing capacity, GOx was introduced to generate hydrogen peroxide *via* glucose feedstock, which then reacted with hydroxide ions to generate hydroxyl radicals to initiate the polymerization by the bacteria-triggered Fenton reaction. Although a poor blocking efficiency

was achieved when using the macromolecular chain transfer agent (macroCTA), RAFT polymerization traits, such as predictable molar masses, low dispersity and end-group fidelity were acquired. Importantly, successful preparation of nanoparticles was realized with the help of this polymerization-induced self-assembly, offering the possibility for future biomimetic extracellular vesicles (Fig. 4b, II). Interestingly, high monomer conversion was still achieved after three cycles using the original bacterial culture (Fig. 4b, III). This microbial RAFT polymerization method is a versatile method to generate well-defined polymers in living polymerization platforms with specific properties beyond those of chemosynthetic macromolecules.

Being able to realize spatio-temporal controllability and maintain the chain-end fidelity and the dispersity of radical polymerizations, PET-RAFT polymerization reactions have received great attention since 2014. Due to their great potential in biomedicine and “green” chemistry fields, photosensitizers with wideband and

near-infrared (NIR) absorption are superior for PET-RAFT polymerization.<sup>80–82</sup> Although some advanced photosensitizers have been developed to initiate RAFT polymerization reactions under a series of light sources, including blue, green, red light and natural sunlight, the requirement of non-aqueous solvent systems has not been violated.<sup>83</sup> Qiao *et al.* presented the first example using the self-assembly of carboxylated porphyrin (SA-TCPP) as a photosensitizer for NIR-mediated controlled radical polymerization reactions in an aqueous solution (Fig. 5a).<sup>84</sup> SA-TCPP showed a broad absorbance spectrum in the range of 300–950 nm, and the micro-fibre-shaped morphology extended the lifetime of the excited electron-hole pairs, thus significantly improving the efficiency of polymerization. The polymerization rate ranked from high to low in the order of white, blue, green, red and NIR light, which was in accordance with the absorbance of SA-TCPP. Importantly, PET-RAFT polymerization also successfully proceeded in mammalian fibroblast cells at the cost of cell viability, suggesting that in future, programmable multi-block polymerization reactions may be conducted in mechanized microliter injection systems after the problem of cell viability is solved. These biocompatible NIR-mediated controlled radical polymerizations are good pioneers for future *in vivo* biomedical polymerizations and “green” polymerizations.

Grafting synthetic polymers to cell surfaces offers potential to regulate cellular functions and expand the structural repertoire of cells. However, the conventional “grafting-to” strategies involving chemical or physical polymer conjugation are often

challenged by low grafting efficiency and the abuse of polymers. In contrast, “grafting-from” strategies in which the designed polymers directly grow from cell surfaces, display multiple advantages, such as enhanced grafting efficacy, controlled chain length and high adaptivity and specificity. Hawker *et al.* reported a cytocompatible “grafting-from” strategy to engineer living yeast and mammalian cells *via* PET-RAFT (Fig. 5b).<sup>40</sup> For yeast cells, a two-step method was first developed to conjugate chain-transfer agents (CTAs) onto cell surfaces. After surface-initiated polymerization, a strong purple fluorescence (Alexa Fluor 647) was observed around the cell surface of yeast cells Y2, suggesting that PET-RAFT successfully proceeded on the cell surface. Furthermore, there was distinct fluorescence arising from fluorescein diacetate in the cytoplasm, indicating the high viability of polymer-modified yeast cells. Without addition of tannic acid (TA) which can cross-link poly(ethylene glycol) (PEG) polymers *via* hydrogen bonding, few cell aggregates were observed, whereas considerable aggregated cells were monitored in the presence of TA, clearly demonstrating that cytocompatible polymer coatings exhibited feasible capability to control cell assembly and aggregation. Similar to yeast cells, an obvious Alexa Fluor 647 fluorescence emerged from the Jurkat cell surface after surface polymerization, confirming that polymers also efficiently grew from mammalian cell surfaces. In addition, high viability was also acquired for the polymer-anchored Jurkat cells, indicating that the active metabolism and intact cell membranes were maintained after polymerization. In comparison with

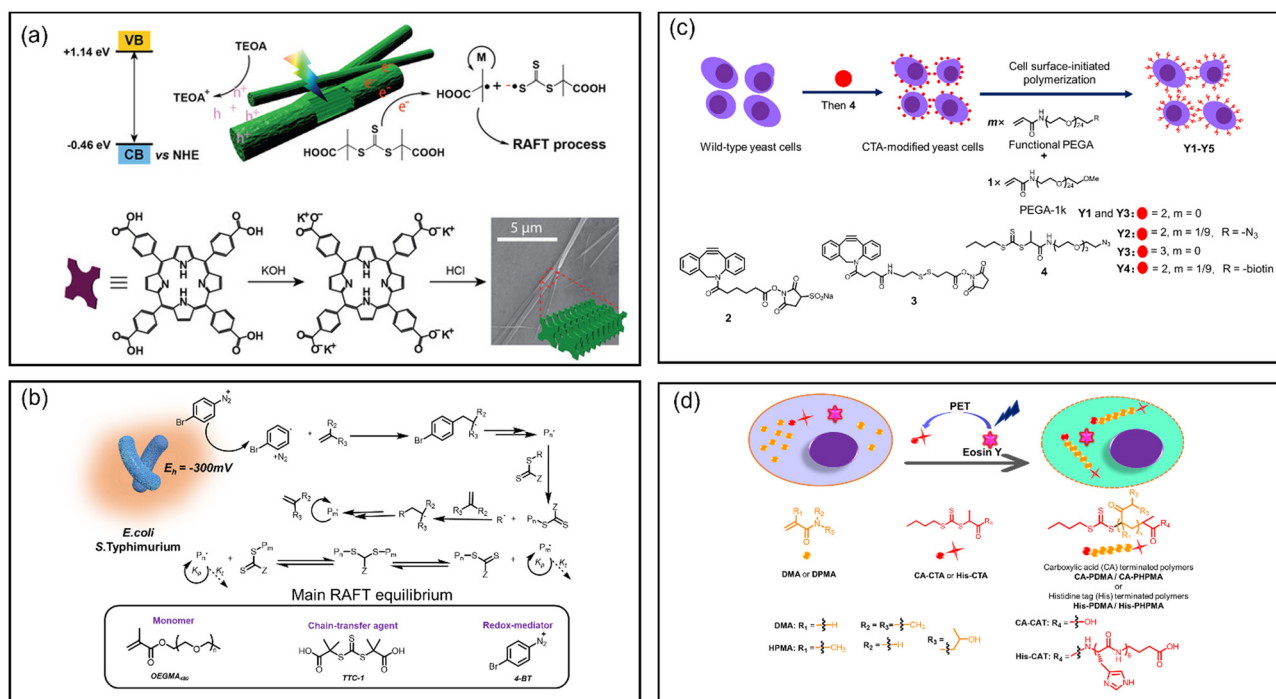


Fig. 5 (a) Synthetic route of SA-TCPP and the mechanism of SA-TCPP-catalyzed PET-RAFT polymerization reactions. Reproduced with the permission from ref. 84. Copyright 2020, Wiley-VCH GmbH. (b) Schematic diagram of the yeast cells modified with SI PET-RAFT. Reproduced with the permission from ref. 40. Copyright 2017, Springer Nature. (c) Controlled radical polymerization initiated by the terminal electron flux of *E. coli* and *S. Typhimurium*. Reproduced with the permission from ref. 86. Copyright 2020, American Chemical Society. (d) Schematic diagram of the intracellular PET-RAFT. Reproduced with the permission from ref. 89. Copyright 2022, American Chemical Society.

conventional “grafting-to” strategies, these “grafting-from” approaches not only greatly improve the grafting efficiency but also actively manipulate cellular phenotypes. Based on the diversity of functional polymers in this “grafting-from” strategy, a wide range of applications may be possible. For example, grafting high density glycopolymers to rewire signalling pathways and spatiotemporally controlling polymer distributions on cell surface to manipulate cell–cell interactions, *etc.*

Recently, construction of ELMs by harnessing the reducing power of bacteria has been developed, but the specific metal bio-reduction pathways and the cytotoxicity of metal catalysts are always involved.<sup>85</sup> Qiao *et al.* reported a metal-free biosynthesis strategy to initiate a “living” radical polymerization reaction, in which bacterial electron flux was captured to generate abiotic radical species (Fig. 5c).<sup>86</sup> Two bacterial species including *S. Typhimurium* and *E. coli* were utilized to reduce aryl diazonium salt (4-bromobenzenediazonium tetrafluoroborate, 4-BT) into aryl radicals near microbial membranes. The generated aryl radicals initiated “living” RAFT polymerization to synthesize vinyl polymers using methacrylate monomers. Multiple excellent polymerization features including high fidelity of chain-transfer agents, low dispersity and first-order chain growth were observed in the regulation of polymerization conditions, suggesting that this bacteria-facilitated polymerization was well controlled. In addition, it was demonstrated that the reduced contents in bacteria, such as metal ions with a low redox state and glutathione, facilitated transmembrane electron transfer and speeded up the reduction of 4-BT. Meanwhile, active metabolism was necessary for the sustained generation of radicals, guaranteeing the following “living” RAFT polymerization. The universal mechanism of redox equilibrium and the validity of the reducing environment of active bacterial cultures provides significant potential to extend this “living” radical polymerization to other microorganisms and replaceable redox-activated chemistry. Based on the performance of this “living” radical polymerization, hijacking microbial redox force to synthesize artificial polymers instead of reliance on the conventional metal-catalyzed polymerization reactions provides a new method for constructing ELMs at the abiotic/biotic interface.

**2.2.2 Intracellular light-triggered RAFT polymerization.** Photo-induced polymerization is developed rapidly and has been applied in a variety of medical and biological areas.<sup>87</sup> However, uncontrollable molecular weight of polymers is one practical issue for the photo-induced radical polymerization reactions. Attributing to the oxygen tolerance and special energy transfer mechanism, PET-RAFT polymerization can ensure polymers with predictable molecular weight<sup>88</sup> and narrow dispersity in the physiological environments. Geng *et al.* developed a “prodrug” system through the visible light-mediated intracellular RAFT polymerization to fight against cancer (Fig. 5d).<sup>89</sup> Under irradiation of visible light at 470 nm, PET-RAFT polymerization was initiated in HeLa cells treated with polymerization cocktails containing monomers, CTA and photosensitizer eosin Y. This intracellular polymerization changed a series of cell functions including cell cycle, apoptosis, necroptosis, cell proliferation and motility. It was important that the intracellular polymerization

greatly inhibited tumor growth, prolonged the survival of mice and suppressed tumor metastasis *in vivo*. There was no obvious change in body weight, hematological indexes and the histology of major organs, suggesting the high biosafety of this “polymeric prodrug” system. It can be concluded that a combination of “prodrug” monomers and intracellular targeted polymerization would be a new approach of cancer treatment, in which nontoxic monomers could be transformed into active polymers only at the irradiated site. This therapeutic strategy on the basis of molecular weight-controllable PET-RAFT polymerization will set a new direction for the directed and targeted cancer chemotherapy.

### 2.3 Other light-triggered free radical polymerization

Engineering a single cell surface with compact organic or inorganic shells is an appropriate way to protect them from the adverse environments and improve their tolerance to rigorous conditions.<sup>90,91</sup> Owing to their diverse structures and durable stability, chemical polymerization methods are considered more promising for cell surface modification. Although some mild reaction conditions have been adopted to preserve the cell viability during polymerization reactions, a toxic pretreatment or complicated process is always needed. Therefore, mild and simple polymerization strategies for cell surface engineering are urgently needed. Yang *et al.* developed a cytocompatible and facile strategy to construct polymeric shells with controllable thickness on living yeast cells based on a visible light-initiated polymerization (Fig. 6a, I).<sup>92</sup> Owing to the benign polymerization conditions, such as room temperature, oxygen resistance and visible light irradiation, the cell viability remained higher than 85% after polymerization (Fig. 6a, II and III), suggesting that the shell was not fabricated at the cost of cell viability. Because of the mechanical confinement of the poly(ethylene glycol) diacrylate (PEGDA) shell, cell division was retarded (Fig. 6a, IV) and could be flexibly regulated by the thickness of the PEGDA shell. Moreover, the PEGDA shell also greatly enhanced the tolerating ability of yeasts against lyticase-mediated lysis (Fig. 6a, V). Therefore, this simple and mild engineering approach provides a new concept for the shell functionalization *via* copolymerization.

Various artificial coating techniques have been engaged to endow organisms with additional functionalities and protection from hostile conditions.<sup>93–95</sup> However, a full coating or uniform coverage may inevitably block functional receptors on cell membranes, impairing their communication with surrounding cells, therefore partial or asymmetric coating is a more feasible surface modification approach.<sup>96–98</sup> Yang *et al.* developed a visible light-initiated graft polymerization for symmetric or asymmetric surface coating on individual yeast cells (Fig. 6b, I).<sup>99</sup> The degree of coating could be tuned by simply regulating irradiation time and density and high viability of yeasts was invariably retained (Fig. 6b, II). As expected, the yeast cells with polymer shells showed a delayed division and enhanced lysis resistance. In addition, obvious incomplete ellipse emerged on the PEGDA-decorated yeast cells (Janus-poly(PEGDA)-cells) after adding poly(sodium acrylate) (PAAS), suggesting PAAS was selectively introduced in the PEGDA-patched area of cell surfaces (Janus-PAAS-cells) (Fig. 6b, III).

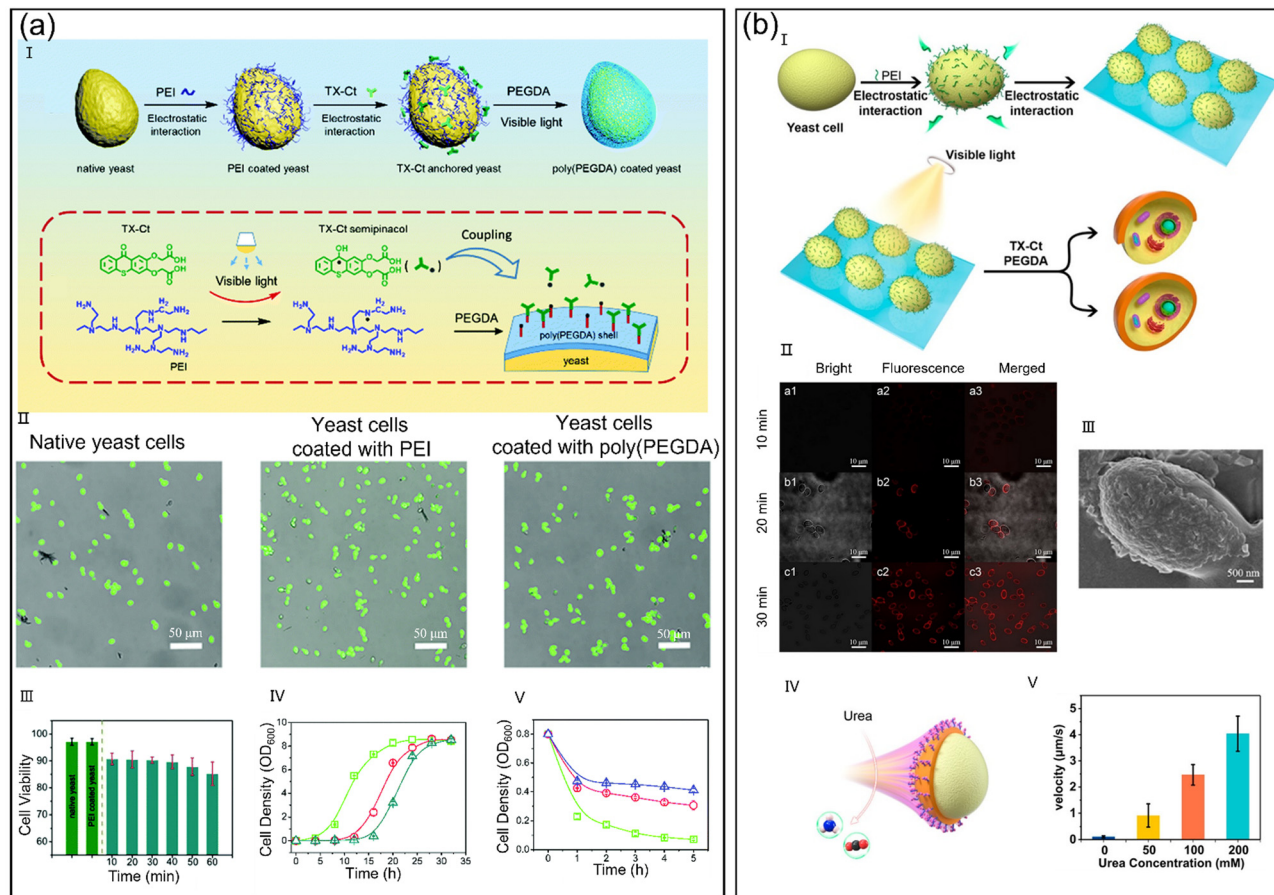


**Fig. 6** (a) Decorating yeasts with the controllable shell. (I) Mechanism of the visible light-initiated graft polymerization on the yeast surface. (II) CLSM images of different yeasts stained with fluorescein diacetate. (III) Cell viability of different yeasts. (IV) Growth curves of native ( $\square$ ) and poly(PEGDA)-coated yeasts with a 30 min polymerization ( $\circ$ ) or 60 min polymerization ( $\Delta$ ). (V) Survival curves of the native ( $\square$ ) and poly(PEGDA)-coated yeasts with a 30 min polymerization ( $\circ$ ) or 60 min polymerization ( $\Delta$ ) in the presence of lyticase. Reproduced with the permission from ref. 92. Copyright 2018, The Royal Society of Chemistry. (b) Coating individual cells partially/fully with polymer shells on yeast cells to obtain self-propelling ability. (I) Synthetic route of partially and fully coated yeast cells. (II) CLSM images of poly(PEGDA)-coated cells. (III) SEM photograph of Janus-PAAS-cell. (IV) Migrating mechanism of Janus-Urease-cells in urea solution with different concentrations. Reproduced with the permission from ref. 99. Copyright 2018, The Royal Society of Chemistry.

It was worth noting that the asymmetrically decorated yeast cells exhibited a strong self-propelling capability in the urea-containing fermentation broth by anchoring urease on the surface of Janus-PAAS-cells (Fig. 6b, IV and V). Considering the structural diversity of living graft polymerization and the loading functionality of the hydrogel layer, this flexible cell coating strategy provides great potential in multiple fields, such as cell therapy, cell-based advanced drug delivery, tissue engineering and biocatalysis.

Although fluorescent quantum dots<sup>100</sup> and inorganic nanomaterials have been successfully synthesized in human cells and microorganisms, radical polymerization in living organisms has rarely been reported and we still lack a deep understanding that how these endogenous polymers modulate cellular functions or track cells. Bradley *et al.* reported a light-mediated radical polymerization reaction for *in situ* polymer synthesis in cells using a series of monomers and a biocompatible initiator (Fig. 7a, I).<sup>101</sup> The monomer conversion of these polymerization reactions remained high in different media, such as  $\sim 50\%$  in

PBS and cell lysate, and  $\sim 68\%$  inside cells, suggesting that the complex cellular microenvironment rarely interfered with this radical polymerization. Furthermore, high viability was acquired for different cell lines even on the 7th day post-polymerization, indicating the good biocompatibility of these polymerization reactions. There was no obvious difference in the  $G_0/G_1$  and M phase for the cells, but a delayed S phase was observed (Fig. 7a, II), demonstrating that this intracellular polymerization affected the cell cycle. In addition, cell motility (Fig. 7a, III) and actin polymerization (Fig. 7a, IV) were also regulated by the cellular polymerization. Direct evidence for intracellular polymerization was obtained by using 4-styrenesulfonate (NaSS) as a monomer. Even after five passages, strong fluorescence signals were still observed in the polymerized cells (Fig. 7a, V), providing a possibility for long-term tracking of the implanted cells. After incubating HeLa cells with ferrocenylmethyl methacrylate (FMMA) monomers, spherical nanoparticles with a diameter of 50–70 nm were observed both in the cytoplasm and nucleus (Fig. 7a, VI), suggesting that FMMA not only crossed the cellular

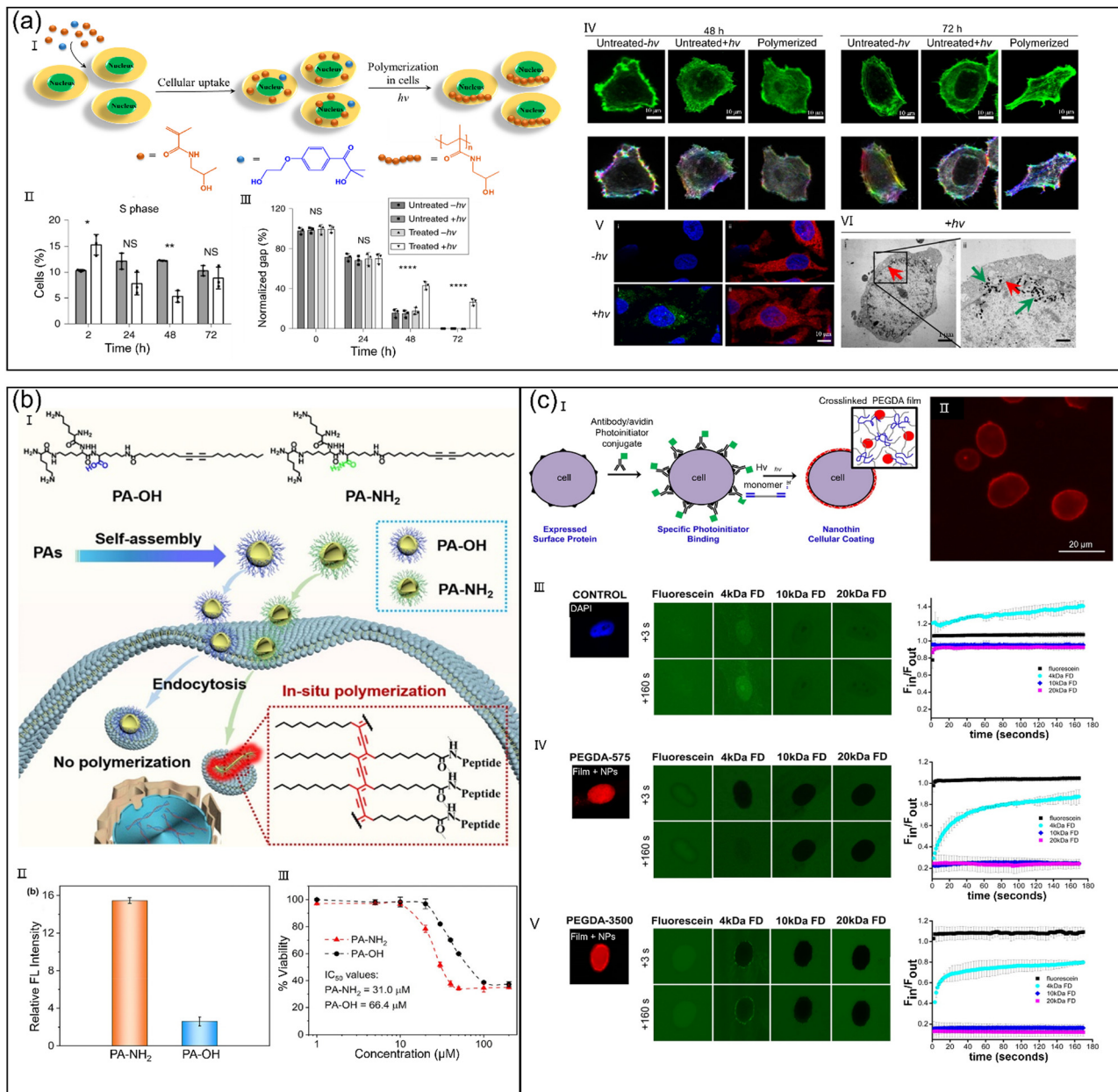


**Fig. 7** (a) Light-mediated radical polymerization for manipulating, tracking and controlling cellular behavior. (I) Illustration of intracellular polymerization. (II) Changes of the S phase over time after photopolymerization. (III) Normalized gaps vs. time. (IV) CLSM images of HeLa cells after different treatments. (V) CLSM images of HeLa cells displaying the intracellular photopolymerization of NaSS. (VI) Transmission electron microscopy (TEM) images of HeLa cell showing the intracellular photopolymerization of FMMA. Reproduced with the permission from ref. 101. Copyright 2019, Springer Nature. (b) Electrostatically controlled polymerization of diacetylene-conjugated peptide amphiphiles in living cells. (I) Illustration of the extracellular self-assembly and intracellular polymerization of DPAs. (II) Relative fluorescence intensity of HeLa cells treated with PA-OH and PA-NH<sub>2</sub>. (III) Viability of HeLa cells treated with PA-OH and PA-NH<sub>2</sub>. Reproduced with the permission from ref. 110. Copyright 2022, American Chemical Society. (c) Coating ultrathin hydrogel on cell surface through photo-polymerization for cellular immunoprotection. (I) Schematic diagram of antigen-specific photo-polymerization to coat nanothin hydrogels on cell surfaces. (II) Fluorescent image of Jurkats coated with PEGDA film. (III–V) Quantity analysis of different molecular diffusions through different nanoscale coatings. Reproduced with the permission from ref. 50. Copyright 2015, American Chemical Society.

membrane, but also penetrated into the nucleus. Using light-mediated polymerization reactions to synthesize new-to-nature polymers in living cells paves a new way for intracellular engineering where the *in situ* formed functional polymers can be applied in controlling cytoskeleton functions, fluorescence imaging and cellular motility. The applicability and potential power

of this approach permits us to add intracellular synthetic macromolecules into a toolkit of cyto-compatible chemistries and further intracellular polymerization exploration promises to be a great adventure.

Peptide amphiphile (PA)-constructed biomaterials have been broadly used in diverse fields of biomedicine, such as

biosensors, drug delivery and tissue engineering.<sup>102–107</sup> Importantly, the biofunctionalities of PAs are closely related with their supramolecular assembling behaviors, and therefore a deep understanding of the assembly mechanism of supramolecular architectures is crucial for the applications of peptide biomaterials.<sup>108,109</sup> Jiang *et al.* reported two kinds of diacetylene-containing peptide amphiphiles (DPAs) (zwitterionic PA-OH and cationic PA-NH<sub>2</sub>), which exhibited entirely different polymerization behaviors in living cells and aqueous solution (Fig. 7b, I).<sup>110</sup> For example, PA-NH<sub>2</sub> did not undergo polymerization in a series of aqueous solutions owing to the irregular arrangement of diacetylene chains but finished *in situ* polymerization in response to the microenvironment of tumor cells. In contrast, PA-OH accomplished the polymerization in aqueous solution, but not in cells (Fig. 7b, II). Because of the higher positive charge and intracellular polymerization of PA-NH<sub>2</sub>, PA-NH<sub>2</sub> achieved a lower half inhibitory concentration (IC<sub>50</sub>) than that of PA-OH (Fig. 7b, III), serving as a potential anticancer agent. This work not only provides indications on the relationship between the charge characters of PAs and their polymerization behaviors, but also demonstrates that diacetylene-containing PAs with the polymerizing capability in cells can serve as a highly effective anticancer agent.

For cell replacement therapy, exogenous cells are encapsulated in hydrogels to prevent the recognition of immune biomacromolecules but allow the free entry and exit of small molecular weight nutrients and water.<sup>212</sup> Therefore, hydrogel coatings with size selectivity are the key for cell transplantation therapy. Berron *et al.* developed a free-radical polymerization reaction to coat ultrathin hydrogel films on mammalian cell surfaces, realizing the selective transport of small molecular nutrients (Fig. 7c, I).<sup>50</sup> Photoinitiators with a low concentration were first grafted on the cell surface, and thus the subsequent restricted chain growth induced a thin polymer coating (Fig. 7c, II). These thin hydrogel films displayed similar size-selective behaviors to the corresponding bulk hydrogel materials, and the lower thickness led to a higher flux of species with a low molecular weight (Fig. 7c, III–V). Hence, in the post-transplantation cellular environment, it is expected that the delivery of vital small nutrients across the gellified cell membrane is slightly affected while host immune response is efficiently prevented. Because cells are engineered in the solution, the cell suspension can be injected into target tissues in a less invasive manner than the conventional cross-linked cell scaffolds with a large bulk, potentially shortening the recovery time and decreasing the frequency of cell therapy.

### 3. Bioorthogonal polymerization

#### 3.1 Extracellular bioorthogonal polymerization

Although linear polymers have been engineered on the surface of yeasts and even mammalian cells, the limited sorts of monomers and uncontrollable structures of polymers are still the challenges. With the help of bioorthogonal chemistry, Lilienkamp *et al.* synthesized dendrimers *in situ* on the cell surface, exponentially amplifying the signals of fluorescent markers anchored on the surface of antibody-targeted living

cells (Fig. 8a).<sup>111</sup> Three bioorthogonal building blocks 5–7 were designed. 5 possessed an NHS ester unit and three aldehyde groups, in which the NHS ester unit was used to conjugate the primary amines (*e.g.*, antibody herceptin, Her-1), whereas three aldehyde groups acted as bioorthogonal units for hydrazide ligation. The branched building block 6 consisted of an aminoxy unit and three norbornene motifs could be amplified to nine norbornenes after aminoxy/aldehyde reaction with 1 (Her-2). Building block 7 containing a tetrazine unit and two aldehyde groups could be grafted to Her-2 to construct Her-3 with the aid of the inverse electron-demand Diels–Alder (IEDDA) reaction. The final antibody dendrimer Her-4 was obtained by labelling fluorescein hydrazide 8 on Her-3. After three-generation amplification from Her-1 to Her-4, the fluorescence intensity of Her-4-bearing SK-BR-3 cells increased by 4.6-fold compared with the cells stained with FAM-Her (fluorescein-conjugated Herceptin), suggesting that the bioorthogonal “swarming” was successfully achieved on cells. This novel “swarming” strategy provides a new method to conjugate artificial chemical structures on mammalian cells, and the formation of nanostructures paves a new way to form artificial cellular organisms for regulating cellular behaviors.

Owing to the similar mechanical properties with many substances in living systems, hydrogels have been applied to encapsulate and stabilize many biological entities, such as oligonucleotides, proteins and living cells.<sup>112–115</sup> However, precisely controlled release of biological objects is a crucial challenge in these applications. Although some acid-degradable hydrogels have been recently reported by utilizing copper(i)-catalyzed azide–alkyne cycloaddition (CuAAC)<sup>116</sup> and free radical cross-linking,<sup>117</sup> sensitive biomolecules are hardly encapsulated by these hydrogels, attributed to the cytotoxicity of metal ions and free radicals.<sup>118</sup> Combining the droplet-based microfluidics and bioorthogonal strain-promoted azide–alkyne cycloaddition (SPAAC), Haag *et al.* fabricated a series of pH-responsive microgels for living cells (Fig. 8b).<sup>119</sup> Cytocompatible poly(ethylene glycol)-dicyclooctyne (PEG-DIC) and dendritic poly(glycerol azide) (dPG) were utilized as bioinert macromonomers. Azide groups were covalently connected to dPG *via* changing the substituted acid-sensitive benzacetal linkers, realizing accurate control of release kinetics in the pH range of 4.5–7.4. Integrating the bioorthogonal encapsulation with the pH-controlled release, an on-demand release of encapsulated cells was achieved without impact on cell activity and viability. Thus, these microgel particles can be applied for short-term cell encapsulation, permitting the cells to be manipulated and studied during encapsulation and eventually be isolated and collected *via* the decomposition of microgel scaffolds.

Seiffert *et al.* prepared hydrogel particles with micrometer-size and cell-laden ability through a combination of droplet-based microfluidics (technically) and bioorthogonal bioinert polymers (chemically) (Fig. 8c).<sup>120</sup> The gelation of microgels was realized through the thiol-ene click reactions between dithiolated PEG and acrylated hyperbranched PG without any initiator. The microgel properties were systematically investigated through simply varying the molecular weights and concentrations of macromonomers, to deeply understand the impacts to the proliferation

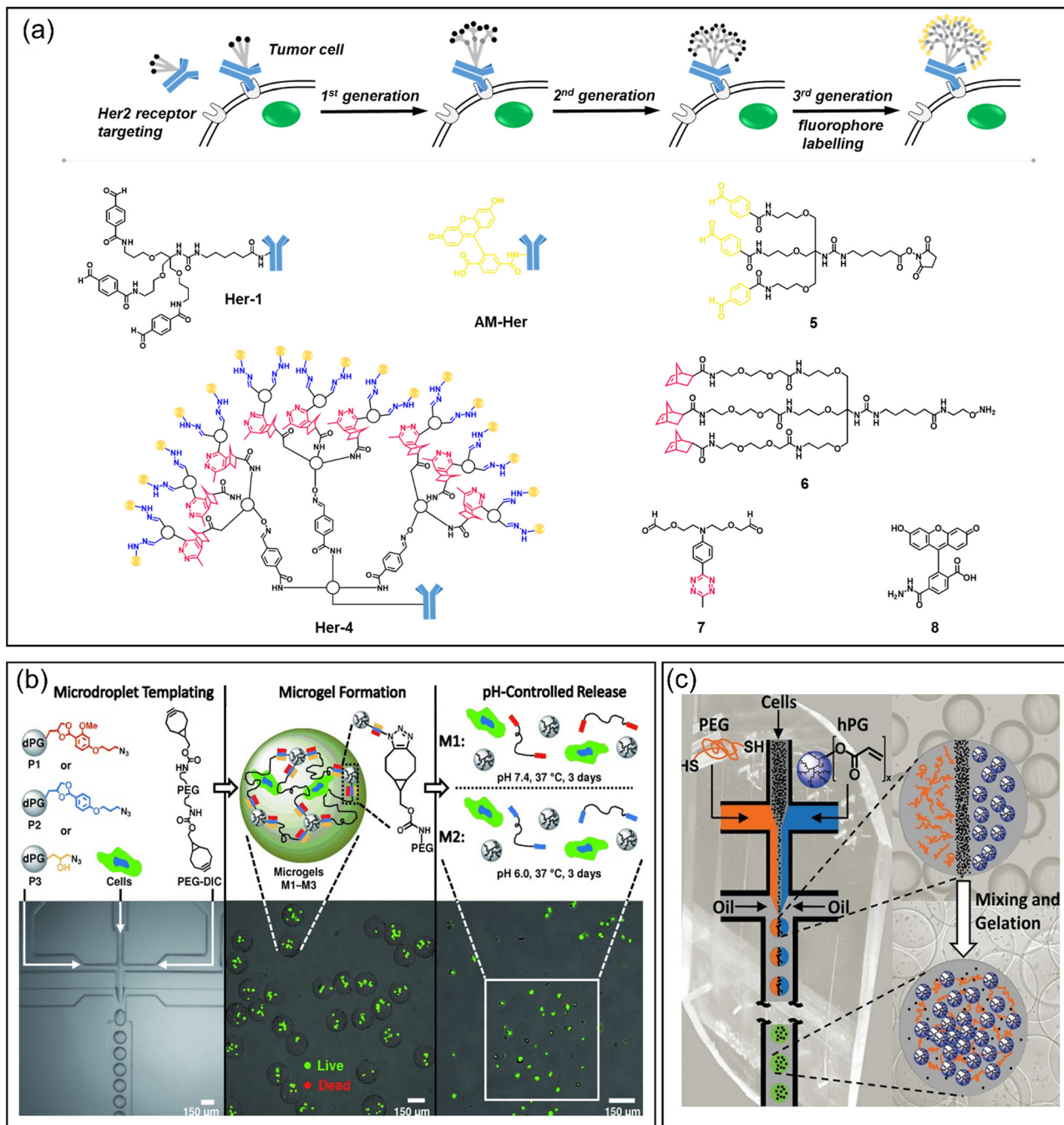


Fig. 8 (a) Concept of bioorthogonal "swarming" on the cell surface and the chemical structures of building blocks 5–8. Reproduced with the permission from ref. 111. Copyright 2020, American Chemical Society. (b) Microgel strategy for bioorthogonal encapsulation of living cells and following pH-controlled release. Reproduced with the permission from ref. 119. Copyright 2013, Wiley-VCH Verlag GmbH & Co. KGaA, Weinheim. (c) Droplet microfluidics-controlled radical-free gelation for the preparation of cell-laden microgels. Reproduced with the permission from ref. 120. Copyright 2012, American Chemical Society.

and viability of these encapsulated yeast and mammalian cells. Further optimization of cell-laden microgel structures could be achieved *via* integrating droplet-based microfluidic technologies for single cell encapsulation followed by the fluorescence-activated classification to separate living cell-containing microgels from dead cell-containing microgels.

*Staphylococcus aureus* (*S. aureus*) infection is one of the principal reasons for numerous severe epidemic diseases

including bacteraemia, osteomyelitis and pneumonia.<sup>121</sup> Early and rapid detection of *S. aureus* infection can be treated directly, to reduce the abuse of antibiotics and harness long-term beneficial results.<sup>122</sup> The diagnostic approaches of *S. aureus* on tissue biopsies or blood sample analyses are time-consuming, complicated and invasive procedures.<sup>123,124</sup> Benefiting from the merits of low cost, easy operation, real-time, non-invasiveness and superb sensitivity, fluorescence

imaging represents one of the most hopeful techniques for diagnosis of bacterial infection.<sup>125</sup> The “turn-on” probes display a better sensitivity than the traditional “always-on” probes when considering signal-to-noise ratios,<sup>126</sup> yet rare “turn-on” fluorescence probes have been exploited for real-time monitoring of *S. aureus* infection. Liang *et al.* developed an NIR fluorescence probe Cys(StBu)-EDA-thioketal-Lys(Cy5.5)-CBT (TK-CBT) that assembled into fluorescence-quenched TK-CBT-NPs through

the supramolecular polymerization driven by noncovalent interactions, including hydrophobic interaction and  $\pi$ - $\pi$  stacking (Fig. 9a).<sup>127</sup> The disulfide bond of TK-CBT-NPs could be oxidated through the elevated reactive oxygen species (ROS) in *S. aureus*-tainted macrophages, leading to the disintegration of TK-CBT-NPs, thus turning on the NIR fluorescence for real-time detection of *S. aureus* infection in cells and animals. It is expected that TK-CBT-like “turn-on” NIR probes may be used to clarify the

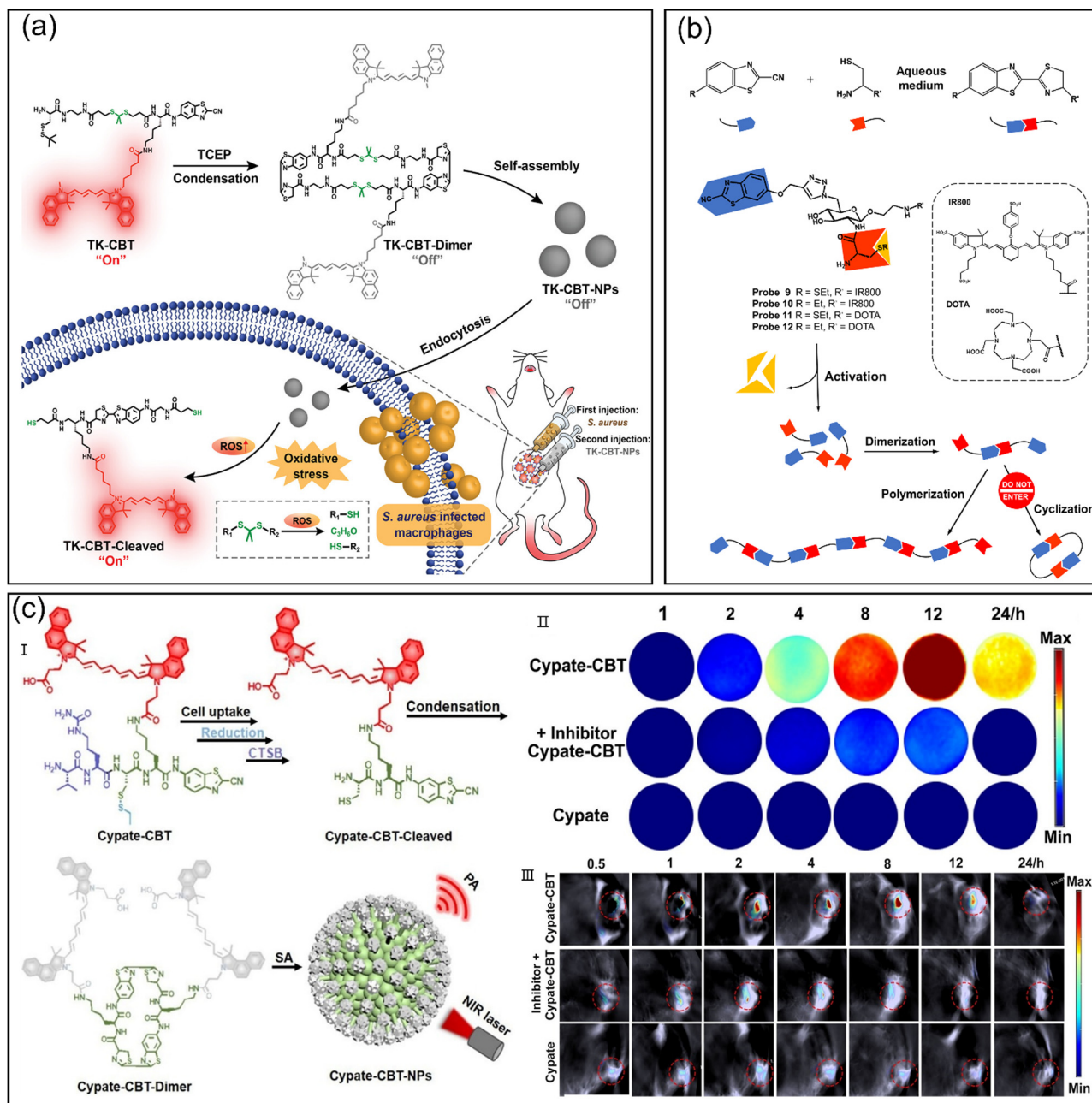


Fig. 9 (a) Fluorescence imaging of *S. aureus* infection based on the ROS-responsive disassembly of nanoparticles formed from bioorthogonal polymerization. Reproduced with the permission from ref. 127. Copyright 2022, Wiley-VCH GmbH. (b) Illustration of reduction-triggered bioorthogonal polymerization. Reproduced with the permission from ref. 131. Copyright 2020, American Chemical Society. (c) GSH and cathepsin B-triggered cypate nanoparticles formation for PA imaging. (I) Illustration of the GSH and cathepsin B-activated self-assembly of cypate nanoparticles. (II) Time-course PA imaging of MDA-MB-231 cells treated with cypate-CBT, inhibitor + cypate-CBT or cypate. (III) Time-course PA imaging of the mice bearing MDA-MB-231 tumor injected with cypate-CBT. Reproduced with the permission from ref. 137. Copyright 2021, Wiley-VCH GmbH.

mechanism of biological pathology in ROS-related theranostics and to diagnose the clinical *S. aureus*-infected diseases in near future.

### 3.2 Intracellular bioorthogonal polymerization

Bioorthogonal reactions have been used to assemble macromolecules in complex physiological environments. However, bioorthogonal units with stimuli-responsiveness are rare, because they are not easily biochemically masked. Although some enzymes or light-modulated bioorthogonal reactions<sup>128–130</sup> have been realized *in vitro*, their *in vivo* applications are rarely reported. Rao *et al.* used a reductase-responsive cyanobenzothiazole (CBT)–cysteine condensation to *in situ* synthesize polymers *in vivo* (Fig. 9b).<sup>131</sup> Cysteine and CBT units were respectively linked to the C2 and C6 positions of equator-configurational  $D$ -glucosamine *via* peptide bonds and click reaction, in which  $D$ -glucosamine served as a rigid backbone to form linear polymers. After cleavage of disulfide bonds on cysteine in a reducing environment, free N-terminal cysteine moieties were released and CBT–cysteine condensation reactions were immediately initiated. Aqueous solution containing GSH was first injected subcutaneously in the back of mice to form a locally reductive microenvironment at two spots, and then probes 9 and 10 were injected. Fluorescence signals arising from probe 9 significantly decreased within the first 0.5 h owing to the aggregation-caused quenching (ACQ) effect of the formed polymers, and the intensity became brighter afterwards. In contrast, the fluorescence of probe 10 showed a maximum at 0.5 h, while it subsequently decreased due to their diffusion effect, indicating that *in situ* assembled polymers prolonged the retention time of probe 9. Different from fluorescence imaging, the photoacoustic (PA) imaging signal from probe 9 increased in the initial 0.5 h and remained strong even after 24 h; nevertheless the PA signal of probe 10 could not be detected after 24 h, demonstrating that the GSH-catalyzed bioorthogonal reactions indeed triggered the polymerization process in mice, and the PA signal of GSH-activated tumor injected with probe 9 reached the peak at 4 h post-injection. Notably, it is the fluorescence signal from the polymer which intensified at 0.5–1 h post-injection. Furthermore, the PA signal around tumor was intense even after a whole day, but the fluorescence signal faded away rather fast, which further proved the effectiveness of *in situ* polymerization in living mice. Inspired by this GSH-activated bioorthogonal polymerization *in vivo*, other smart stimuli-responsive bioorthogonal systems may be put into practice in living organisms based on other stimuli, such as enzymatic activity in tumor tissues.

Because there is a big difference in the 5-year survival rate of cancer patients at early stages and late stages, early diagnosis of tumors plays an extremely important role in cancer therapy.<sup>132</sup> Cathepsin B (CTSB) is overexpressed at early stages of numerous tumors; thus it is considered as a potential biomarker for the early cancer diagnosis.<sup>133</sup> Precise monitoring of the CTSB expression will provide useful information for the early detection of tumors.<sup>134</sup> With high spatial resolution and prominent tissue-penetrating depth, PA imaging has been regarded as a promising and noninvasive imaging modality to screen early stage tumors.<sup>135</sup> Although the fluorescence of most imaging

agents is often quenched after aggregation owing to the ACQ effect, their PA signal displays an amusing aggregation-induced enhancement,<sup>136</sup> which can combine intracellular self-assembly to provide an “off-on” fluorescence method for detection of CTSB activity *in vivo*. Liang *et al.* developed a CTSB-activatable PA probe Val-CitCys(SET)-Lys(cypate)-CBT (cypate-CBT), which polymerized into cypate nanoparticles (near infrared fluorophore) through a supramolecular way after GSH reduction and CTSB catalysis inside tumor cells (Fig. 9c, I).<sup>137</sup> These nanoformulations showed unparalleled advantages for monitoring of CTSB activity with high specificity and sensitivity (Fig. 9c, II). Attributed to the enhanced intracellular accumulation, the cypate-CBT probe exhibited a nearly 5-fold enhancement of PA signals in CTSB-overexpressed tumor cells or solid tumors (Fig. 9c, III), showing a potential for clinical diagnosis of early tumors. It is expected that this intelligent cypate-CBT probe could be used as a PA agent to diagnose CTSB-overexpressing tumors at early stages with a high precision and sensitivity in clinics after reasonable refinement.

## 4. Oxidative polymerization

### 4.1 Extracellular chemical oxidative polymerization

Being able to meet the requirements of waste water treatment and sustainable energy production simultaneously, microbial fuel cells (MFCs) which utilize the metabolic activity of exoelectrogenic bacteria strains to gather electric energy from organic matrix, have drawn increasing attentions recently.<sup>138</sup> However, some bacterial cells cannot come in close contact with conductive materials, thus resulting in a low efficiency of EET.<sup>139</sup> *In situ* coating conjugated polymers on bacteria is expected a promising strategy to address this issue, as such an arrangement will permit the efficient electron transportation from inner bacteria to the electrode. Zhang *et al.* coated conductive polypyrrole on the surface of several bacteria through an *in situ* oxidative polymerization process. In detail, bacteria including *E. coli*, *S. oneidensis MR-1*, *Ochrobacterium anthropic* and *Streptococcus thermophilus* were tried using this method.<sup>140</sup> Enhanced conductivities (Fig. 10a, I and II) were acquired from all of these coated bacterial species without impairing their viability (Fig. 10a, III), indicating the general applicability of this *in situ* polymerization method. Polypyrrole, as conductive polymer, was coated on the surface of *S. oneidensis MR-1*, and this coating material was used as the anode of the MFC. It was found that not only the facilitated EET between electrogens and electrodes was highly enhanced (Fig. 10a, IV–VI), but also cell viability was improved. It is believed that this cell-surface modification provides not only a new direction for developing high-performance anodes in MFCs but also a good start for their application in microbial electrochemical systems.

*In situ* coating of polypyrrole on the surface of microorganisms not only improves the efficiency of extracellular electron transfer, but also provides great promise to regulate their biology catalytic activity.<sup>141,142</sup> Wang *et al.* endowed thermally-sensitive *Aspergillus oxyzae* (Asp cells) with photo-sensitivity *via* coating a layer of photothermal polypyrrole clothing on their surfaces.<sup>143</sup>

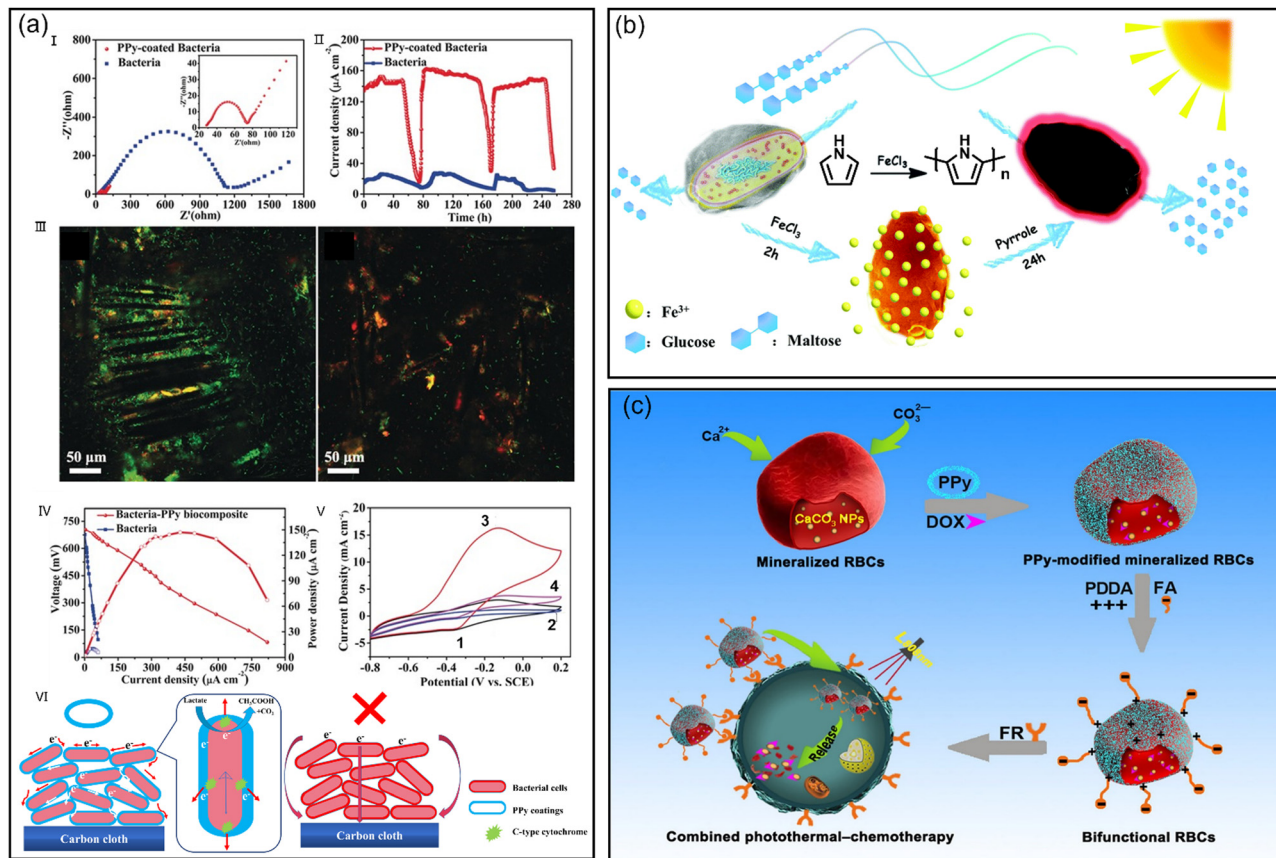


**Fig. 10** (a) Individual bacteria coated with polypyrrole generated *in situ* for enhancing their conductivity without impairing viability. (I) Nyquist curves of native *S. oneidensis* MR-1/CC electrodes and PPY-coated *S. oneidensis* MR-1/CC electrodes. (II) Current density of MFCs equipped with different anodes. (III) CLSM images of native *S. oneidensis* MR-1/CC electrodes (right) and PPY-coated *S. oneidensis* MR-1/CC electrodes (left). (IV) Power-density curves and polarization of MFCs equipped with distinct electrodes. (V) Current–voltage curves with (curves 3 and 4) and without (curves 1, 2) turnover current for MFCs with native *S. oneidensis* MR-1/CC electrodes (curves 2 and 4) and PPY-coated *S. oneidensis* MR-1/CC electrodes (curves 1 and 3). (VI) Schematic diagram of the EET mechanism of the native *S. oneidensis* MR-1/CC anode (right) and PPY-coated *S. oneidensis* MR-1/CC anode (left). Reproduced with the permission from ref. 140. Copyright 2017, Wiley-VCH Verlag GmbH & Co. KGaA, Weinheim. (b) Coating photothermal cloth on fungus for improving their solar activation. Reproduced with the permission from ref. 143. Copyright 2020, The Royal Society of Chemistry. (c) Intra/extracellular dual-modified red blood cells for synergistic photothermal and chemotherapy. Reproduced with the permission from ref. 145. Copyright 2020, Elsevier B.V.

The production and catalytic activity of  $\alpha$ -amylase from *Asp* cells were obviously enhanced under the irradiation of solar light (Fig. 10b). Attributing to the low cost, biocompatibility and non-contact modulation, this photothermal modification strategy offers a great promise for coating living cell–polymer hybrid structures on microorganism systems to improve their low-temperature environmental adaptation.

Except for extracellular surface modification, formation of nanomaterials inside cells is also a novel approach to adjust cellular functions.<sup>144</sup> Yang *et al.* reported an extra/intracellular dual-modified strategy based on the red blood cell (RBC) template to realize synergistic photothermal-chemotherapy.<sup>145</sup>  $\text{CaCO}_3$  nanoparticles were first generated in RBCs *via* the mineralization of  $\text{Ca}^{2+}$  and  $\text{CO}_3^{2-}$  followed by extracellular pyrrole oxidative polymerization (PPy) and folic acid (FA) modification, finally establishing a  $\text{CaCO}_3@RBC@PPy\text{-FA}$  structure (Fig. 10c). Attributed to the coordination interactions between  $-\text{CO}/-\text{OH}$  groups of DOX and  $\text{CaCO}_3$ , targeting ability of FA and photothermal effects of PPy, dual-modified RBCs possessed a

high drug loading and a targeted and light-controlled drug release behavior, greatly inhibiting the growth of tumor cells combining photothermal therapy and chemotherapy. This intra/extracellular dual-modification of RBCs provides new insights for future clinical cancer therapy based on their synergistic photothermal-chemotherapy.

Living cell-based therapies, such as fecal microbiota transplantation, infusion of hemopoietic stem cells and T-cell therapy, have been successfully applied in the treatment of various intractable diseases, including inflammatory bowel disease, cancers, and congenital defects.<sup>146,147</sup> Nevertheless, cells are fragile to hostile environmental stressors, transplantation-conducted metabolic microenvironments and host immune systems, resulting in a low therapeutic efficacy and undesired cell death.<sup>148</sup> Therefore, methods simultaneously integrating therapeutic modalities with protective functions are highly desired to frame satisfied cells for cell-based therapy. Liu *et al.* reported a new cell engineering approach for coating individual living cells with multimodal motifs.<sup>149</sup> Dopamine was first deposited on the surface of living

cells by a cascade dopamine oxidation and polymerization reaction. Functional molecules such as amino-terminated polyethylene oxide (PEO-NH<sub>2</sub>), rhodamine B and fluorescein isothiocyanate (FITC) were then co-deposited with dopamine to construct multifunctional coatings on the surface of individual cells, including fungi, bacteria and mammalian cells. The main driving forces for this surface polymerization included  $\pi$ - $\pi$  stacking, hydrogen bonding, Schiff base reaction and Michael addition (Fig. 11a, I–III). Importantly, no obvious change was detected in bioactivity and viability after coating. Owing to the strong tolerance against bile salts and gastric acid due to the presence of the coating, engineered cells presented an obviously improved retention in the stomach and gut compared with bare bacteria (Fig. 11a, IV). Benefiting from the targeting ability of chitosan to inflamed colonic mucosa, coated cells showed a higher accumulation in sick tissue (Fig. 11a, V) and significantly increased the treatment efficacy (Fig. 11a, VI) of the dextran sulfate sodium-lured murine colitis. Bandaging using a multifunctional and biocompatible coating opens a new window for engineering living cells for treatment and prevention. It is anticipated that this approach can be expanded to the decoration of other cells, especially immune cells, aiming to treat cancer and autoimmune disease.

The pharmaceutical efficacy of anticancer drugs is often hampered by their poor tumor invasiveness and limited accumulation in tumors.<sup>150,151</sup> Although a number of excellent nanomedicines have been designed to detain active ingredients in tumor tissues with the aid of enhanced permeability and retention effects,<sup>152</sup> the total enrichment is still disappointing. Therefore, methods that are able to disperse antitumor drugs lastingly and homogeneously throughout the whole tumor tissue are desirable to maximize their therapeutic efficacy. Liu *et al.* reported a bacteria-directed spatio-temporally controllable allocation of synergistic therapeutics in tumor tissues to reverse the immunosuppression microenvironment for maximizing anti-tumor efficacy (Fig. 11b, I).<sup>153</sup> By combining genetic engineering and polymerization reaction, bacteria were first remoulded from inside and outside synchronously to express photothermal melanin (Bac<sup>MeI</sup>). The immune checkpoint inhibitor ( $\alpha$ PD-1) was then deposited onto the surface of Bac<sup>MeI</sup> which was pre-coated with polydopamine (B- $\alpha$ PD-1). Because bacteria tended to colonize in intratumoral hypoxia circumstances, both Bac<sup>MeI</sup> and  $\alpha$ PD-1 could be lastingly and homogeneously distributed in excised human (Fig. 11b, II) and intravital mouse tumors, leading to a uniform heating area of tumor tissue. Benefiting from the dual photothermal-stimulated and immune checkpoint inhibitor-primed immune activation effect (Fig. 11b, III), the immunosuppressive tumor microenvironment was synergistically reprogrammed (Fig. 11b, IV). As expected, tumor growth was significantly inhibited, and the survival of mice was prolonged in both subcutaneous and eutopic 4T1-tumor murine models with the aid of Bac<sup>MeI</sup> + NIR irradiation. This bacteria-guided collaborative treatment combining photothermal therapy and immunotherapy paves a new avenue for a lasting and homogeneous distribution of antitumor therapeutics in solid tumors. Considering the future translation, some underlying challenges

like the mode of administration, the frequency and dosage of modified bacteria, the mechanism of bacterial distribution and safety issue, should be evaluated systematically.

Inflammatory bowel diseases (IBDs) are closely connected with elevated ROS and highly disordered gut microbiota.<sup>154–156</sup> Although antioxidants have been applied to eliminate ROS from the intestine,<sup>157–159</sup> and probiotic-guided methods have been developed to help recover the normal gut microbes,<sup>160,161</sup> great limitations are still present in the process of application. Nonspecific biodistribution, rapid clearance and weak ROS-scavenging ability determine the inconsistent efficacy of antioxidants for the treatment of inflammatory disease. Simultaneously, probiotics are greatly sensitive to the unfriendly circumstances in the gastrointestinal (GI) tract, significantly limiting their retention time and viability in the intestine. Hu *et al.* synthesized a amphiphilic hyaluronic acid-poly(propylene sulfide) (HA-PPS) polymer which self-assembled into HA-PPS nanoparticles (HPN) with ROS-scavenging ability (Fig. 11c, I).<sup>162</sup> To improve the delivery of probiotics (*E. coli* Nissle 1917, EcN) to the colons for enhancing bacteriotherapy, they were encapsulated with norepinephrine (NE), which underwent auto-oxidization and self-polymerization to deposit a poly-NE coat on the surface of probiotics (NE-EcN) to buffer them from hostile environmental assaults and prolong their detention time in the intestinal tract owing to their strong mucoadhesive ability. Based on the colon tissue-targeting capability of probiotics, HPN was conjugated onto the modified probiotic surface (HPN-NE-EcN) and efficiently delivered to the inflamed colons to regulate ROS levels with minimum side effects (Fig. 11c, II). In the dextran sulfate sodium-lured murine colitis model, HPN-NE-EcN displayed sharply improved prophylactic and treatment efficacy. Moreover, the diversity and abundance of gut microbes were boosted after HPN-NE-EcN treatment (Fig. 11c, III), conducive to the remission of IBDs. Because some research studies disclosed that the EcN-included *E. coli* strain shows the probability of facilitating colon cancer, the biosafety of this EcN strain-based study requires to be carefully assessed before clinical application, and other bacterial strains with a higher safety factor may be considered.

#### 4.2 Intracellular oxidative polymerization triggered by bioactive oxidizing molecules

The functional complexity of organisms originates from the functions and structures of component cells, exemplified by the important roles of neurocytes in nervous systems. From this perspective, the specific cells may be genetically remoulded to construct new structures with designed forms and functions. Although some electrochemical strategies have been developed to change cell activity and the impedance of living tissues,<sup>163,164</sup> the gene modification-based strategy is absent. By integrating polymer chemistry and engineered enzymes, Deisseroth *et al.* realized chemical synthesis of insulating and conductive polymers on the plasma membrane of living neurons (Fig. 12a, I).<sup>165</sup> Rat hippocampal neurons were selected and transfected with ascorbate peroxidase Apex2-modified adeno-associated virus (AAV) to construct Apex2(+) neurons. Under the trigger of the Apex2 reactive center, the polymerization of aniline monomers

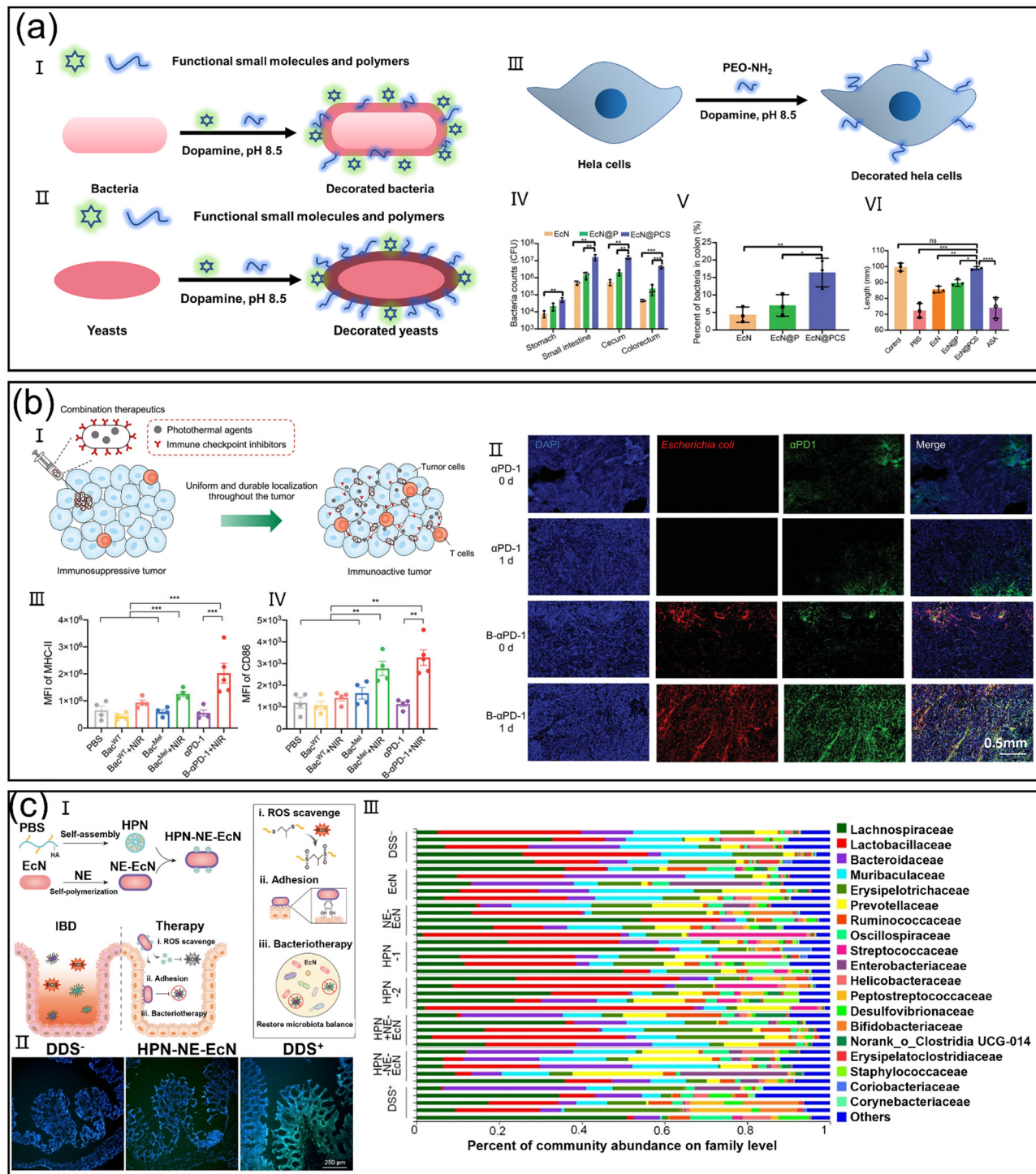
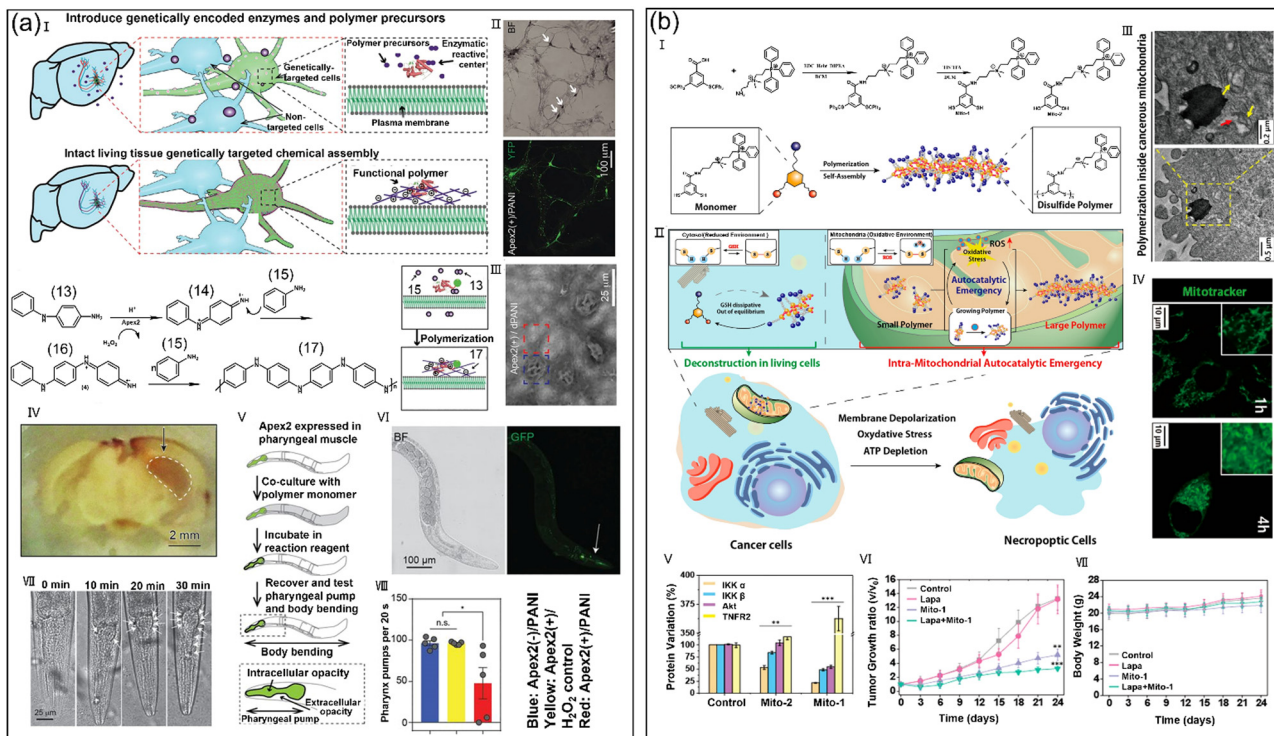


Fig. 11 (a) Multiple functionalization of living cells based on polymerization for cell therapy. Reproduced with the permission from ref. 149. Copyright 2021, Wiley-VCH GmbH. (b) New strategy for cancer therapy on the basis of *in situ* polymerization. (I) Schematic diagram of spatio-temporally controllable distribution of antitumor drugs in solid tumors combining genetic engineering and interfacial chemistry. (II) Slice analysis of B- $\alpha$ PD-1 distribution in excised human tumor tissue. Mean fluorescence intensity of MHC-II (III) and CD86 (IV) on DCs. Reproduced with the permission from ref. 153. Copyright 2021, Wiley-VCH GmbH. (c) Mucoadhesive probiotics carrying ROS nanoscavengers to facilitate the treatment of enteropathy-associated bacteria. (I) Preparation process of HPN-NE-EcN and the mechanism of bacteriotherapy for IBD treatment. (II) CLSM images of colon tissues revealing the ROS level. (III) Relative richness assessment of gut microbiome in mice from different groups. Reproduced with the permission from ref. 162. Copyright 2022, American Association for the Advancement of Science.

(PANI) was obviously observed at the juxtamembranous location (Fig. 12a, II). Compared with Apex2(-)/PANI neurons, a higher

contrast was observed on the Apex2(+)/PANI neurons (Fig. 12a, III), suggesting that there was a substantial enhancement of



**Fig. 12** (a) Genetically targeted enzyme/H<sub>2</sub>O<sub>2</sub>-catalyzed radical cation polymerization in living cell, tissue and animal. (I) Schematic illustration of the Apex2-mediated polymerization on plasma membrane. (II) *In situ* Apex2-targeted synthesis of PANI. (III) Variable-pressure SEM image of Apex2(+)/dPANI neurons. (IV) Micrograph of a brain slice after Apex2-driven polymerization. (V) Illustration of the Apex2-targeted polymerization in pharyngeal muscle. (VI) Micrograph and fluorescence photographs of *C. elegans* labeled with Apex2-green fluorescent protein. (VII) Time-course micrograph photographs of pharyngeal muscle after PANI reaction. (VIII) Body-bending rate of *C. elegans* after different treatments. Reproduced with the permission from ref. 165. Copyright 2020, The American Association for the Advancement of Science. (b) Intramitochondrial disulfide polymerization for cancer treatment. (I) Structures of the monomer and disulfide polymers. (II) Schematic illustration of intramitochondrial PISA to induce the necroptosis of tumor cells. (III) TEM images of HeLa cells treated with Mito-1. (IV) CLSM images showing intramitochondrial polymerization-induced mitochondrial fragmentation. (V) Quantification of protein involved in the necroptotic signaling pathways. (VI) Tumor growth curves of SCC7 tumor-bearing mice after different treatments. (VII) Body weight changes of SCC7 tumor-bearing mice after different treatments. Reproduced with the permission from ref. 169. Copyright 2021, American Chemical Society.

surface conductivity in the Apex2(+)/PANI neurons. In addition, Apex2-catalyzed polymerization was also monitored in the human cortical spheroids and brain (Fig. 12a, IV). In order to investigate the impact of genetically-targeted electroactive polymers on the behavior of moving animals, a worm pharyngeal muscle cell model expressing Apex2-green fluorescent protein (GFP) was built (Fig. 12a, V and VI). Robust polymers were localized on the cytomembrane of pharyngeal muscle cells (Fig. 12a, VII) and there was a reduction in the pumping periodicity of pharyngeal muscle (Fig. 12a, VIII), indicating that the formed polymers limited the movement of pharyngeal muscle. Although the chemical assemblies of genetically targeted electroactive polymers have been realized in live cells, tissue and animals, some potential opportunities and limitations need to be considered. For example, the retention time of polymers in living systems, which may lead to superiority or cytotoxicity. Distinct strategies for triggering chemical synthesis could be concentrated on genetically modified cells, anatomically targeted reactants, catalysts, reaction conditions, *etc.* Meanwhile, multifarious cell-specific chemical synthesis may be developed to obtain functional characteristics in the goal structures.

It has been demonstrated that the polymerization-induced self-assembly (PISA) method in living systems is able to regulate cellular functions<sup>166,167</sup> and even acts as superior therapeutics.<sup>168</sup> Nevertheless, PISA proceeding in a specific organelle has not been implemented. Ryu *et al.* developed a mitochondria-targeting PISA method to induce the necroptosis of tumor cells (Fig. 12b, I).<sup>169</sup> Under the effect of mitochondria targeting groups (triphenylphosphonium, TPP), monomers with two thiol units (Mito-1) highly accumulated in the mitochondria of tumor cells which contained a high level of ROS. The ROS in the mitochondria acted as a chemical fuel to catalyze the disulfide polymerization. Furthermore, this intramitochondrial polymerization induced oxidative stress that further elevated the ROS level, thus auto-catalyzing polymerization (Fig. 12b, II). The formed long polymer chains self-assembled into fibrous structures and penetrated mitochondrial membranes (Fig. 12b, III), disrupting the integrity of mitochondria (Fig. 12b, IV) and eventually inducing cellular necroptosis (Fig. 12b, V). Because mitochondria are crucial organelles responsible for the energetic metabolism, this energy-outage strategy may overcome multidrug resistance in tumor treatment. Based on the synergistic effect of Mito-1 and

$\beta$ -lapachone (Lapa) which generated abundant ROS after the catalysis by the intracellular NQO1 enzyme, the tumor growth of SCC7 (Fig. 12b, VI) and 4T1 tumor-bearing mice was significantly inhibited. Of note, negligible systemic toxicity was detected after the synergistic treatment (Fig. 12b, VII). This *in situ* polymerization in mitochondria shows huge potential for cancer treatment including multidrug-resistant cancers.

Polymerization on cell surfaces has been widely explored, but polymerization in living cells remains challenging owing to the complex cellular environment. However, from another point of view, the cellular microenvironment is abundant in various biological molecules, full of opportunities to regulate cell activities. For example, the high concentration of ROS in tumor microenvironments, may be a favorable condition to initiate oxidative polymerization in cells. Xu *et al.* developed a ROS-initiated oxidative polymerization reaction to synthesize functional polymers in an ROS-abundant intracellular microenvironment (Fig. 13a).<sup>170</sup> In order to elevate the local concentration of monomers for polymerization, a nanoreservoir containing plentiful organotellurides was constructed based on the coordination interaction between gold and organotelluride (Fig. 13b). Attributed to their ultrasensitive redox responsiveness and coordination properties, organotellurides were oxidized into Te–O polymers by the ROS in tumor cells. The obtained Te–O polymers perturbed the intracellular antioxidant system by inhibiting the expression of selenoproteins. As a consequence, a high concentration of ROS was induced in the tumor microenvironment, which continuously fueled the synthesis of Te–O polymers *via* a self-amplification mechanism (Fig. 13c). Because the ROS

level in normal cells was not enough to activate oxidative polymerization of organotellurides, the self-amplification effect was prevented. Therefore, a selective anticancer activity was achieved by the Te nanoreservoir. With a continuous increase in ROS, the ROS-associated apoptosis pathway in tumor cells was activated; thus Te–O polymers exhibited a high anticancer activity and a low systemic toxicity (Fig. 13d). Compared with previous approaches, this oxidative polymerization was initiated without an external stimulus and highly concentrated monomers. The only initiator of the reaction was the intracellular microenvironment. Based on the advantages, such as easy preparation, strong targeting ability and high efficiency, this oxidative polymerization will create a new sensation for the selective regulation of cell behaviors *in vivo*.

## 5. Supramolecular polymerization

In contrast to covalent polymerization, supramolecular polymerization refers to the construction of macroaggregates from the noncovalent interaction-directed self-assembly of small molecular monomers. As a classic example of supramolecular polymerization reactions, 3D and 4D protein assembly in organisms involves actins and tubulins in cells. As an integration of supramolecular chemistry and polymer science, supramolecular polymerization displays superiority in a variety of biomedical applications. Benefiting from the diversity of supramolecular chemistry, multifarious dynamic noncovalent interactions including electrostatic interactions, hydrogen bonds,  $\pi$ - $\pi$  stacking and host-guest interactions, have been utilized as driving

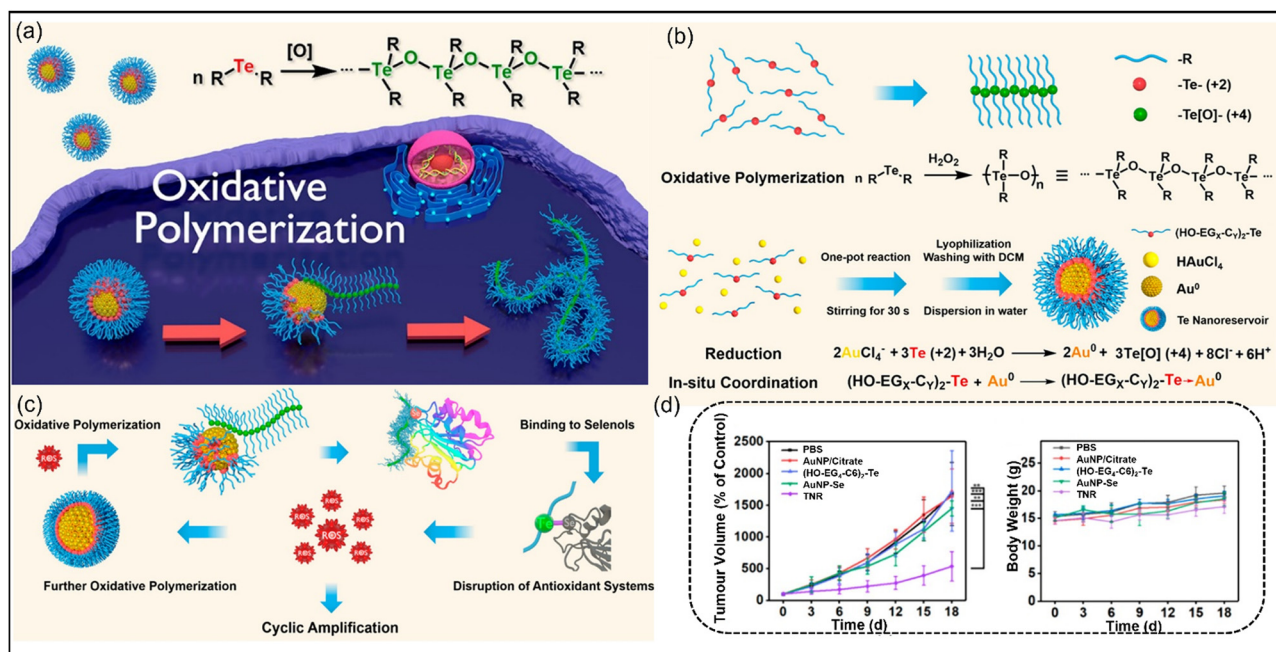


Fig. 13 Te–O polymerization in living cells. (a) Schematic diagram of oxidative polymerization in living cells. (b) Synthetic process of Te–O polymerization and Te nanoreservoirs. (c) Te–O polymerization with a self-amplification mechanism in cancer cells. (d) Tumor growth curves of HepG2 tumor-bearing mice after different treatments. (e) Body weight changes of HepG2 tumor-bearing mice after different treatments. Reproduced with the permission from ref. 170. Copyright 2021, American Chemical Society.

forces to fabricate biomimetic supramolecular polymers. Profiting from the reversible and dynamic noncovalent interactions, stimuli-responsiveness and biodegradability will be granted to the living supramolecular polymers, thus reducing toxic side effects on normal cells and avoiding long-term immunotoxicity.

### 5.1 Extracellular supramolecular polymerization triggered by the DNA pairing principle and redox systems of microorganisms

Currently, many efforts and representative works have been carried out to enhance the environmental tolerance of cells by depositing materials on the cell membrane of mammalian cells.<sup>171–173</sup> However, existing methods all rely on directly depositing coating materials onto the cell membrane, which often mean that the interaction between cells and the outside world is completely blocked (the failure of material transport and information transmission).<sup>174</sup> The reports of building structures simulating the cytoderm of microbial and plant cells are rare. DNA is one of the three elementary polymers in nature, and its synthetic counterpart has been broadly applied to establish materials for biomedical and biological applications.<sup>175–177</sup> Wang *et al.* developed a biomimetic cell wall (BCW) on plasma

membranes based on a framing template (supramolecular DNA structure) and a cross-linked matrix (alginate and polylysine-consisted polyelectrolyte) to protect live mammalian cells (Fig. 14a, I).<sup>178</sup> The whole process of BCW construction did not involve any harsh conditions. The cationic polylysine mainly interacted with DNA-targeted anionic alginate, rather than the plasma membrane; thus the BCW-coated mammalian cells maintained a high bioactivity (Fig. 14a, II). Importantly, BCW could not only shield living mammalian cells from physical assaults including centrifugal force (Fig. 14a, III and IV) and osmotic imbalance (Fig. 14a, V and VI), but also avoid immune attack-like biological assaults (Fig. 14a, VII). It indicated that BCW could be a conspicuous tool for bioprinting and cell transport for tissue regeneration. While this study is not concentrated on the exploration of BCW for therapeutic applications, it provides a great possibility to acquire a “permanent” shielding shelter for live mammalian cells or islets *via* the optimization of BCW synthesis conditions. For example, islet transport for the treatment of diabetes in which shielding materials own a long-term stability, high integrity and a satisfied molecular delivery efficiency to support cell survival.

It is well known that cellular interactions are mainly regulated by the membrane proteins, the conformations and

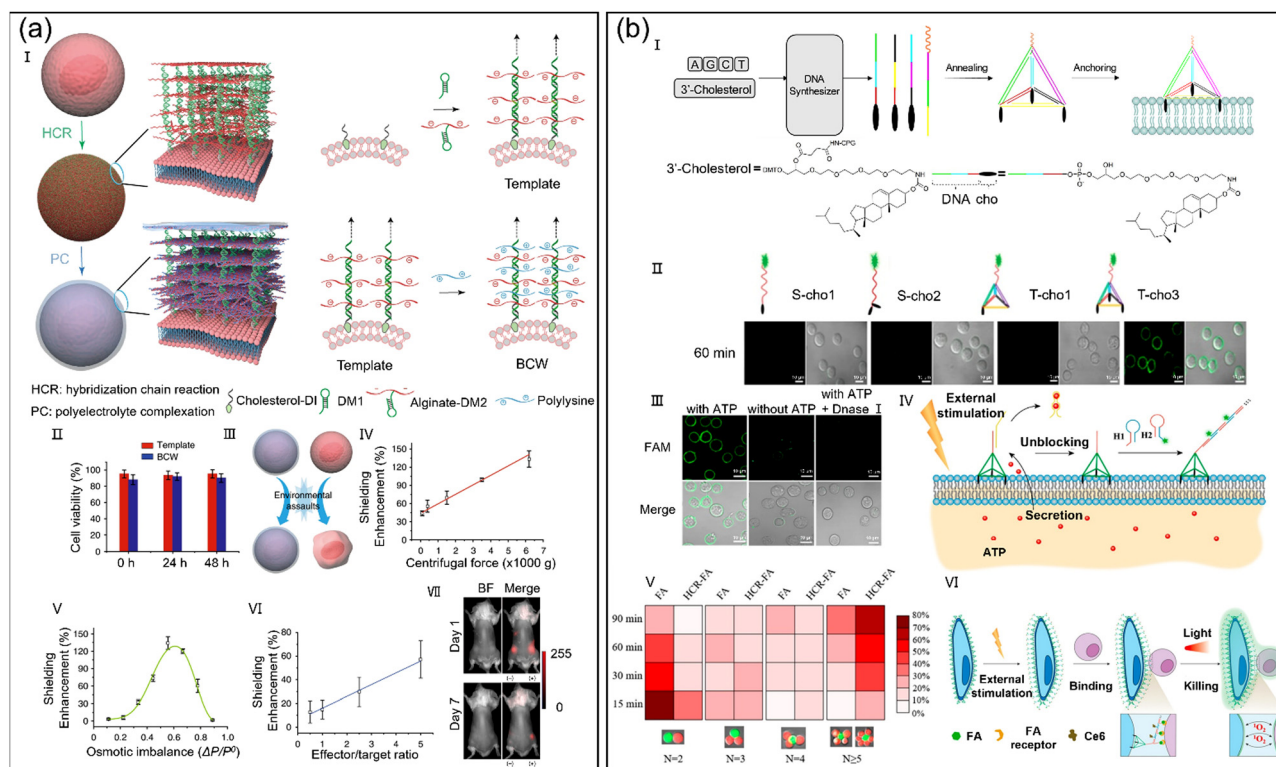


**Fig. 14** (a) DNA-constructed bionic cell wall for encapsulating and protecting mammalian cells. (I) Schematic diagram of BCW synthesis. (II) Cell viability after different treatments. (III) Stability comparison of the native cells (right) and BCW-covered cells (left). (IV) Relationship between shielding enhancement and centrifugal force. (V) Relationship between shielding enhancement and osmotic imbalance. (VI) Relationship between shielding enhancement and immune attack. (VII) *In vivo* imaging of human mesenchymal stem cells (MSCs)-transplanted mice. Reproduced with the permission from ref. 178. Copyright 2021, Springer Nature. (b) Supramolecular polymerization of DNA on cell surfaces to imitate the dynamical behaviors of membrane proteins. (I) Schematic diagram of the T-cho3 formation and its anchoring manner on cell-membranes. (II) Evaluation of the membrane-anchoring ability of T-cho3 by CLSM. (III) Evaluation of the ATP-responsiveness of HCR by CLSM. (IV) Schematic diagram of cellular adaptive establishment of DNA polymerization on membrane. (V) Evaluation of the formation of cell clusters. (VI) Diagrammatic representation of dynamic-DNA nanoarchitecture-controlled cell-cell interactions. Reproduced with the permission from ref. 184. Copyright 2021, American Chemical Society.

expression of which are dynamically adjusted *via* intracellular programs.<sup>179,180</sup> Therefore, development of membrane protein-simulated architectures that are able to recognize cell-responsive signals in response to environmental stimuli and consequently perform allosteric modulation to control cellular interactions will offer new opportunities for the study of cell-signaling networks. With the advantages of predictable structures, good biocompatibility and high programmability, DNA nanostructures are considered as one of the most prospective membrane protein-mimicking materials.<sup>181–183</sup> Tan *et al.* engineered a cell surface-anchored nanoarchitecture that implemented molecular recognition-activated DNA polymerization to imitate the dynamical behaviors of membrane proteins, realizing the perception of cellular adaptive response to environmental changes (Fig. 14b, I).<sup>184</sup> Amphiphilic DNA tetrahedrons (T-cho3) could be stably and efficiently anchored onto cell membranes with a low ratio of detachment and internalization (Fig. 14b, II). Upon sensing the cellular adaptive response to intracellular and extracellular stimulations, such as endogenous and exogenous adenosine triphosphate (ATP), these membrane-anchored DNA nanostructures were activated followed by the tandem polymerization of multiple functional nucleic acids *via* the hybridization chain reaction (HCR) (Fig. 14b, III and IV). The multivalent effect of HCR not only enhanced cell aggregation efficiency and facilitated the generation of the highly clustered cells (Fig. 14b, V), but also recognized the targeted cells for a precise killing effect (Fig. 14b, VI). Profiting from the fast dynamics of nucleic acid chemistry and the modular assembly, this approach could be broadened to manipulate and mimic diversiform biological events such as cellular communication and adaptation, providing a new prototype for intelligent synthetic biology and customized cell engineering.

Although some polymer-based cell encapsulation approaches have been developed, encapsulation of target living cells into mechanically and biotunable polymer shells is a major challenge in current research.<sup>185–187</sup> Li *et al.* proposed a biocompatible and programmable DNA-oriented polymerization approach (isDOP) to *in situ* weave DNA oocysts on living cells (Fig. 15a, I).<sup>188</sup> By the feat of DNA isothermal duplication and programmed DNA assembly, the surface chemistry, mechanical properties and polymer density can be tailored. Since DNA polymers are molecularly precise assemblies with high homogeneity, they can be precisely addressed by DNA base pairing (G–C and A–T) and DNA-modifying enzymes. Rolling cyclic replication (R1) and branching replication (R2) were employed in weaving DNA polymer networks, seeded by initiation primers (IP) and branch primers (BP), respectively. First, IP initiated R1, which generated the long and periodic DNA polymers (LonDNA) based on the replication template of single-stranded circular DNA (cirDNA). Then, BP initiated R2, which generated another single-stranded DNA polymer (LatDNA). LatDNA cross-linked with LonDNA to induce the assembly of connections based on the replication templates; thus *in situ* DNA cocoons on the cell surface were fabricated (Fig. 15a, I). When an increase in concentration of IP or BP, the density and thickness of DNA polymers also increased (Fig. 15a, II), whereas the pore size of DNA cocoons decreased, suggesting that the structure of DNA cocoons could be regulated

by adjusting the IP or BP concentration. After DNA weaving, over 95.6% MCF-7 cells were encapsulated and remained alive (Fig. 15a, III), indicating that this isDOP was highly efficient and biocompatible. Different fluorescent color-labeled DNA cocoons were specifically caught in different regions of the DNA-stereotyped slide surface which was pretreated with the corresponding capture strands (CSs), indicating that LatDNA and LogDNA were automatically synthesized and assembled according to the sequence codes (Fig. 15a, IV). Most importantly, with the aid of DNA-modifying enzymes which can cleave the designed encoding sequences in DNA cocoons, the DNA-weaved cells were selectively released from the capture zones (Fig. 15a, V). This precise isDOP not only enables to overcome cell encapsulation challenges but also provides flexible mechanisms to regulate physiological and biophysical phenomena at cell interfaces. Aside from DNA weaving technique, other tunable natural materials for the control of rigidity, permeability and stimuli-responsiveness of the coating, and the ability to vest the cells with specific functions, including targeted cell delivery, specified assembly manners and designed cell–cell interactions, should be given more attentions.

The transmembrane redox potentials originating from prokaryote respiration, have been successfully applied for *in situ* construction of biomedical materials over recent years. Compared with traditional biomedical materials, functional materials fabricated *in situ* can omit the transporting process and targeting ability, thus greatly promoting their adaptivity and specificity.<sup>189–191</sup> Meanwhile, supramolecular polymerization reactions are able to endow the final materials with excellent stimuli-responsiveness and biodegradability, attributed to the reversible and dynamic nature of the noncovalent interactions, which are excellent qualities for biomedical applications. Benefitting from the advantages of the *in situ* fabrication strategy and supramolecular polymerization reactions, it is expected that supramolecular polymers constructed *in situ* may become novel diagnostic and therapeutic tools. Xu *et al.* developed a cucurbit[8]uril (CB[8])-based supramolecular polymerization strategy, in which the bifunctional monomer VDV was equipped with a positively charged 1,4-diazabicyclo[2.2.2]octane unit and two viologen groups at the ends (Fig. 15b, I).<sup>192</sup> Under anaerobic conditions, the redox potential of *E. coli* reduced VDV into cation radicals which then self-assembled into supramolecular polymers (VR-SP) driven by the 1 : 2 ternary host–guest complexation between CB[8] and viologen cation radicals (Fig. 15b, II and III). Free radicals with one or more unpaired single electrons are characterized by a special open-shell structure, and their band gaps are always narrow. It is expected that organic free radicals can show NIR absorption and are good choices for NIR photosensitizers for photothermal therapy. Upon NIR irradiation, the photothermal effect of VR-SP efficiently killed *E. coli*, displaying a high antibacterial efficiency (Fig. 15b, IV). Because the positively charged VR-SP owned a strong adhesion ability to the negatively charged bacteria (Fig. 15b, V), the photothermal antibacterial ability of supramolecular polymers was further enhanced by the local enrichment of VR-SP. After killing *E. coli*, VR-SP were easily oxidized by the dissolved oxygen, thus

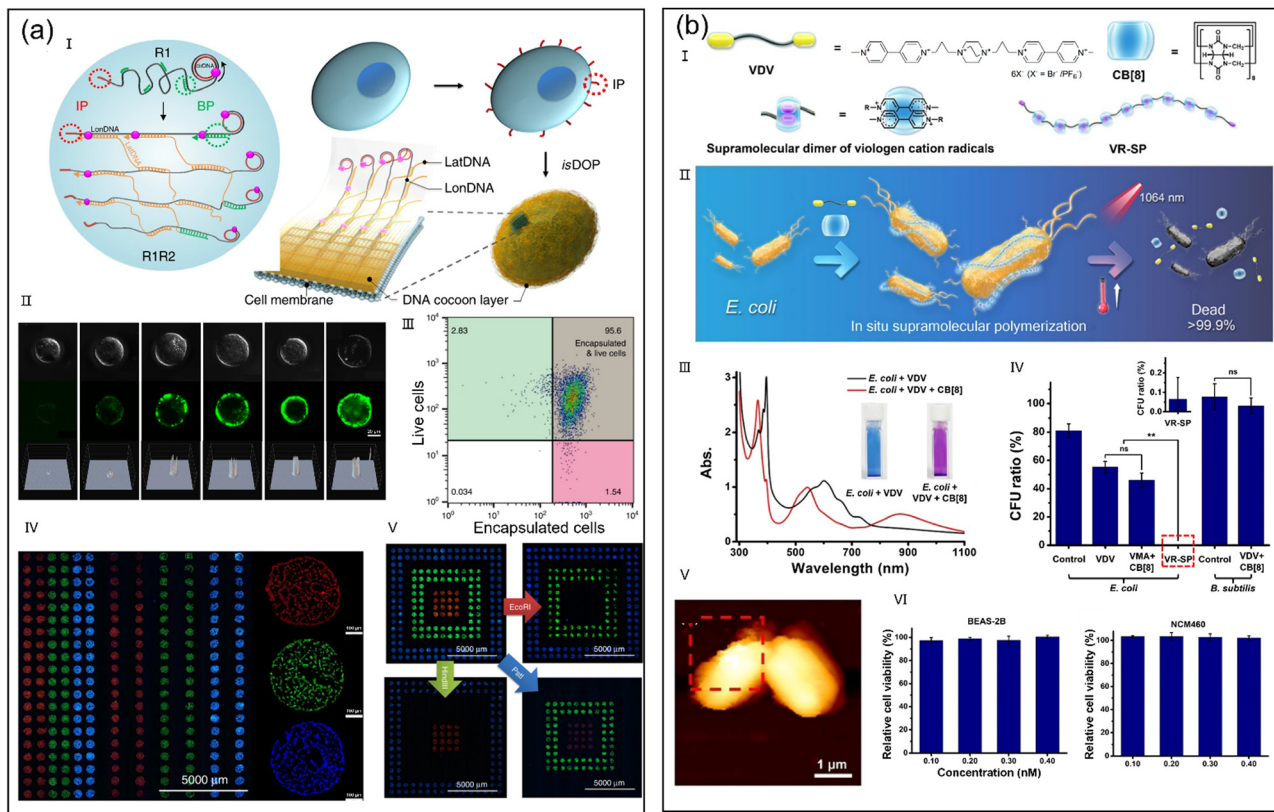


**Fig. 15** (a) Deposition of DNA onto living cells like cocoons. (I) Mechanism of isDOP for cell encapsulation. (II) CLSM images of the DNA-covered MCF-7 cells. (III) Flow cytometry result revealing the encapsulation productivity and cell viability of MCF-7 cells. (IV) Fluorescent scanning images showing the encoded cells were captured in the specific capture zones. (V) Fluorescent scanning images showing the site-specific release of cells after treatments with different restriction endonucleases. Reproduced with the permission from ref. 188. Copyright 2019, Springer Nature. (b) *E. coli*-powered supramolecular polymerization for NIR photothermal antibacteria. (I) Structures of VDV, CB[8] and VR-SP. (II) Schematic representation of the NIR photothermal antibacteria. (III) Images and UV-vis spectra of the *E. coli* + VDV solution with or without CB[8]. (IV) Colony-forming unit ratio of *B. subtilis* and *E. coli* after different treatments. (V) Atomic force microscopy (AFM) image of *E. coli* treated with VDV and CB[8]. (VI) Cytotoxicity of the equimolar VDV and CB[8] against BEAS-2B cells and NCM460 cells. Reproduced with the permission from ref. 192. Copyright 2021, Chinese Chemical Society.

automatically turning off their antibacterial activity. Importantly, the building blocks were biocompatible and exhibited negligible cytotoxicity against mammalian cells (Fig. 15b, VI), suggesting that VR-SP was a safe photothermal agent in potential applications. Better selectivity to specific microbes and antimicrobial performance would be acquired by integrating bio-responsive units and photothermal motifs in this system. This *in situ* supramolecular polymerization provides a new idea for the fabrication of novel biomedical materials with high adaptivity and programmability.

## 5.2 Intracellular supramolecular polymerization triggered by non-covalent interactions and bioactive molecules

Inspired by the intelligence of nature, numerous artificial self-assembled nano-architectures, especially the supramolecular structures built on the basis of macrocyclic receptors, have been constructed and applied to regulate the physiological and biological events.<sup>193–198</sup> As a fundamental component of eukaryotic cells, microtubules (MTs) assembled from the dynamically alternate  $\alpha/\beta$  tubulin heterodimers undertake an important role in the mitosis-associated cell cycle. Controlling the self-assembly of MTs is expected to blaze a trail for the MTs-related disease

therapy. Based on the host–guest complexation between photochromic arylazopyrazole (AAP) and  $\beta$ -cyclodextrin ( $\beta$ -CD), Liu *et al.* realized the reversible light-controlled inter-tubular aggregation of MTs in cellular environments (Fig. 16a, I).<sup>197</sup> Since paclitaxel (PTX) was able to stabilize MTs against depolymerization *via* selectively binding to  $\beta$ -monomer, PTX was covalently linked to AAP and  $\beta$ -CD respectively to regulate the interconnection of MTs. The morphology of MTs changed from nanoribbons and nanofibers to diverse spherical nanoparticles of various sizes after co-incubation with different PTX-containing building units (Fig. 16a, II). Furthermore, 4–8  $\mu\text{m}$  aggregates were observed near cell nuclei after the treatment with *trans*-PTX-AAP  $\subset$  PTX-CD, rather than in other groups, which suggested that the host–guest complexation-triggered inter-tubular aggregation of MTs could be implemented in the cellular microenvironment. More importantly, high cell death rates and more shrunken cells were induced by the *trans*-PTX-AAP  $\subset$  PTX-CD complex, demonstrating that supramolecular complex-induced MT aggregation resulted in a strong cytotoxicity. This work not only deepens our understanding of dynamic protein self-assembly at a molecule level but also provides a new chance for the theranostics of MTs-related diseases.

Self-assembly is a useful tool to prepare supramolecular materials.<sup>199</sup> However, efforts have been mainly concentrated on applying a single-step catalytic reaction or a molecule to initiate the self-assembly (also called supramolecular polymerization) process;<sup>200</sup> thus the structures of self-assemblies are relatively plain. Recently, a two-reaction controlled supramolecular strategy has attracted increasing interest and has presented diversified self-assemblies with smart functions.<sup>201–203</sup> Yang *et al.* reported a peptide derivative-based tandem molecular self-assembly which was hierarchically controlled by the synergistic effect of extracellular alkaline phosphatase (ALP) catalysis and intracellular GSH reduction (Fig. 16b, I).<sup>204</sup> Because hepatoma cells possess higher concentrations of ALP and GSH than normal cells, the hierarchical supramolecular polymerization of the peptide derivative (18) occurred in HepG2 and QGY7703 cells. The peptide 18 first formed nanoparticles outside the cell membrane and then transformed into nanofibers around karyotheca or inside the cell membrane (Fig. 16b, II). Attributed to this tandem supramolecular mechanism, the

peptide derivative 18 exhibited stronger cellular uptake and inhibition effects against liver cancer cells than against normal liver cells (Fig. 16b, III–V). This extracellular and intracellular tandem molecular self-assembly mechanism will push the further development of supramolecular self-assemblies with improved performances in cancer theranostics.

Drug resistance is a major obstacle for ovarian cancer treatment. Among various approaches reversing drug resistance, cisplatin-involved combination chemotherapies are most explored because of the high efficiency of cisplatin (CDDP) in clinical therapeutics.<sup>205</sup> However, the 5-year survival rate of ovarian cancer patients has hardly increased over the past decade.<sup>206</sup> Thus, innovative cisplatin-based combination therapies are urgently needed. Xu *et al.* used enzyme-instructed self-assembly to construct intracellular supramolecular assemblies which greatly enhanced the capability of CDDP to reverse the drug-resistance of ovarian cancer cells (Fig. 17a, I).<sup>207</sup> The pre-installed ester groups on the small peptide precursors (L-22 and D-22) could be cleaved by carboxylesterase (CES), and they

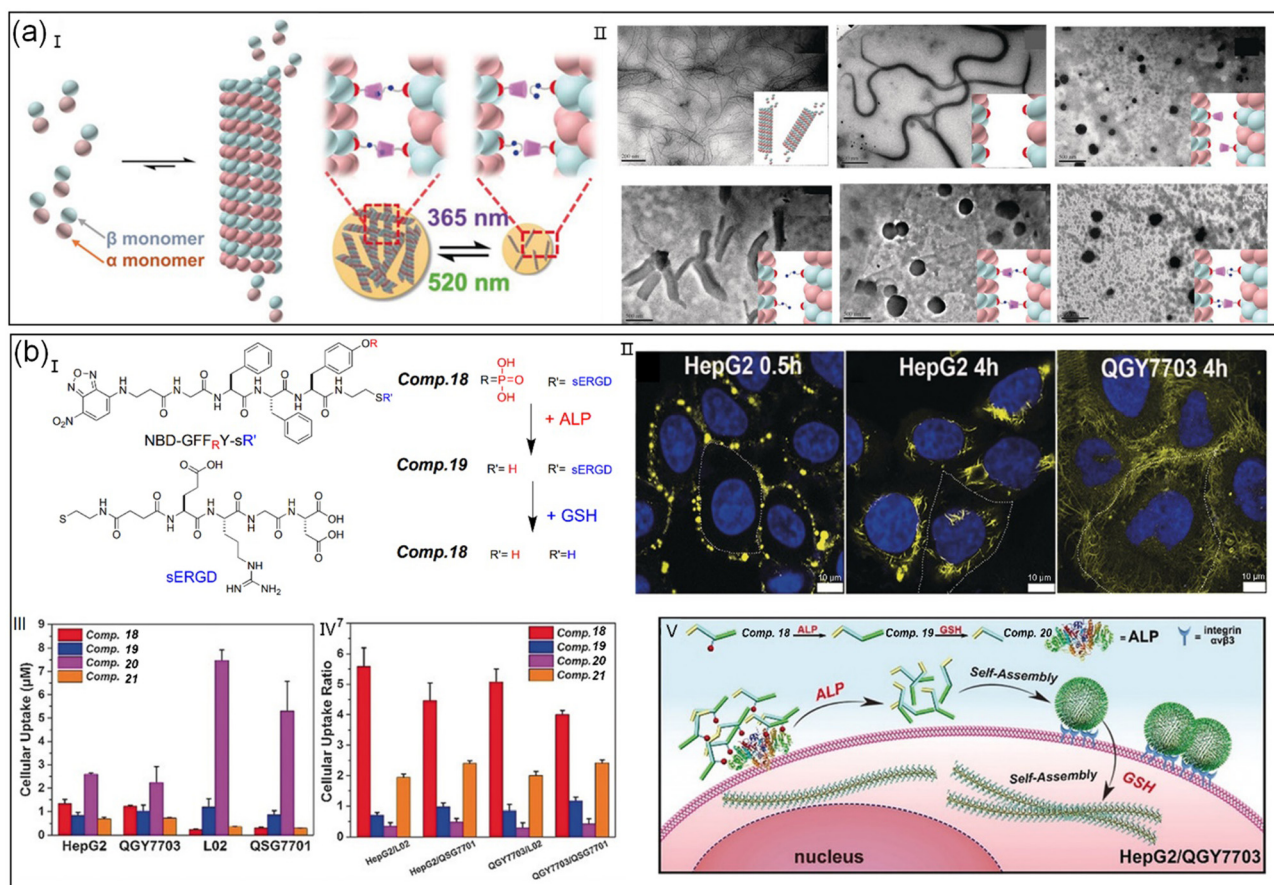


**Fig. 16** (a) Photo-controlled microtubule assembly based on the host–guest complexation. (I) Schematic diagram of photo-controlled microtubule assembly. (II) TEM images of microtubules after different treatments. (III) CLSM images of A549 cells after treatment with *trans*-PTX-AAP  $\subset$  PTX-CD. Reproduced with the permission from ref. 197. Copyright 2018, Wiley-VCH Verlag GmbH & Co. KGaA, Weinheim. (b) Supramolecular polymerization of hierarchical peptide in tumor cells. (I) Chemical structures of compounds 18–20 and the transformational relationship between them. Chemical 21 without GSH-responsiveness was chosen as a control. (II) CLSM images of QGY7703 and HepG2 cells cultured with 18. (III) Cellular uptake assessment of compounds 18–21 by different cells. (IV) Cellular uptake ratios of compounds 18–21 by different cells. (V) Proposed mechanism of supramolecular polymerization in the tumor microenvironment. Reproduced with the permission from ref. 204. Copyright 2018, Wiley-VCH Verlag GmbH & Co. KGaA, Weinheim.

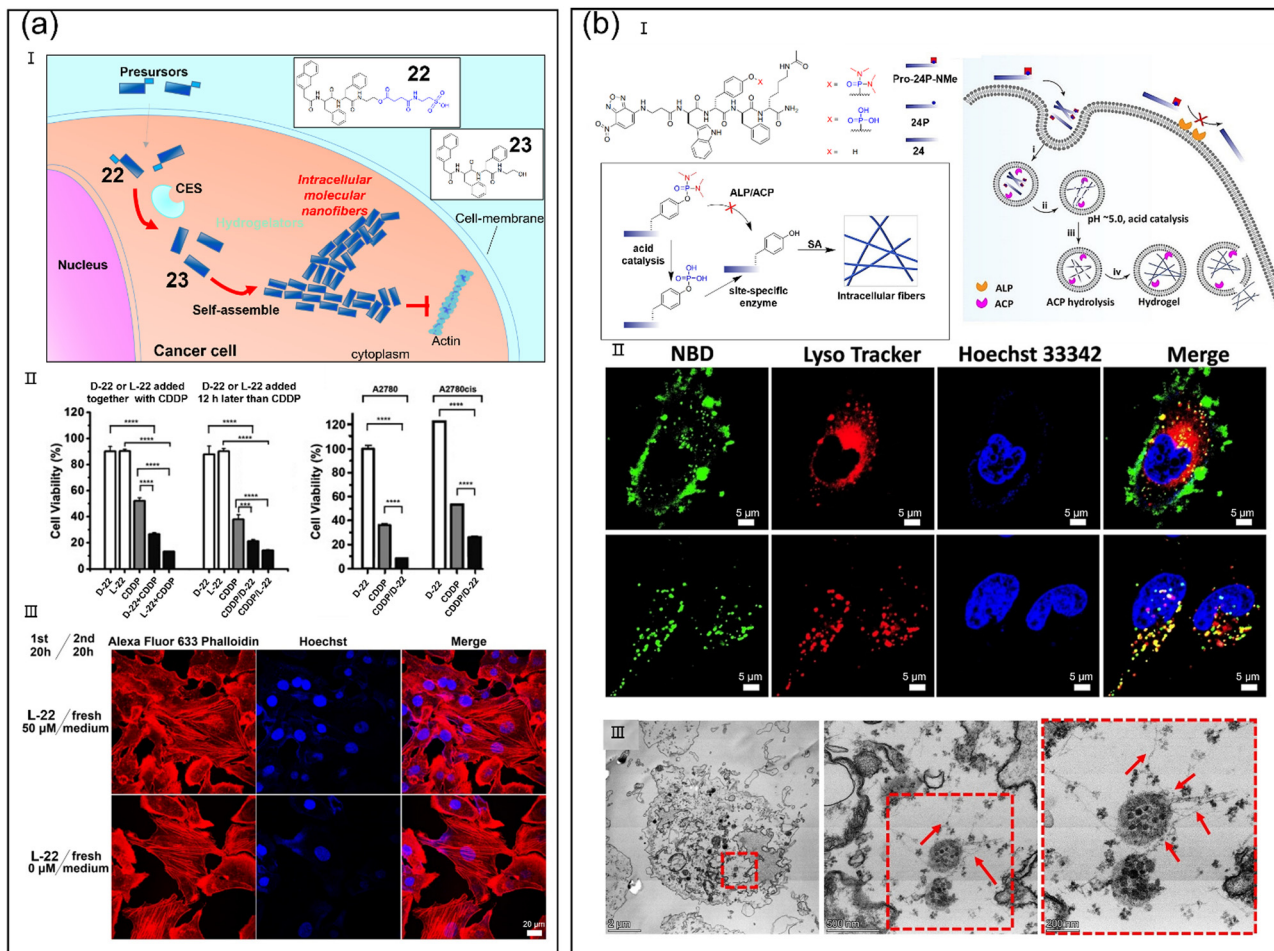


Fig. 17 (a) Enzyme-activated intracellular supramolecular polymerization of peptides to reverse the drug resistance of ovarian cancer cells. (I) Schematic diagram of enzyme-activated supramolecular polymerization inside cells. (II) Cell viability of two ovarian cancer cells after different treatments. (III) CLSM images of SKOV3 cells after different treatments. Reproduced with the permission from ref. 207. Copyright 2015, Wiley-VCH Verlag GmbH & Co. KGaA, Weinheim. (b) Spatio-temporally controlled supramolecular polymerization of peptides in living cells. (I) Chemical structures and schematic illustration of multistage peptide polymerization in living cells. (II) CLSM images of Saos-2 cells after different treatments (top row: 24, bottom row: Pro-24P-NMe). (III) Electron microscopy photographs of peptide fibre formation inside the cells in the Pro-24P-NMe group. Reproduced with the permission from ref. 210. Copyright 2021, Wiley-VCH GmbH.

were then transformed into L-23 and D-23, respectively, which eventually self-assembled into nanofibers in cells through supramolecular polymerization. At appropriate concentrations, both precursors were innocuous to cancer cells, but significantly boosted the activity of CDDP against the resistant ovarian cancer cells (Fig. 17a, II). Intracellular nanofibers exhibited transient cytotoxicity which minimized the long-term system toxicity in combination therapy (Fig. 17a, III). This enzyme-instructed self-assembly strategy promises a new method for drug-resistant cancer treatment. Other antitumor platinum drugs such as carboplatin which is regarded as a preferred platinum-based drug may display a better anticancer effect in synergy with this enzyme-instructed supramolecular self-assembly strategy.

Molecular self-assembly has developed into a cogent strategy to construct versatile structures with suitable association and folding in living cells.<sup>208,209</sup> Although impressive successes have been acquired *in vitro*, precise construction of molecular assemblies in living cells remains challenging, because the

self-assembly precursors will inevitably experience hydrolysis by the non-specific hydrolytic enzymes with similar activities. Wang *et al.* reported an easily accessible and efficient multistage strategy to accurately control the formation of supramolecular assembly in live cells (Fig. 17b, I).<sup>210</sup> *O*-[bis(dimethylamino)phosphono]tyrosine motifs in the precursor NBD-<sup>D</sup>Wp<sup>D</sup>Y(NMe<sub>2</sub>)<sub>2</sub>-<sup>D</sup>F<sup>D</sup>-K(Ac)-NH<sub>2</sub> (Pro-24P-NMe) acted as the Trojan horse, which resisted hydrolysis by moving phosphatases in and out of the cells as the enzymatic cleavage occurred selectively in lysosome-like acidic environments. After phagocytosis by Saos-2 cells, the phosphodiester groups of Pro-24P-NMe underwent acid-triggered hydrolysis to generate the substrate (24P) by acid phosphatase only inside the lysosome. Acid phosphatase cleaved the phosphate group of 24P and induced the multilevel self-assembly of Pro-24PNMe. The supramolecular polymerization from oligomers to nanofibrous networks was confirmed by CLSM (Fig. 17b, II) and biological electron microscopy (Fig. 17b, III). Replacing the acid-catalyzed unit and the type of enzyme by other

functional groups, this precise controllable nanostructure formation strategy is expected to develop more functional higher-order structures.

## 6. Other polymerization strategies

### 6.1 Extracellular polymerization triggered by metal catalysts

For the *in situ* radical polymerization reactions on cell surfaces, except for the free radicals which may induce cytotoxicity against cells, tracing the surface-initiated polymers is also difficult. Therefore, developing novel non-radical and imaging-guided surface polymerization approaches is imperative. Cell surfaces often have abundant Pd-binding sites. Coordinatable functional groups, such as amino, carboxyl, and phosphate groups, are the right candidates to trigger the generation of Pd nanoparticles for Pd-mediated cell surface aggregation. Wang *et al.* reported a biocompatible Pd-catalyzed polymerization reaction on the basis of the Sonogashira reaction for *in situ* synthesis of photoactive

polyphenyleneethynylene (PPE) on living cells (Fig. 18a, I).<sup>211</sup> Cationic 1,4-bis(oxy-hexamethylene-trimethylammonium bromide)-2,5-diiodobenzene (M1) and 1,4-bis(oxyhexamethylene-trimethylammonium bromide)-2,5-diethynylbenzene (M2) were selected as the monomers for polymerization. Owing to the positive charge of photoactive PPE, it could tightly anchor on cell surfaces with negative charge. Since PPE emitted blue fluorescence, polymerization could be easily characterized and traced. A concentration-dependent fluorescence enhancement was observed on *E. coli* surfaces in the experimental group compared to the control group (Fig. 18a, II), suggesting that polymerization proceeded on the *E. coli* surface. In addition, PPE-modified *E. coli* displayed a low bacterial viability (Fig. 18a, III), further demonstrating that cationic PPE was *in situ* synthesized on the bacteria surface. Similar to *E. coli*, *in situ* Sonogashira coupling also efficiently proceeded on the surface of *C. pyrenoidosa*, and increased ATP synthesis *via* a PS I activity enhancement mechanism (Fig. 18a, IV and V). Extending this Pd-catalyzed polymerization to other metal-catalyzed polymerization reactions, more

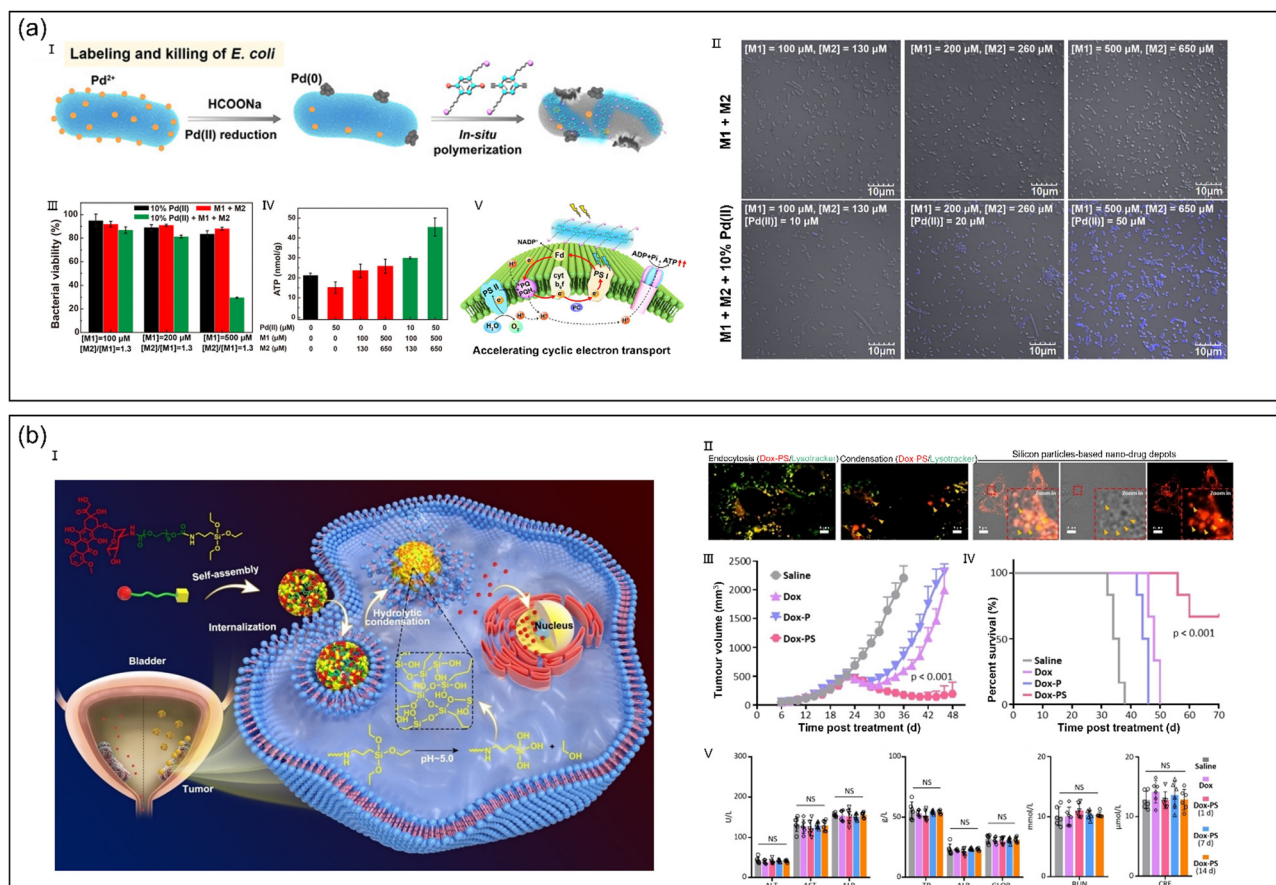


**Fig. 18** (a) *In situ* polymerization on cell surfaces triggered by the Sonogashira coupling reaction. (I) Schematic diagram of the bio-Pd-catalyzed synthesis on cell surfaces and its antibacterial ability. (II) CLSM images of the polymerization on cell surfaces using different monomer concentrations. (III) Viability of *E. coli* after polymerization. (IV) ATP production of *C. pyrenoidosa* after different polymerization reactions. (V) Proposed mechanism of polymerization-triggered ATP augment. Reproduced with the permission from ref. 211. Copyright 2020, Wiley-VCH Verlag GmbH. (b) *In situ* construction of nano-drug depots *via* the intracellular hydrolytic condensation for bladder cancer treatment. (I) Schematic diagram of the IHC system. (II) Fluorescence images of EJ tumor cells after 2 h, 4 h and 8 h incubation with Dox-PS. (III) Tumor growth curves of EJ tumor-bearing mice after different treatments. (IV) Survival curves of EJ tumor-bearing mice after different treatments. (V) Index of hematology including liver function and kidney function. Reproduced with the permission from ref. 214. Copyright 2022, Wiley-VCH Verlag GmbH, Weinheim.

functional polymers will be *in situ* generated on the living cell surface, and more artificial strategies will be developed to regulate cell functions.

## 6.2 Intracellular polymerization triggered by hydrolytic condensation

In the clinical treatment of bladder tumor, the common therapeutic method is intravesical perfusion of chemotherapeutic drugs with a high concentration.<sup>213</sup> However, the efficacy of intravesical chemotherapy is always low because of the short retention time of chemotherapeutics in the bladder owing to the continuous cycling of urine. Furthermore, the repeated perfusion of chemotherapeutic drugs with a high concentration usually induces serious side effects, such as inflammation, infection and hematuria. Hence, developing therapeutic strategies with a prolonged tumor retention time and low side effects for bladder tumor is extremely demanded. Xu *et al.* reported an intracellular hydrolytic condensation (IHC) reaction to build nano-drug depots which steadily released drugs *in situ*, efficiently inhibiting the growth of bladder tumors and reducing the side effects of chemotherapy (Fig. 18b, I).<sup>214</sup> In aqueous solution, doxorubicin (Dox)-silane (Dox-PS) prodrugs self-assembled into silane-based nanoparticles which displayed favorable lysosomal escape *via* the acid-catalyzed intracellular hydrolysis and eventually reconstituted into nano-drug depots in the cytoplasm of tumor cells (Fig. 18b, II). Attributed to the sustained drug release from nano-drug depots, the IC<sub>50</sub> values of Dox against three bladder cancer cells greatly decreased. Importantly, the IHC system exhibited potent antitumor efficacies in EJ xenograft tumor and EJ-air pouch bladder xenograft tumor models (Fig. 18b, III), and simultaneously extended the overall survival of mice (Fig. 18b, IV). Furthermore, the IHC system effectively reduced the severe side effects of Dox, such as hepatotoxicity and nephrotoxicity (Fig. 18b, V), showing a good biosafety. This IHC strategy on the basis of intracellular polymerization optimizes the design of nanomedicines, providing a unique strategy to significantly promote therapeutic efficacy of cancer chemotherapy.

## 7. Conclusions

Cells, as a basic unit of life, exhibit specific metabolic activities and diverse physiological functions, such as the high redox potential of active microbial, abundant Pd binding sites, reducing and oxidizing microenvironments, different levels of enzymes, and subphysiological pH, and have tremendous advantages in fabricating living bio-templated materials and other biohybrid systems with biomorphic or bioactive traits. In recent years, cell-mediated “living” polymerization has been rapidly developed, with significant advances in methods to engineer cell surfaces and construct sophisticated sequence-controlled materials in cells, offering unheard-of possibilities in multiple domains ranging from processing and information storage to biomedical imaging and drug delivery (Fig. 19).

Various polymerization reactions, including metal/enzyme/photo-catalyzed radical polymerization, reduction/oxidation

polymerization, bioorthogonal polymerization, and the latest bacteria-powered radical polymerization, have been successfully implemented extra/intracellularly. Most of the numerous designed cell-mediated polymerization reactions require catalysts, toxic conditions (ultraviolet light, free radicals, and organic solvent), harsh conditions (hypoxic or anaerobic), and complicated pretreatment processes (genetic modification). Thus, developing new strategies depending on simple and biologically benign reaction conditions is extremely urgent.

As a result, diverse supramolecular polymers have been *in situ* established extra/intracellularly. The reversible and dynamic noncovalent interactions endow supramolecular polymers with stimuli-responsiveness and biodegradability properties, thus reducing toxic side effects on normal cells and avoiding long-term immunotoxicity. Unlike traditional supramolecular structures developed based on weak and single noncovalent interactions, supramolecular polymers are the products of multiple noncovalent forces, making their structure formation and maintenance under dynamic environments relatively feasible. Nevertheless, ELMs still face some challenges: (1) intracellular ELMs are rarely generated in selected cells or a specific organelle; (2) extracellular fabrication of polymeric materials seems easy because most ELMs are initiated on or near the cell membrane, but intracellular biomimetic self-assemblies, which must survive in the complex intracellular microenvironment are rare, thus requiring more efforts to be concentrated on the development of intracellular or even *in vivo* ELMs; (3) the chemical structures of ELMs are usually systematically characterized *in vitro*, but their theranostic mechanisms are not well investigated. A rational combination of high therapeutic efficiency and the thorough treatment mechanism can push the rapid expansion of the *in situ* biomimetic ELMs.

We propose the five most critical issues hindering the development of ELMs and figure out some possible solutions, which will enrich readers' knowledge and facilitate in-depth research.

### (a) Precise regulation of polymerization reaction rate and conversion rate

The long-term existence of highly active free radical states in cells can often damage the cells. Therefore, it is significant to enhance the polymerization reaction kinetics to minimize the influence of harmful free radicals. The polymerization reaction kinetics can be enhanced as follows:

(1) Improving the polymerization activity of monomer molecules. The stability of free radicals of monomer molecules determines the regulation of monomer activity, which can be considered from the following aspects: resonance effects, charge effects (push-pull effects), and steric effects. For example, methacrylate has more stable free radicals than acrylate due to the steric hindrance effect of methacrylate, and the reaction rate is much faster. Thus, the monomers can be rationally modified with different groups according to the specific circumstances and cells for polymerization.

(2) Enhancing the initiation efficiency. Conventional initiation methods, such as light-initiating or thermal-initiating methods, are not applicable due to the poor penetration of light and heat *in vivo* (initiation energy). Therefore, to enhance

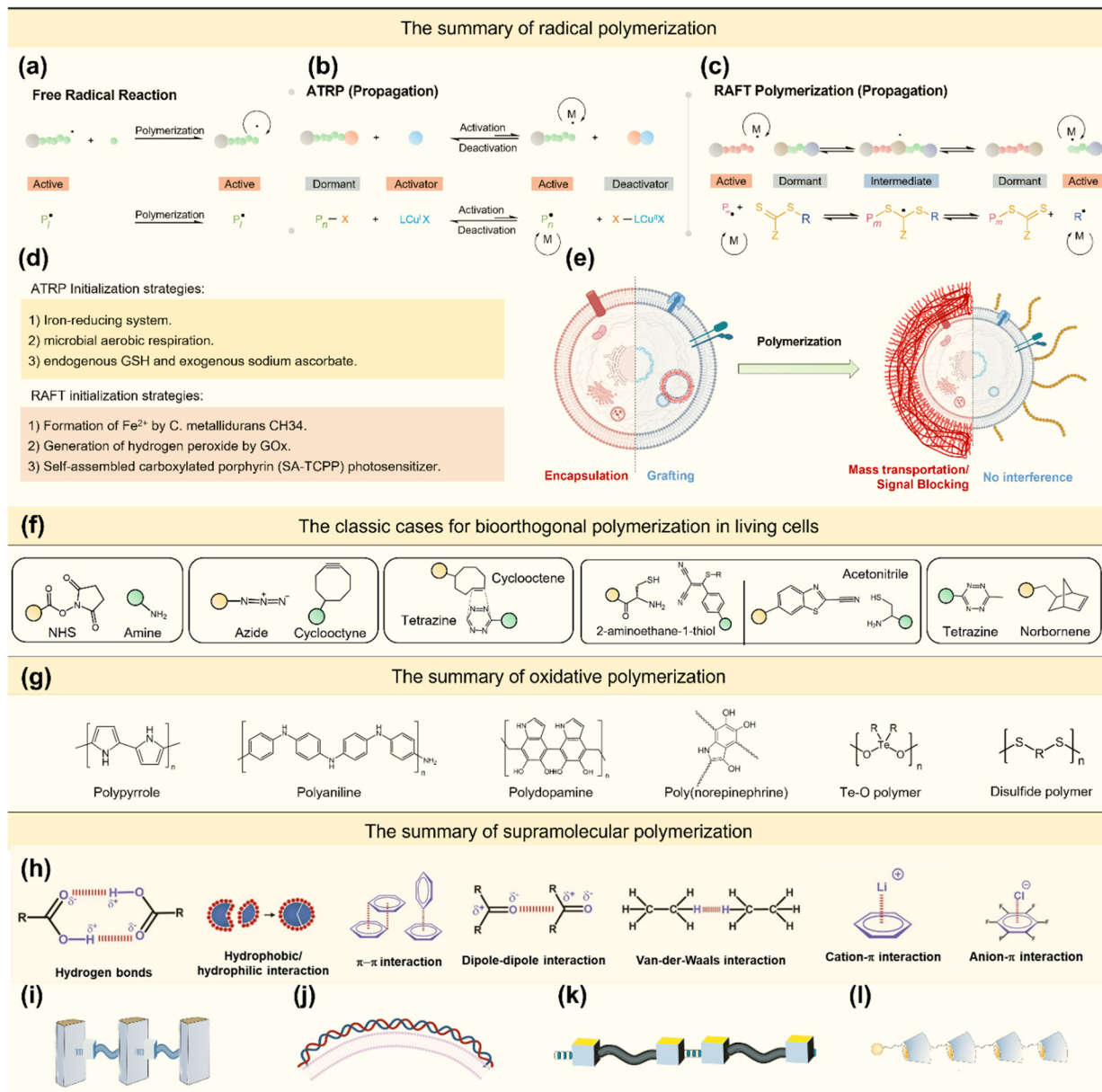


**Fig. 19** Overall summary of polymerization in living organisms. (a–c) Depiction of radical polymerization in living organisms. (a) Basic principle of free radical polymerization. (b) and (c) Two most common polymerization modes in the living organisms, and their special initiation modes in living organisms. (e) New generation polymerization strategy (grafting methods) for the modification of cells compared to traditional encapsulation methods. (f) Toolbox for bioorthogonal polymerization. (g) Reported polymer mini-library based on oxidative polymerization. (h–l) Overall guidelines for supramolecular polymerization. (h) List of common met supramolecular interactions. (i–l) Reported interaction modes between the supramolecular monomers. (i) Stacking of building blocks. (j) Adsorption of two parts. (k) Direct polymerization of monomers. (l) Polymerization driven by the host-guest recognition.

the initiation efficiency of polymerization, the current mainstream method uses peroxides as initiators in the body or photoinitiators with longer absorption wavelengths. Notably, newly proposed electrochemical-regulated radical polymerization and ultrasonically regulated controlled radical polymerization reactions are promising, because the high penetration depth of ultrasound and electrical field is remarkably favorable to initiate the polymerization *in vitro* and *in vivo*.

(3) Choosing suitable catalysts. Most catalyst used in polymerization are pristine ions, metal-ligand complexes, or bulky clusters,

biosafety of which is always considered. In addition, the catalytic capability can be easily diminished by the intracellular components, especially for the sulfur-containing compounds. The incorporation of active catalysts into nanoparticles might resolve the issue. For example, the chelator ligands can be grafted or physically encapsulated by polymeric or inorganic nanoformulations to protect the active catalytic sites during delivery. The catalytic capability is activated at the sites of interest by de-shielding the matrix materials in response to the intracellular microenvironment, thus optimizing the polymerization and preventing unwanted cytotoxicity.

### (b) Precise polymerization in specific cells or organelles

For biomedical applications, the polymerization should be precisely controlled at a cellular or even an organelle level. To reduce the disturbance to the rest of the body the organism, specific transportation of drugs to the pathological sites can effectively improve curative performances and reduce systemic toxicity. Encapsulation of functional monomers into nano-sized delivery systems with sophisticated stimuli-responsiveness is believed to be a straightforward method to realize precise polymerization *in vitro* and *in vivo*. We conceptualize a new targeting methodology, tertiary-mediated targeting (TMT), which is promising in targeting specific organelles of specific cells in specific organs. Compared with conventional non-selective polymerization, precise polymerization can significantly improve disease diagnosis and efficiently restore cellular function.

(1) The first order: organ targeting. It can be achieved by manipulating the physical and chemical properties of delivery systems, including size, charge, components, amphiphilicity and stability. For example, selective organ-targeting nanoparticles can be fabricated by varying the zeta potential of lipid nanoparticles. The nanoparticles are delivered specifically to the lungs, liver, spleen, and lymph nodes. In addition, nanoformulations can be enshrouded by a layer of biomolecules in the bloodstream to form a protein corona, which plays a pivotal role in organ-targeted delivery. The protein compositions in the corona vary according to the amphiphilicity and stability of nanoformulations. The interactions between the surface-bound proteins and cognate receptors highly expressed in specific tissues lead to organ-targeting effects.

(2) The second order: cell targeting. It can be achieved by modifying the nanoformulations with targeting ligands, such as antibodies, peptides and other small molecules that can interact with the receptors on the cell membrane. Antibodies exhibit extremely high binding affinity, and chemical modifications possibly denature these ligands. Moreover, the introduction of antibodies on the surface might increase the size of the resulting delivery systems. Peptides and other small molecules show outstanding tolerance to chemical reactions, while their stability and targeting effect *in vivo* are sometimes unsatisfactory. Thus, it is necessary to establish a balance between their advantages and disadvantages in biomedical applications.

(3) The third order: organelle targeting. It can be achieved by conjugating ligands to monomers. Morpholine, TPP, and methyl sulphonamide moieties have demonstrated excellent targeting ability toward lyso/endosomes, mitochondria, and endoplasmic reticulum, respectively. These groups can be easily conjugated to the monomers, thus facilitating the polymerization in targeting organelles.

### (c) Expanding the types of monomers

The problem of short fluorescence lifetime of imaging probes and poor pharmacokinetics of small-molecule drugs can be overcome by coupling the molecules to polymer segments, or directly designing imaging probes and small molecules into polymerizable monomers followed by initiation of polymerization reaction.

Therefore, broadening the current library of polymerizable small-molecule drugs or imaging probes is a key issue.

To enrich the theranostic functions, diagnostic and therapeutic monomers are urgently desired for *in situ* polymerization. Fluorescence dyes, radiolabeling chelators, chemotherapeutics, and immune-regulating drugs can be modified with polymerizable groups, such as acrylate and methacrylate. Owing to the multivalent effect of polymerization, it is expected to improve the sensitivity and resolution of imaging signals. For therapeutic applications, the efflux phenomenon responsible for drug resistance can be solved through the intracellular polymerization of prodrug monomers. The use of cleavable linkers facilitates the release of potent drugs from the formed polymers or assemblies to activate their therapeutic functions. Moreover, the polymerization modifications should be scrutinized during design. There are also ideas to screen small molecules with both polymerizable sites and pharmacodynamic activity from the molecule database through high-throughput screening using artificial intelligence with powerful prediction ability.

In addition to the pharmacophoric moiety that exerts therapeutic effects and polymerizable functional groups, domains that can regulate the solubility of the entire drug, activate pharmacophoric moieties, or have an enrichment effect on specific organs or cells, can also be integrated. For example, the introduction of sugar compounds and peptides consistently improves solubility, favoring their pharmacokinetic behaviors and final therapeutic performances.

### (d) Development of novel polymerization methods

The current polymerization methods mainly focus on free radical-mediated polymerization. However, due to the damage caused by free radicals to the cells and the rigorous reaction conditions, it is necessary to develop new polymerization methods.

(1) Cascade reactions for polymerization. After delivery of non-toxic and inactive molecular precursors to targeting cells, specific enzymes in the cells endow monomers with pharmacological activity and polymerization activity, thereby realizing cascade polymerization reactions. At present, there are very few reported cases of this line of thought. However, the polymerization cascade reaction has a broad application, because it can solve the issue of toxic and side effects of monomer molecules due to off-targeting, that is, to exert drug efficacy only at the active sites.

(2) Bioorthogonal polymerization. Several cases of bioorthogonal polymerization in living organisms have been reported. However, various polymerization modes can be developed combined with the high-efficiency characteristics of bioorthogonal reactions. For example, the modification of monomers with orthogonal groups (Fig. 19f) endows the monomers with the ability to polymerize in complex microenvironments.

(3) Biological enzyme-catalyzed polymerization. Biological enzymes have specific and highly efficient catalytic activities. As a result, the monomers can be directly polymerized into polymer chains using enzymes in living organisms. For example, horseradish peroxidase and soybean peroxidase can be used to catalyze the polymerization of phenolic compounds. In addition,

some highly expressed enzymes in the tumor have the ability of targeted enrichment. Tyrosinase in malignant cancer cells can catalyze the polymerization of short peptides to promote antigen cross-presentation, which plays a pivotal role in cancer immunotherapy.

(4) Supramolecular polymerization. It is important to take full advantage of the reversible and stimuli-responsive ability of supramolecular polymeric substances. Noncovalent interactions occur when building blocks are incorporated into monomers, initiating supramolecular polymerization in living organisms. Considering the specific microenvironment in tumors, it is possible to construct supramolecular polymers that can self-assemble only in tumors triggered by abnormal conditions.

Naturally, the assembly of tubulins, and the double helical structure of DNA or DNA origami are identical to hybridization covalent polymerization and supramolecular polymerization. Specifically, the first step can be realized *in situ via* covalent polymerization. The second part of supramolecular polymerization can be recognized by influential intermolecular forces, such as multiple hydrogen bonds. This direction has the potential to realize polymer-based molecular machines in living organisms.

#### (e) Manipulation of cells, bacteria, and viruses

(1) Bacterial manipulation. The regulation of bacteria can be considered from the perspective of antimicrobial resistance. One effective method is the use of a positively charged cationic polymer *via in situ* polymerization, which can agglutinate bacteria in targeting sites through electrostatic interactions due to the negatively charged cell membranes of the bacteria. This approach shows great promise in many post-surgery operations that are highly susceptible to infection, as well as in addressing the problems associated with traditional antibiotics that come with serious side effects and require continuous usage.

(2) Virus manipulation. Virus activity can be influenced by chemical reactions. For example, amine groups on the surface of the virus can react with epoxy compounds or formaldehyde, which is the basic principle for manufacturing inactivated or attenuated virus vaccines. Therefore, the spike proteins on the surface of the virus can possibly be engineered as the sites for polymerization, inhibiting the ability of the virus to infect and multiply. Thus, the virus can be converted into a potential vaccine in one step.

(3) Cell manipulation. Intracellular polymerization can significantly change the cell cycle, cytoskeleton structure, cell motility, and other properties. Liver fibrosis, thrombosis and other vital diseases are expected to be regulated through intracellular polymerization. For example, liver fibrosis is often caused by excessive accumulation of extracellular matrix. The metabolism of the superfluous extracellular matrix plays a vital role in chronic inflammatory diseases. Long-term regulation of the microenvironment in the pathological area can be achieved through *in situ* polymerization of inflammatory regulatory molecules in the extracellular matrix.

Unlike the regulation of other cellular functions, direct manipulation of immune cells is of a higher value, especially

in cancer therapy and autoimmune diseases. T cells, responsible for the elimination of cancer cells, are often tricked by immune checkpoints on cancer cells, which lead to premature exhaustion of T cells. One of the important reasons is that the glycosylation signal recognition on the surface of cancer cells can manipulate T cells. As a result, it has become a promising alternative to traditional antibodies with glycan molecules through polymerization reactions, especially sugar polymerization reactions. However, manipulating sugar synthesis *in vivo* remains blank or unknown. As the most critical and powerful antigen-presenting cells of acquired immunity, the development of dendritic cells (DCs) is one of the most effective ways to stimulate the body's immune system to resist cancer and virus invasion. It will be a milestone if the activation and antigen-presentation of DCs can be regulated by polymerizing unique monomers inside the cells. In addition, the repolarization of macrophages in the tumor microenvironment and the disruption of interactions between tumors and T cells need to be further explored using the tool of *in situ* polymerization by researchers.

The Nobel Prize of 2022 was awarded for the scientists who found the click chemistry and bioorthogonal chemistry.<sup>215</sup> Bioorthogonal chemistry is particularly attractive for its ability to conduct reactions within living organisms without interfering with intrinsic chemical reactions. On the other hand, *in situ* polymerization involves creating multifunctional polymers within living organisms, and polymers play a central role in all stages of life activities. *In vivo* polymerization that can be achieved through bioorthogonal chemistry and free radicals has emerged as a direct regulator of metabolism, immunity, and signal transduction. Therefore, it is of great significance to explore the *in situ* polymerization reaction *in vivo*. By combining advanced nanotechnology with polymer chemistry,<sup>216–218</sup> more breakthroughs can be expected in the field of polymerization in living organisms, which will ultimately benefit humanity in the near future.

## Conflicts of interest

There are no conflicts to declare.

## Acknowledgements

This work was supported by the National Key Research and Development Program of China (2021YFA0910100), the Vanke Special Fund for Public Health and Health Discipline Development, Tsinghua University (2022Z82WKJ005 and 2022Z82WKJ013), the Tsinghua University Spring Breeze Fund (2021Z99CFZ007), the National Natural Science Foundation of China (22175107), the Starry Night Science Fund of Zhejiang University Shanghai Institute for Advanced Study (SN-ZJU-SIAS-006), the Zhejiang Provincial Natural Science Foundation of China (LQ20B040001 and LZ21E030002).

## References

- 1 N. S. Simmons and E. R. Blout, *Biophys. J.*, 1960, **1**, 55–62.
- 2 A. C. H. Durham and A. Klug, *Nat. New Biol.*, 1971, **229**, 42–46.

- 3 T. Lino, *J. Supramol. Struct.*, 1974, **2**, 372–384.
- 4 T. D. Pollard and G. G. Borisy, *Cell*, 2003, **112**, 453–465.
- 5 D. M. Fowler, A. V. Koulov, W. E. Balch and J. W. Kelly, *Trends Biochem. Sci.*, 2007, **32**, 217–224.
- 6 M. D. Shoulders and R. T. Raines, *Annu. Rev. Biochem.*, 2009, **78**, 929–958.
- 7 D. A. Fletcher and R. D. Mullins, *Nature*, 2010, **463**, 485–492.
- 8 F. Huber, J. Schnauß, S. Rönicke, P. Rauch, K. Müller, C. Fütterer and J. Kas, *Adv. Phys.*, 2013, **62**, 1–112.
- 9 T. P. J. Knowles, M. Vendruscolo and C. M. Dobson, *Nat. Rev. Mol. Cell Biol.*, 2014, **15**, 384–396.
- 10 J. Bromberg and J. E. Darnell Jr, *Oncogene*, 2000, **19**, 2468–2473.
- 11 D. Jo, D. Liu, S. Yao, R. D. Collins and J. Hawiger, *Nat. Med.*, 2005, **11**, 892–898.
- 12 H. Ishikawa, Z. Ma and G. N. Barber, *Nature*, 2009, **461**, 788–792.
- 13 V. Hornung and E. Latz, *Nat. Rev. Immunol.*, 2010, **10**, 123–130.
- 14 M. Kushwaha, W. Rostain, S. Prakash, J. N. Duncan and A. Jaramillo, *ACS Synth. Biol.*, 2016, **5**, 795–809.
- 15 L. He, D. Lu, H. Liang, S. Xie, X. Zhang, Q. Liu, Q. Yuan and W. Tan, *J. Am. Chem. Soc.*, 2018, **140**, 258–263.
- 16 S. Li, Q. Jiang, S. Liu, Y. Zhang, Y. Tian, C. Song, J. Wang, Y. Zou, G. J. Anderson, J.-Y. Han, Y. Chang, Y. Liu, C. Zhang, L. Chen, G. Zhou, G. Nie, H. Yan, B. Ding and Y. Zhao, *Nat. Biotechnol.*, 2018, **36**, 258–264.
- 17 L.-S. Lin, T. Huang, J. Song, X.-Y. Ou, Z. Wang, H. Deng, R. Tian, Y. Liu, J.-F. Wang, Y. Liu, G. Yu, Z. Zhou, S. Wang, G. Niu, H.-H. Yang and X. Chen, *J. Am. Chem. Soc.*, 2019, **141**, 9937–9945.
- 18 D.-B. Cheng, D. Wang, Y.-J. Gao, L. Wang, Z.-Y. Qiao and H. Wang, *J. Am. Chem. Soc.*, 2019, **141**, 4406–4411.
- 19 W. Tan, Q. Zhang, J. Wang, M. Yi, H. He and B. Xu, *Angew. Chem., Int. Ed.*, 2021, **60**, 12796–12801.
- 20 T. Li, S. Pan, S. Gao, W. Xiang, C. Sun, W. Cao and H. Xu, *Angew. Chem., Int. Ed.*, 2020, **59**, 2700–2704.
- 21 S. Gao, T. Li, Y. Guo, C. Sun, B. Xianyu and H. Xu, *Adv. Mater.*, 2020, **32**, e1907568.
- 22 M. Pieszka, S. Han, C. Volkmann, R. Graf, I. Lieberwirth, K. Landfester, D. Y. W. Ng and T. Weil, *J. Am. Chem. Soc.*, 2020, **142**, 15780–15789.
- 23 W. Xuan, Y. Xia, T. Li, L. Wang, Y. Liu and W. Tan, *J. Am. Chem. Soc.*, 2020, **142**, 937–944.
- 24 R. F. Fakhrullin, A. I. Zamaleeva, R. T. Minullina, S. A. Konnova and V. N. Paunov, *Chem. Soc. Rev.*, 2012, **41**, 4189–4206.
- 25 R. F. Fakhrullin and Y. M. Lvov, *ACS Nano*, 2012, **6**, 4557–4564.
- 26 I. Drachuk, M. K. Gupta and V. V. Tsukruk, *Adv. Funct. Mater.*, 2013, **23**, 4437–4453.
- 27 P. Q. Nguyen, N.-M. D. Courchesne, A. Duraj-Thatte, P. Praveschotinunt and N. S. Joshi, *Adv. Mater.*, 2018, **30**, e1704847.
- 28 C. Gilbert and T. Ellis, *ACS Synth. Biol.*, 2019, **8**, 1–15.
- 29 M. F. Moradali and B. H. A. Rehm, *Nat. Rev. Microbiol.*, 2020, **18**, 195–210.
- 30 C. M. Heveran, S. L. Williams, J. Qiu, J. Artier, M. H. Hubler, S. M. Cook, J. C. Cameron and W. V. Sruubar, *Matter*, 2020, **2**, 481–494.
- 31 N. Kampf, *Polym. Adv. Technol.*, 2002, **13**, 895–904.
- 32 J. H. Park, S. H. Yang, J. Lee, E. H. Ko, D. Hong and I. S. Choi, *Adv. Mater.*, 2014, **26**, 2001–2010.
- 33 V. X. Truong, M. P. Ablett, S. M. Richardson, J. A. Hoyland and A. P. Dove, *J. Am. Chem. Soc.*, 2015, **137**, 1618–1622.
- 34 Z. M. Liu, X. R. Xu and R. K. Tang, *Adv. Funct. Mater.*, 2016, **26**, 1862–1880.
- 35 D. Hong, M. Park, S. H. Yang, J. Lee, Y.-G. Kim and I. S. Choi, *Trends Biotechnol.*, 2013, **31**, 442–447.
- 36 Q. Wei, K. Achazi, H. Liebe, A. Schulz, P.-L. M. Noeske, I. Grunwald and R. Haag, *Angew. Chem., Int. Ed.*, 2014, **53**, 11650–11655.
- 37 H. C. Yang, J. Q. Luo, Y. Lv, P. Shen and Z. K. Xu, *J. Membr. Sci.*, 2015, **483**, 42–59.
- 38 M. Tanaka, K. Sato, E. Kitakami, S. Kobayashi and K. Fukushima, *Polym. J.*, 2015, **47**, 114–121.
- 39 A. S. Mao, J.-W. Shin, S. Utech, H. Wang, O. Uzun, W. Li, M. Cooper, Y. Hu, L. Zhang, D. A. Weitz and D. J. Mooney, *Nat. Mater.*, 2017, **16**, 236–243.
- 40 J. Niu, D. J. Lunn, A. Pusuluri, J. I. Yoo, M. A. O'Malley, S. Mitragotri, H. T. Soh and C. J. Hawker, *Nat. Chem.*, 2017, **9**, 537–545.
- 41 N. George, H. Pick, H. Vogel, N. Johnsson and K. Johnsson, *J. Am. Chem. Soc.*, 2004, **126**, 8896–8897.
- 42 S. Boonyarattanakalin, S. E. Martin, Q. Sun and B. R. Peterson, *J. Am. Chem. Soc.*, 2006, **128**, 11463–11470.
- 43 S. T. Laughlin, J. M. Baskin, S. L. Amacher and C. R. Bertozzi, *Science*, 2008, **320**, 664–667.
- 44 J. T. Wilson, V. R. Krishnamurthy, W. Cui, Z. Qu and E. L. Chaikof, *J. Am. Chem. Soc.*, 2009, **131**, 18228–18229.
- 45 N. A. A. Rossi, I. Constantinescu, D. E. Brooks, M. D. Scott and J. N. Kizhakkedathu, *J. Am. Chem. Soc.*, 2010, **132**, 3423–3430.
- 46 J. T. Wilson, W. Cui, V. Kozlovskaya, E. Kharlampieva, D. Pan, Z. Qu, V. R. Krishnamurthy, J. Mets, V. Kumar, J. Wen, Y. Song, V. V. Tsukruk and E. L. Chaikof, *J. Am. Chem. Soc.*, 2011, **133**, 7054–7064.
- 47 C. S. Bahney, T. J. Lujan, C. W. Hsu, M. Bottlang, J. L. West and B. Johnstone, *Eur. Cell Mater.*, 2011, **22**, 43–55.
- 48 H. Shih and C.-C. Lin, *Macromol. Rapid Commun.*, 2013, **34**, 269–273.
- 49 E. P. Magennis, F. Fernandez-Trillo, C. Sui, S. G. Spain, D. J. Bradshaw, D. Churchley, G. Mantovani, K. Winzer and C. Alexander, *Nat. Mater.*, 2014, **13**, 748–755.
- 50 J. L. Lilly, G. Romero, W. Xu, H. Y. Shin and B. J. Berron, *Biomacromolecules*, 2015, **16**, 541–549.
- 51 I. Cobo, M. Li, B. S. Sumerlin and S. Perrier, *Nat. Mater.*, 2015, **14**, 143–159.
- 52 T. Klaus, R. Joerger, E. Olsson and C.-G. Granqvist, *Proc. Natl. Acad. Sci. U. S. A.*, 1999, **96**, 13611–13614.

- 53 R. Y. Sweeney, C. Mao, X. Gao, J. L. Burt, A. M. Belcher, G. Georgiou and B. L. Iverson, *Chem. Biol.*, 2004, **11**, 1553–1559.
- 54 X. Ma, H. Chen, L. Yang, K. Wang, Y. Guo and L. Yuan, *Angew. Chem., Int. Ed.*, 2011, **50**, 7414–7417.
- 55 W. A. El-Said, H.-Y. Cho, C.-H. Yea and J.-W. Choi, *Adv. Mater.*, 2014, **26**, 910–918.
- 56 R. Cui, H.-H. Liu, H.-Y. Xie, Z.-L. Zhang, Y.-R. Yang, D.-W. Pang, Z.-X. Xie, B.-B. Chen, B. Hu and P. Shen, *Adv. Funct. Mater.*, 2009, **19**, 2359–2364.
- 57 Y. Li, R. Cui, P. Zhang, B.-B. Chen, Z.-Q. Tian, L. Li, B. Hu, D.-W. Pang and Z.-X. Xie, *ACS Nano*, 2013, **7**, 2240–2248.
- 58 A. Ramanavicius, E. Andriukonis, A. Stirke, L. Mikoliunaite, Z. Balevicius and A. Ramanaviciene, *Enzyme Microb. Technol.*, 2016, **83**, 40–47.
- 59 R.-B. Song, Y. Wu, Z.-Q. Lin, J. Xie, C. H. Tan, J. S. C. Loo, B. Cao, J.-R. Zhang, J.-J. Zhu and Q. Zhang, *Angew. Chem., Int. Ed.*, 2017, **56**, 10516–10520.
- 60 E. Andriukonis, A. Stirke, A. Garbaras, L. Mikoliunaite, A. Ramanaviciene, V. Remeikis, B. Thornton and A. Ramanavicius, *Colloids Surf., B*, 2018, **164**, 224–231.
- 61 H. G. Sherman, J. M. Hicks, A. Jain, J. J. Titman, C. Alexander, S. Stolnik and F. J. Rawson, *ChemBioChem*, 2019, **20**, 1008–1013.
- 62 M. R. Bennett, P. Gurnani, P. J. Hill, C. Alexander and F. J. Rawson, *Angew. Chem., Int. Ed.*, 2020, **59**, 4750–4755.
- 63 C. W. Pester, B. Narupai, K. M. Mattson, D. P. Bothman, D. Klinger, K. W. Lee, E. H. Discekici and C. J. Hawker, *Adv. Mater.*, 2016, **28**, 9292–9300.
- 64 B. Narupai, Z. A. Page, N. J. Treat, A. J. McGrath, C. W. Pester, E. H. Discekici, N. D. Dolinski, G. F. Meyers, J. R. de Alaniz and C. J. Hawker, *Angew. Chem., Int. Ed.*, 2018, **57**, 13433–13438.
- 65 A. J. Gormley, J. Yeow, G. Ng, Ó. Conway, C. Boyer and R. Chapman, *Angew. Chem., Int. Ed.*, 2018, **57**, 1557–1562.
- 66 J. Yeow, R. Chapman, A. J. Gormley and C. Boyer, *Chem. Soc. Rev.*, 2018, **47**, 4357–4387.
- 67 G. Fan, A. J. Graham, J. Kolli, N. A. Lynd and B. K. Keitz, *Nat. Chem.*, 2020, **12**, 638–646.
- 68 J. Y. Kim, B. S. Lee, J. Choi, B. J. Kim, J. Y. Choi, S. M. Kang, S. H. Yang and I. S. Choi, *Angew. Chem., Int. Ed.*, 2016, **55**, 15306–15309.
- 69 T. J. Little, J. E. Allen, S. A. Babayan, K. R. Matthews and N. Colegrave, *Nat. Med.*, 2012, **18**, 217–220.
- 70 T.-Y. Liu, K.-T. Tsai, H.-H. Wang, Y. Chen, Y.-H. Chen, Y.-C. Chao, H.-H. Chang, C.-H. Lin, J.-K. Wang and Y.-L. Wang, *Nat. Commun.*, 2011, **2**, 538.
- 71 E. J. Smith, W. Xi, D. Makarov, I. Mönch, S. Harazim, V. A. B. Quiñones, C. K. Schmidt, Y. Mei, S. Sanchez and O. G. Schmidt, *Lab Chip*, 2012, **12**, 1917–1931.
- 72 K. Matyjaszewski, W. Jakubowski, K. Min, W. Tang, J. Huang, W. A. Braunecker and N. V. Tsarevsky, *Proc. Natl. Acad. Sci. U. S. A.*, 2006, **103**, 15309–15314.
- 73 C. Boyer, N. A. Corrigan, K. Jung, D. Nguyen, T.-K. Nguyen, N. N. M. Adnan, S. Oliver, S. Shanmugam and J. Yeow, *Chem. Rev.*, 2016, **116**, 1803–1949.
- 74 D. C. Kennedy, C. S. McKay, M. C. B. Legault, D. C. Danielson, J. A. Blake, A. F. Pegoraro, A. Stolow, Z. Mester and J. P. Pezacki, *J. Am. Chem. Soc.*, 2011, **133**, 17993–18001.
- 75 Q. Shen, Y. Huang, Y. Zeng, E. Zhang, F. Lv, L. Liu and S. Wang, *ACS Mater. Lett.*, 2021, **3**, 1307–1314.
- 76 G. Fan, C. M. Dundas, A. J. Graham, N. A. Lynd and B. K. Keitz, *Proc. Natl. Acad. Sci. U. S. A.*, 2018, **115**, 4559–4564.
- 77 M. Ouchi and M. Sawamoto, *Macromolecules*, 2017, **50**, 2603–2614.
- 78 S. Perrier, *Macromolecules*, 2017, **50**, 7433–7447.
- 79 M. R. Bennett, C. Moloney, F. Catrambone, F. Turco, B. Myers, K. Kovacs, P. J. Hill, C. Alexander, F. J. Rawson and P. Gurnani, *ACS Macro Lett.*, 2022, **11**, 954–960.
- 80 N. Corrigan, L. Zhernakov, M. H. Hashim, J. Xu and C. Boyer, *React. Chem. Eng.*, 2019, **4**, 1216–1228.
- 81 J. Xu, S. Shanmugam, H. T. Duong and C. Boyer, *Polym. Chem.*, 2015, **6**, 5615–5624.
- 82 C. Wu, S. Shanmugam, J. Xu, J. Zhu and C. Boyer, *Chem. Commun.*, 2017, **53**, 12560–12563.
- 83 F. Zhou, R. Li, X. Wang, S. Du and Z. An, *Angew. Chem., Int. Ed.*, 2019, **58**, 9479–9484.
- 84 S. Allison-Logan, Q. Fu, Y. Sun, M. Liu, J. Xie, J. Tang and G. G. Qiao, *Angew. Chem., Int. Ed.*, 2020, **59**, 21392–21396.
- 85 Y. Luo, Y. Gu, R. Feng, J. Brash, A. M. Eissa, D. M. Haddleton, G. Chen and H. Chen, *Chem. Sci.*, 2019, **10**, 5251–5257.
- 86 M. D. Nothling, H. Cao, T. G. McKenzie, D. M. Hocking, R. A. Strugnell and G. G. Qiao, *J. Am. Chem. Soc.*, 2021, **143**, 286–293.
- 87 T. Mazaki, Y. Shiozaki, K. Yamane, A. Yoshida, M. Nakamura, Y. Yoshida, D. Zhou, T. Kitajima, M. Tanaka, Y. Ito, T. Ozaki and A. Matsukawa, *Sci. Rep.*, 2014, **4**, 4457.
- 88 M. Chen, M. Zhong and J. A. Johnson, *Chem. Rev.*, 2016, **116**, 10167–10211.
- 89 Y. Zhang, Q. Gao, W. Li, R. He, L. Zhu, Q. Lian, L. Wang, Y. Li, M. Bradley and J. Geng, *JACS Au*, 2022, **2**, 579–589.
- 90 M. T. Stephan, J. J. Moon, S. H. Um, A. Bershteyn and D. J. Irvine, *Nat. Med.*, 2010, **16**, 1035–1041.
- 91 W. Youn, E. H. Ko, M.-H. Kim, M. Park, D. Hong, G. A. Seisenbaeva, V. G. Kessler and I. S. Choi, *Angew. Chem., Int. Ed.*, 2017, **56**, 10702–10706.
- 92 G. Wang, K. Zhang, Y. Wang, C. Zhao, B. He, Y. Ma and W. Yang, *Chem. Commun.*, 2018, **54**, 4677–4680.
- 93 B. J. Kim, H. Cho, J. H. Park, J. F. Mano and I. S. Choi, *Adv. Mater.*, 2018, **30**, e1706063.
- 94 M. Matsusaki, K. Kadowaki, Y. Nakahara and M. Akashi, *Angew. Chem., Int. Ed.*, 2007, **46**, 4689–4692.
- 95 V. M. Gaspar, P. Lavrador, J. Borges, M. B. Oliveira and J. F. Mano, *Adv. Mater.*, 2020, **32**, e1903975.
- 96 K. Liang, J. J. Richardson, J. Cui, F. Caruso, C. J. Doona and P. Falcaro, *Adv. Mater.*, 2016, **28**, 7910–7914.
- 97 K. Liang, J. J. Richardson, C. J. Doonan, X. Mulet, Y. Ju, J. Cui, F. Caruso and P. Falcaro, *Angew. Chem., Int. Ed.*, 2017, **56**, 8510–8515.

- 98 W. Zhu, J. Guo, S. Amini, Y. Ju, J. O. Agola, A. Zimpel, J. Shang, A. Nouredine, F. Caruso, S. Wuttke, J. G. Croissant and C. J. Brinker, *Adv. Mater.*, 2019, **31**, e1900545.
- 99 C. Jiao, C. Zhao, Y. Ma and W. Yang, *ACS Nano*, 2021, **15**, 15920–15929.
- 100 L. Tan, A. Wan and H. Li, *ACS Appl. Mater. Interfaces*, 2014, **6**, 18–23.
- 101 J. Geng, W. Li, Y. Zhang, N. Thottappillil, J. Clavadetscher, A. Lilienkampf and M. Bradley, *Nat. Chem.*, 2019, **11**, 578–586.
- 102 S. Soukasene, D. J. Toft, T. J. Moyer, H. Lu, H.-K. Lee, S. M. Standley, V. L. Cryns and S. I. Stupp, *ACS Nano*, 2011, **5**, 9113–9121.
- 103 Z. Song, X. Chen, X. You, K. Huang, A. Dhinakar, Z. Gu and J. Wu, *Biomater. Sci.*, 2017, **5**, 2369–2380.
- 104 M. Urello, W.-H. Hsu and R. J. Christie, *Acta Biomater.*, 2020, **117**, 40–59.
- 105 P. Neuberg, A. Wagner, J.-S. Remy and A. Kichler, *Int. J. Pharm.*, 2019, **566**, 141–148.
- 106 S. Pavan and F. Berti, *Anal. Bioanal. Chem.*, 2012, **402**, 3055–3070.
- 107 C. Karavasili and D. G. Fatouros, *Adv. Drug Delivery Rev.*, 2021, **174**, 387–405.
- 108 A. Dasgupta and D. Das, *Langmuir*, 2019, **35**, 10704–10724.
- 109 I. W. Hamley, *Chem. Commun.*, 2015, **51**, 8574–8583.
- 110 N. Lv, X. Yin, Z. Yang, T. Ma, H. Qin, B. Xiong, H. Jiang and J. Zhu, *ACS Macro Lett.*, 2022, **11**, 223–229.
- 111 Y. Zhang, M. Üçüncü, A. Gambardella, A. Baibek, J. Geng, S. Zhang, J. Clavadetscher, I. Litzen, M. Bradley and A. Lilienkampf, *J. Am. Chem. Soc.*, 2020, **142**, 21615–21621.
- 112 T.-A. Read, D. R. Sorensen, R. Mahesparan, P. O. Enger, R. Timpl, B. R. Olsen, M. H. B. Hjelstuen, O. Haraldseth and R. Bjerkgvig, *Nat. Biotechnol.*, 2001, **19**, 29–34.
- 113 D. Seliktar, *Science*, 2012, **336**, 1124–1128.
- 114 T. Vermonden, R. Censi and W. E. Hennink, *Chem. Rev.*, 2012, **112**, 2853–2858.
- 115 H. J. Kong and D. J. Mooney, *Nat. Rev. Drug Discovery*, 2007, **6**, 455–463.
- 116 D. Steinhilber, M. Witting, X. Zhang, M. Staegemann, F. Paulus, W. Friess, S. Küchler and R. Haag, *J. Controlled Release*, 2013, **169**, 289–295.
- 117 M. C. Parrott, J. C. Luft, J. D. Byrne, J. H. Fain, M. E. Napier and J. M. DeSimone, *J. Am. Chem. Soc.*, 2010, **132**, 17928–17932.
- 118 D. Steinhilber, S. Seiffert, J. A. Heyman, F. Paulus, D. A. Weitz and R. Haag, *Biomaterials*, 2011, **32**, 1311–1316.
- 119 D. Steinhilber, T. Rossow, S. Wedepohl, F. Paulus, S. Seiffert and R. Haag, *Angew. Chem., Int. Ed.*, 2013, **52**, 13538–13543.
- 120 T. Rossow, J. A. Heyman, A. J. Ehrlicher, A. Langhoff, D. A. Weitz, R. Haag and S. Seiffert, *J. Am. Chem. Soc.*, 2012, **134**, 4983–4989.
- 121 S. Y. Tong, J. S. Davis, E. Eichenberger, T. L. Holland and V. G. Fowler Jr., *Clin. Microbiol. Rev.*, 2015, **28**, 603–661.
- 122 A. S. Lee, H. de Lencastre, J. Garau, J. Kluytmans, S. Malhotra-Kumar, A. Peschel and S. Harbarth, *Nat. Rev. Dis. Primers*, 2018, **4**, 18033.
- 123 L. Varadi, J. L. Luo, D. E. Hibbs, J. D. Perry, R. J. Anderson, S. Orenga and P. W. Groundwater, *Chem. Soc. Rev.*, 2017, **46**, 4818–4832.
- 124 V. Templier and Y. Roupioz, *J. Appl. Microbiol.*, 2017, **123**, 1056–1067.
- 125 C. Yang, C. Ren, J. Zhou, J. Liu, Y. Zhang, F. Huang, D. Ding, B. Xu and J. Liu, *Angew. Chem., Int. Ed.*, 2017, **56**, 2356–2360.
- 126 L. Wu, Y. Ishigaki, W. Zeng, T. Harimoto, B. Yin, Y. Chen, S. Liao, Y. Liu, Y. Sun, X. Zhang, Y. Liu, Y. Liang, P. Sun, T. Suzuki, G. Song, Q. Fan and D. Ye, *Nat. Commun.*, 2021, **12**, 6145.
- 127 L. Xu, W. Zhan, Y. Deng, X. Liu, G. Gao, X. Sun and G. Liang, *Adv. Healthcare Mater.*, 2022, **11**, e2200453.
- 128 E. R. Ruskowitz and C. A. DeForest, *Nat. Rev. Mater.*, 2018, **3**, 1–17.
- 129 K. T. Nguyen and J. L. West, *Biomaterials*, 2002, **23**, 4307–4314.
- 130 E. Jalali and J. S. Thorson, *Curr. Opin. Biotechnol.*, 2021, **69**, 290–298.
- 131 L. Cui, S. Vivona, B. R. Smith, S.-R. Kothapalli, J. Liu, X. Ma, Z. Chen, M. Taylor, P. H. Kierstead, J. M. J. Fréchet, S. S. Gambhir and J. Rao, *J. Am. Chem. Soc.*, 2020, **142**, 15575–15584.
- 132 R. L. Siegel, K. D. Miller and A. Jemal, *Ca-Cancer J. Clin.*, 2020, **70**, 7–30.
- 133 Z. Zeng, S. S. Liew, X. Wei and K. Pu, *Angew. Chem., Int. Ed.*, 2021, **60**, 26454–26475.
- 134 B. Bian, S. Mongrain, S. Cagnol, M.-J. Langlois, J. Boulanger, G. Bernatchez, J. C. Carrier, F. Boudreau and N. Rivard, *Mol. Carcinog.*, 2016, **55**, 671–687.
- 135 Y. Zhang, S. He, W. Chen, Y. Liu, X. Zhang, Q. Miao and K. Pu, *Angew. Chem., Int. Ed.*, 2021, **60**, 5921–5927.
- 136 J. Wu, L. You, S. T. Chaudhry, J. He, J.-X. Cheng and J. Mei, *Anal. Chem.*, 2021, **93**, 3189–3195.
- 137 C. Wang, W. Du, C. Wu, S. Dan, M. Sun, T. Zhang, B. Wang, Y. Yuan and G. Liang, *Angew. Chem., Int. Ed.*, 2022, **61**, e202114766.
- 138 R.-B. Song, K. Yan, Z.-Q. Lin, J. S. C. Loo, L.-J. Pan, Q. Zhang, J.-R. Zhang and J.-J. Zhu, *J. Mater. Chem. A*, 2016, **4**, 14555–14559.
- 139 J. Xie, C.-E. Zhao, Z.-Q. Lin, P.-Y. Gu and Q. Zhang, *Chem. – Asian J.*, 2016, **11**, 1489–1511.
- 140 R.-B. Song, Y. Wu, Z.-Q. Lin, J. Xie, C. H. Tan, J. S. C. Loo, B. Cao, J.-R. Zhang, J.-J. Zhu and Q. Zhang, *Angew. Chem., Int. Ed.*, 2017, **56**, 10516–10520.
- 141 B. Guo and P. X. Ma, *Biomacromolecules*, 2018, **19**, 1764–1782.
- 142 G. Kaur, R. Adhikari, P. Cass, M. Bown and P. Gunatillake, *RSC Adv.*, 2015, **5**, 37553–37567.
- 143 Q. Pan, R. Li, J. Jia and Y. Wang, *J. Mater. Chem. B*, 2020, **8**, 2466–2470.
- 144 L. Tan, A. Wan and H. Li, *ACS Appl. Mater. Interfaces*, 2014, **6**, 18–23.
- 145 X. Ru, P. Liu, T. Liu, X. Ma and L. Yang, *Mater. Sci. Eng., C*, 2021, **120**, 111708.
- 146 K. O. Kim and M. Gluck, *Clin. Endosc.*, 2019, **52**, 137–143.

- 147 S. S. Li, A. Zhu, V. Benes, P. I. Costea, R. Hercog, F. Hildebrand, J. Huerta-Cepas, M. Nieuwdorp, J. Salojärvi, A. Y. Voigt, G. Zeller, S. Sunagawa, W. M. de Vos and P. Bork, *Science*, 2016, **352**, 586–589.
- 148 Y. Zhao, M. Fan, Y. Chen, Z. Liu, C. Shao, B. Jin, X. Wang, L. Hui, S. Wang, Z. Liao, D. Ling, R. Tang and B. Wang, *Sci. Adv.*, 2020, **6**, eaaw9679.
- 149 C. Pan, J. Li, W. Hou, S. Lin, L. Wang, Y. Pang, Y. Wang and J. Liu, *Adv. Mater.*, 2021, **33**, e2007379.
- 150 I. F. Tannock, C. M. Lee, J. K. Tunggal, D. S. M. Cowan and M. J. Egorin, *Clin. Cancer Res.*, 2002, **8**, 878–884.
- 151 A. I. Minchinton and I. F. Tannock, *Nat. Rev. Cancer*, 2006, **6**, 583–592.
- 152 S. Swain, S. P. Kumar, S. Beg and S. M. Babu, *Curr. Drug Delivery*, 2016, **13**, 1290–1302.
- 153 L. Wang, Z. Cao, M. Zhang, S. Lin and J. Liu, *Adv. Mater.*, 2022, **34**, e2106669.
- 154 Y. Lee, K. Sugihara, M. G. Gilliland 3rd, S. Jon, N. Kamada and J. J. Moon, *Nat. Mater.*, 2020, **19**, 118–126.
- 155 C. Shi, J. Dawulieti, F. Shi, C. Yang, Q. Qin, T. Shi, L. Wang, H. Hu, M. Sun, L. Ren, F. Chen, Y. Zhao, F. Liu, M. Li, L. Mu, D. Liu, D. Shao, K. W. Leong and J. She, *Sci. Adv.*, 2022, **8**, eabj2372.
- 156 D. Zhong, D. Zhang, W. Chen, J. He, C. Ren, X. Zhang, N. Kong, W. Tao and M. Zhou, *Sci. Adv.*, 2021, **7**, eabi9265.
- 157 Y. Li, X. He, J.-J. Yin, Y. Ma, P. Zhang, J. Li, Y. Ding, J. Zhang, Y. Zhao, Z. Chai and Z. Zhang, *Angew. Chem., Int. Ed.*, 2015, **54**, 1832–1835.
- 158 G. Jena, P. P. Trivedi and B. Sandala, *Free Radical Res.*, 2012, **46**, 1339–1345.
- 159 L. Chen, Q. You, L. Hu, J. Gao, Q. Meng, W. Liu, X. Wu and Q. Xu, *Front. Immunol.*, 2018, **8**, 1910.
- 160 J. Liu, W. Li, Y. Wang, Y. Ding, A. Lee and Q. Hu, *Nano Today*, 2021, **41**, 101291.
- 161 Z. Li, Y. Wang, J. Liu, P. Rawding, J. Bu, S. Hong and Q. Hu, *Adv. Mater.*, 2021, **33**, e2102580.
- 162 J. Liu, Y. Wang, W. J. Heelan, Y. Chen, Z. Li and Q. Hu, *Sci. Adv.*, 2022, **8**, eabp8798.
- 163 T. Dvir, B. P. Timko, M. D. Brigham, S. R. Naik, S. S. Karajanagi, O. Levy, H. Jin, K. K. Parker, R. Langer and D. S. Kohane, *Nat. Nanotechnol.*, 2011, **6**, 720–725.
- 164 G. Cellot, E. Cilia, S. Cipollone, V. Rancic, A. Sucapane, S. Giordani, L. Gambazzi, H. Markram, M. Grandolfo, D. Scaini, F. Gelain, L. Casalis, M. Prato, M. Giugliano and L. Ballerini, *Nat. Nanotechnol.*, 2009, **4**, 126–133.
- 165 J. Liu, Y. S. Kim, C. E. Richardson, A. Tom, C. Ramakrishnan, F. Birey, T. Katsumata, S. Chen, C. Wang, X. Wang, L.-M. Joubert, Y. Jiang, H. Wang, L. E. Fenno, J. B.-H. Tok, S. P. Pasca, K. Shen, Z. Bao and K. Deisseroth, *Science*, 2020, **367**, 1372–1376.
- 166 V. Ladmiral, M. Semsarilar, I. Canton and S. P. Armes, *J. Am. Chem. Soc.*, 2013, **135**, 13574–13581.
- 167 S. Y. Khor, J. F. Quinn, M. R. Whittaker, N. P. Truong and T. P. Davis, *Macromol. Rapid Commun.*, 2019, **40**, e1800438.
- 168 B. Peng, X. Zhao, M.-S. Yang and L.-L. Li, *J. Mater. Chem. B*, 2019, **7**, 5626–5632.
- 169 S. Kim, B. Jana, E. M. Go, J. E. Lee, S. Jin, E.-K. An, J. Hwang, Y. Sim, S. Son, D. Kim, C. Kim, J.-O. Jin, S. K. Kwak and J.-H. Ryu, *ACS Nano*, 2021, **15**, 14492–14508.
- 170 Y. Dai, T. Li, Z. Zhang, Y. Tan, S. Pan, L. Zhang and H. Xu, *J. Am. Chem. Soc.*, 2021, **143**, 10709–10717.
- 171 B. Kellam, P. A. De Bank and K. M. Shakesheff, *Chem. Soc. Rev.*, 2003, **32**, 327–337.
- 172 J. H. Park, D. Hong, J. Lee and I. S. Choi, *Acc. Chem. Res.*, 2016, **49**, 792–800.
- 173 S. Zhao, L. Zhang, J. Han, J. Chu, H. Wang, X. Chen, Y. Wang, N. Tun, L. Lu, X.-F. Bai, M. Yearsley, S. Devine, X. He and J. Yu, *ACS Nano*, 2016, **10**, 6189–6200.
- 174 S. Köster, F. E. Angilè, H. Duan, J. J. Agresti, A. Wintner, C. Schmitz, A. C. Rowat, C. A. Merten, D. Pisignano, A. D. Griffiths and D. A. Weitz, *Lab Chip*, 2008, **8**, 1110–1115.
- 175 Y. He, T. Ye, M. Su, C. Zhang, A. E. Ribbe, W. Jiang and C. Mao, *Nature*, 2008, **452**, 198–201.
- 176 F. Praetorius and H. Dietz, *Science*, 2017, **355**, eaam5488.
- 177 Y. Ke, L. L. Ong, W. M. Shih and P. Yin, *Science*, 2012, **338**, 1177–1183.
- 178 P. Shi, N. Zhao, J. Coyne and Y. Wang, *Nat. Commun.*, 2019, **10**, 2223.
- 179 P. Hubert, P. Sawma, J.-P. Duneau, J. Khao, J. Hénin, D. Bagnard and J. Sturgis, *Cell Adhes. Migr.*, 2010, **4**, 313–324.
- 180 D. A. Bleijs, M. E. Binnerts, S. J. van Vliet, C. G. Figdor and Y. van Kooyk, *J. Cell Sci.*, 2000, **113**, 391–400.
- 181 F. Yang, Q. Li, L. Wang, G.-J. Zhang and C. Fan, *ACS Sens.*, 2018, **3**, 903–919.
- 182 P. K. Lo, P. Karam, F. A. Aldaye, C. K. McLaughlin, G. D. Hamblin, G. Cosa and H. F. Sleiman, *Nat. Chem.*, 2010, **2**, 319–328.
- 183 A. V. Pinheiro, D. Han, W. M. Shih and H. Yan, *Nat. Nanotechnol.*, 2011, **6**, 763–772.
- 184 J. Li, K. Xun, L. Zheng, X. Peng, L. Qiu and W. Tan, *J. Am. Chem. Soc.*, 2021, **143**, 4585–4592.
- 185 Y. Reinwald, R. K. Johal, A. M. Ghaemmaghami, F. R. A. J. Rose, S. M. Howdle and K. M. Shakesheff, *Polymer*, 2014, **55**, 435–444.
- 186 H. C. Bygd, K. D. Forsmark and K. M. Bratlie, *Biomaterials*, 2015, **56**, 187–197.
- 187 L. Morsut, K. T. Roybal, X. Xiong, R. M. Gordley, S. M. Coyle, M. Thomson and W. A. Lim, *Cell*, 2016, **164**, 780–791.
- 188 T. Gao, T. Chen, C. Feng, X. He, C. Mu, J.-I. Anzai and G. Li, *Nat. Commun.*, 2019, **10**, 2946.
- 189 L. Zhou, F. Lv, L. Liu, G. Shen, X. Yan, G. C. Bazan and S. Wang, *Adv. Mater.*, 2018, **30**, 1704888.
- 190 L. Zhou, F. Lv, L. Liu and S. Wang, *CCS Chem.*, 2019, **1**, 97–105.
- 191 M. Pieszka, S. Han, C. Volkmann, R. Graf, I. Lieberwirth, K. Landfester, D. Y. W. Ng and T. Weil, *J. Am. Chem. Soc.*, 2020, **142**, 15780–15789.
- 192 Z. Yin, Y. Yang, J. Yang, G. Song, H. Hu, P. Zheng and J.-F. Xu, *CCS Chem.*, 2022, **4**, 3285–3595.

- 193 Á. Martínez, C. O. Mellet and J. M. G. Fernández, *Chem. Soc. Rev.*, 2013, **42**, 4746–4773.
- 194 R. E. McGovern, S. C. Feifel, F. Lisdat and P. B. Crowley, *Angew. Chem., Int. Ed.*, 2015, **54**, 6356–6359.
- 195 M. L. Rennie, A. M. Doolan, C. L. Raston and P. B. Crowley, *Angew. Chem., Int. Ed.*, 2017, **56**, 5517–5521.
- 196 A. M. Doolan, M. L. Rennie and P. B. Crowley, *Chem. – Eur. J.*, 2018, **24**, 984–991.
- 197 Y.-M. Zhang, N.-Y. Zhang, K. Xiao, Q. Yu and Y. Liu, *Angew. Chem., Int. Ed.*, 2018, **57**, 8649–8653.
- 198 S. Engel, N. Möller and B. J. Ravoo, *Chem. – Eur. J.*, 2018, **24**, 4741–4748.
- 199 X. Du, J. Zhou, J. Shi and B. Xu, *Chem. Rev.*, 2015, **115**, 13165–13307.
- 200 A. Tanaka, Y. Fukuoka, Y. Morimoto, T. Honjo, D. Koda, M. Goto and T. Maruyama, *J. Am. Chem. Soc.*, 2015, **137**, 770–775.
- 201 Z. Yang, G. Liang, L. Wang and B. Xu, *J. Am. Chem. Soc.*, 2006, **128**, 3038–3043.
- 202 T.-H. Ku, M.-P. Chien, M. P. Thompson, R. S. Sinkovits, N. H. Olson, T. S. Baker and N. C. Gianneschi, *J. Am. Chem. Soc.*, 2011, **133**, 8392–8395.
- 203 R. J. Amir, S. Zhong, D. J. Pochan and C. J. Hawker, *J. Am. Chem. Soc.*, 2009, **131**, 13949–13951.
- 204 J. Zhan, Y. Cai, S. He, L. Wang and Z. Yang, *Angew. Chem., Int. Ed.*, 2018, **57**, 1813–1816.
- 205 D. K. Armstrong, B. Bundy, L. Wenzel, H. Q. Huang, R. Baergen, S. Lele, L. J. Copeland, J. L. Walker, R. A. Burger and G. O. Group, *N. Engl. J. Med.*, 2006, **354**, 34–43.
- 206 R. L. Siegel, K. D. Miller and A. Jemal, *Ca-Cancer J. Clin.*, 2015, **65**, 5–29.
- 207 J. Li, Y. Kuang, J. Shi, J. Zhou, J. E. Medina, R. Zhou, D. Yuan, C. Yang, H. Wang, Z. Yang, J. Liu, D. M. Dinulescu and B. Xu, *Angew. Chem., Int. Ed.*, 2015, **54**, 13307–13311.
- 208 G. M. Whitesides and B. Grzybowski, *Science*, 2002, **295**, 2418–2421.
- 209 T. Aida, E. W. Meijer and S. I. Stupp, *Science*, 2012, **335**, 813–817.
- 210 X. Yang, H. Lu, Y. Tao, L. Zhou and H. Wang, *Angew. Chem., Int. Ed.*, 2021, **60**, 23797–23804.
- 211 R. Qi, H. Zhao, X. Zhou, J. Liu, N. Dai, Y. Zeng, E. Zhang, F. Lv, Y. Huang, L. Liu, Y. Wang and S. Wang, *Angew. Chem., Int. Ed.*, 2021, **60**, 5759–5765.
- 212 E. Santos, J. L. Pedraz, R. M. Hernández and G. Orive, *J. Controlled Release*, 2013, **170**, 1–14.
- 213 W. S. Tan and J. D. Kelly, *Nat. Rev. Urol.*, 2018, **15**, 667–685.
- 214 D.-Y. Hou, N.-Y. Zhang, M.-D. Wang, S.-X. Xu, Z.-J. Wang, X.-J. Hu, G.-T. Lv, J.-Q. Wang, X.-H. Wu, L. Wang, D.-B. Cheng, H. Wang and W. Xu, *Angew. Chem., Int. Ed.*, 2022, **61**, e202116893.
- 215 D. Wu, K. Yang, Z. Zhang, Y. Feng, L. Rao, X. Chen and G. Yu, *Chem. Soc. Rev.*, 2022, **51**, 1336–1376.
- 216 J. Ouyang, A. Xie, J. Zhou, R. Liu, L. Wang, H. Liu, N. Kong and W. Tao, *Chem. Soc. Rev.*, 2022, **51**, 4996–5041.
- 217 D. Wu, S. Wang, G. Yu and X. Chen, *Angew. Chem., Int. Ed.*, 2021, **60**, 8018–8034.
- 218 P. Zhang, Y. Xiao, X. Sun, X. Lin, S. Koo, A. V. Yaremenko, D. Qin, N. Kong, O. C. Farokhzad and W. Tao, *Med*, 2022, **4**, 147–167.